Defence Research and Development Canada
Recherche et développement pour la défense Canada

DEFENCE R&D DÉFENSE

Evaluation of the TASER eXtended Range Electronic Projectile (XREP)

Donald Sherman and Cynthia Bir

Department of Biomedical Engineering
Wayne State University
Detroit, MI USA

Prepared By:
Wayne State University
5057 Woodward Ave.
Detroit MI 48202
USA
Professor, Biomedical Engineering Department
Contractor's Document Number: 2012 XREP 04F
Contract Project Manager: Cynthia Bir, Ph.D., 313-577-3830
PWGSC Contract Number: W7711-09816/001/SS
CSA: Donna Wood, Project Manager CEWSI, 613-943-2472

Defence R&D Canada – CSS

Contract Report
DRDC CSS CR 2012-003
March 2012

Canada

Principal Author

Original signed by Donald Sherman and Cynthia Bir

Department of Biomedical Engineering

Wayne State University

Approved by

Original signed by Donna Wood

Donna Wood

DRDC Centre for Security Science

Approved for release by

Original signed by Mark Williamson

Mark Williamson

Chair of DRDC-CSS Document Review Panel

This project was sponsored Canadian Police Research Centre.

In conducting the research described in this report, the investigators adhered to the 'Guide to the Care and Use of Experimental Animals, Vol. I, 2nd Ed.' published by the Canadian Council on Animal Care.

Abstract

The TASER XREP was assessed to provide a complete characterization as a less-lethal weapon. The characterization was undertaken to determine how the system performed under normal and special conditions. The characterization included an assessment of the physical/electrical design and durability of the system, in-flight aerodynamics and accuracy, risk of blunt and penetrating injuries as well as a physiological surrogate. Testing was performed in a laboratory setting to allow for control of environmental variables. All fired rounds were tested with a computer-controlled firing system. The overall accuracy of the projectile was found to decrease with distance. Vertical drop from the point of aim to the point of impact at a distance of 20 meters was -51.37 ± 4.79 cm when tested at 23°C. Testing at 50°C and -20°C showed significantly less vertical drop -31.90 ± 3.12 cm and -29.69 ± 10.23 cm respectively. The round was stable in flight and produced a very low risk of blunt trauma although penetration testing at 2 meters showed a high likelihood of penetration. The electrical output of the projectile was within the manufacturer's specification, continued to operate after impact and did not produce any persistent clinically significant effects in the swine model.

Résumé

Le TASER XREP a été évalué pour fournir une caractérisation complète comme arme moins mortelle. La caractérisation a été entreprise pour déterminer comment le système se comporte dans des conditions normales et des conditions spéciales. La caractérisation comprenait une évaluation de la conception physique/électrique et de la durabilité du système, de la précision et de l'aérodynamique en vol, du risque de contusions et de blessures pénétrantes, ainsi qu'un substitut physiologique. Des essais ont été effectués dans un laboratoire pour permettre de contrôler l'environnement. Tous les projectiles lancés ont été testés à l'aide d'un système de tir commandé par ordinateur. On s'est aperçu que la précision globale du projectile diminue au fur et à mesure que la distance augmente. La chute verticale du point de visée au point d'impact à une distance de 20 mètres était de -51,37 ± 4,79 cm lorsque testée à 23 °C. Un essai à 50 °C et un à -20 °C ont démontré qu'il y avait une chute verticale beaucoup moins importante de -31,90 ± 3,12 cm et de -29,69 ± 10,23 cm respectivement. Le projectile était stable en vol et produisait un très faible risque de contusions bien que l'essai de pénétration à 2 mètres démontrait une probabilité élevée de pénétration. L'électricité produite par le projectile respectait la spécification du fabricant, ne cessait pas après l'impact et ne produisait pas d'effets persistants importants au niveau clinique chez le porc.

Executive summary

Evaluation of the TASER eXtended Range Electronic Projectile (XREP)

Donald Sherman; Cynthia Bir; DRDC CSS CR 2012-003; Defence R&D Canada – CSS; March 2012.

Introduction or background: TASER International (TI) announced that they have completed work on a new kind of conducted energy device, the eXtended Range Electronic Projectile or XREP, which is capable of incapacitating dangerous individuals at a greater distance. The XREP was designed as both a kinetic energy device and a conducted energy device.

A tripartite group of the Home Office Scientific Development Branch (United Kingdom), the Canadian Police Research Center (Canada) and the National Institute of Justice (USA) agreed to jointly fund an independent third party assessment of the mechanical, electrical and physical characteristic of the TASER XREP. Wayne State University in Detroit, Michigan was selected as the independent test facility and work began in the February of 2008. WSU neither endorses nor condemns the XREP. Key test parameters were discussed among the funding agencies and a total of 11 tasks were identified to measure the desired test parameters. The parameters identified represented three areas (physical design, in-flight characteristics, and risk of injury).

Results: The overall accuracy of the projectile was found to decrease with distance. Vertical drop from the point of aim to the point of impact at a distance of 20 meters was -51.37 ± 4.79 cm when tested at 23°C. Testing at 50°C and -20°C showed significantly less vertical drop -31.90 ± 3.12 cm and -29.69 ± 10.23 cm respectively. The training round has significant differences in accuracy and vertical drop when compared to the XREP live round. The round was stable in flight and produced a very low risk of blunt trauma although penetration testing at 2 meters showed a high likelihood of penetration. Testing at 5 meters showed a reduction in the risk and severity of penetration. The electrical output of the projectile was within the manufacturer's specifications. Post impact testing showed that the XREP continues to operate after impact. Animal testing indicated that the XREP did not produce any persistent clinically significant arrhythmias or changes physiological values in the swine model.

Significance: The XREP represents an impressive step forward in conducted energy devices. The ability to deploy a conducted energy device at a greater distance allows law enforcement and military personnel the ability to incapacitate a dangerous subject before they are close enough to do harm. The significant changes between the point of aim and point of impact create a specific set of challenges for training. This device is not without merit but end-users and decision makers need to assess all aspects of the XREP testing to determine if the XREP meets their specific needs.

Future plans: At the time of the writing of this report, no additional testing for this version of the XREP is planned. Additional penetration testing at greater ranges would help to better define the risk of penetrating injuries at tactical distances. The results presented in this report present the findings for the specific version of XREP tested. Additional characterizations should be completed if TI updates or changes the design of the XREP.

Sommaire

Évaluation du TASER XREP

Donald Sherman; Cynthia Bir; DRDC CSS CR 2012-003; R&D pour la défense Canada – CSS; mars 2012.

Introduction : La société TASER International a annoncé qu'elle a complété ses travaux sur un nouveau genre de dispositif à impulsions, le XREP (eXtended Range Electronic Projectile), qui est capable de neutraliser des individus dangereux à une plus grande distance. Le XREP a été conçu comme dispositif à énergie cinétique et comme dispositif à impulsions.

Un groupe triparti composé de la *Home Office Scientific Development Branch* (Royaume-Uni), du *Centre canadien de recherches policières* et du *National Institute of Justice* (États-Unis) a accepté de financer une évaluation indépendante par un tiers portant sur la caractéristique physique, la caractéristique électrique et la caractéristique mécanique du TASER XREP. La Wayne State University à Détroit au Michigan a été choisie comme installation d'essais indépendante, et les travaux ont débuté en février 2008. La Wayne State University n'approuve ni ne condamne le XREP. Les paramètres d'essai clés ont fait l'objet d'une discussion tenue par les agences de financement, et un total de 11 tâches ont été identifiées pour mesurer les paramètres d'essai désirés. Les paramètres identifiés représentaient trois domaines : conception physique, caractéristiques en vol et risques de blessures.

Résultats : On s'est aperçu que la précision globale du projectile diminue au fur et à mesure que la distance augmente. La chute verticale du point de visée au point d'impact à une distance de 20 mètres était de -51,37 ± 4,79 cm lorsque testée à 23 °C. Un essai à 50 °C et un essai à -20 °C ont démontré qu'il y avait une chute verticale beaucoup moins importante de -31,90 ± 3,12 cm et de -29,69 ± 10,23 cm respectivement. Le projectile d'entraînement a des différences importantes en termes de précision et de chute verticale par rapport au projectile réel XREP. Le projectile était stable en vol et comportait un risque très faible de contusions bien que l'essai de pénétration à une distance de 2 mètres présentait une probabilité élevée de pénétration. L'essai à une distance de 5 mètres a montré une diminution des risques et de la gravité de la pénétration. Le courant électrique produit par le projectile répondait aux spécifications du fabricant. Un essai après impact a montré que le XREP continue à fonctionner après l'impact. Des essais sur des animaux ont indiqué que le XREP ne produit pas d'arythmies importantes du point de vue clinique et persistantes, et ne modifie pas non plus les valeurs physiologiques chez le porc.

Portée : Le XREP constitue une avancée impressionnante en termes de dispositifs à impulsions. La capacité à déployer un dispositif à impulsions à une plus grande distance permet aux agents de la paix et au personnel militaire de neutraliser une personne dangereuse avant qu'elle soit assez près pour faire du mal. Les modifications importantes entre le point de visée et le point d'impact créent un ensemble spécifique de défis pour l'entraînement. Ce dispositif n'est pas sans avantages, mais les utilisateurs et les décideurs doivent évaluer tous les aspects de l'essai du XREP pour déterminer si le XREP répond à leurs besoins.

Recherches futures : Au moment de la rédaction du présent rapport, aucun essai supplémentaire pour cette version du XREP n'est prévu. Des essais de pénétration supplémentaires à des distances plus grandes aideraient à mieux définir le risque posé par les blessures pénétrantes à des

distances tactiques. Les résultats mentionnés dans le présent rapport donnent les conclusions pour la version spécifique du XREP testé. Des caractérisations supplémentaires doivent être complétées si TASER International met à jour ou modifie le XREP.

Table of contents

List of figures

List of tables

Acknowledgements

The authors wish to thank Mr. Graham Smith, Mr. Joe Cecconi and Mr Steve Palmer for their support of this effort. They provided invaluable insight into the determination of key parameters and feedback of testing setups and data analysis.

The authors also wish to thank Dr. Andy Adler and Mr. Dave Dawson for the expertise in the electrical assessment of the XREP. Their preliminary testing and guidance was helpful in determining optimal test design.

The authors wish to thank Mr. Rick Smith and Mr. Tom Smith for ensuring that the XREP materials would be available to test and for providing the X12 platform.

The authors wish to thank Mr. Jacob Mack for his assistance with data collection and analysis as well as for his assistance with preparing the preliminary test reports.

The authors wish to thank Dr. Elizabeth Dawe, Dr. Javier Sala-Mercado and Mrs. Janine Mathei for their assistance with the physiological model. Their efforts with data collection and analysis were key to fully understanding the physiological effects of the XREP.

This page intentionally left blank.

1 Introduction

1.1 Background

In 2007 TASER International (TI) announced that they had completed work on a new kind of conducted energy device, the eXtended Range Electronic Projectile or XREP. The new device was designed to be fired from a shotgun platform to allow for law enforcement officers to engage and incapacitate dangerous individuals at a greater distance than what was currently possible with other handheld devices. The XREP was designed as both a kinetic energy device and a conducted energy device, an area of less lethal weapons that had never been explored.

A tripartite group of the Home Office Scientific Development Branch (United Kingdom), the Canadian Police Research Center (Canada) and the National Institute of Justice (USA) agreed to jointly fund an independent third party assessment of the mechanical, electrical and physical characteristic of the TASER XREP. Wayne State University (WSU) in Detroit, Michigan was selected as the independent test facility and work began in the February of 2008. WSU neither endorses nor condemns the XREP.

1.2 Goals

The goals of this effort were to perform a thorough and independent characterization of the TASER eXtended Range Electronic Projectile (XREP). Parameters for characterization were identified by stake holders familiar with the device and other less-lethal technologies. The parameters identified represented three areas (physical design, in-flight characteristics, and risk of injury). Similar characteristics were grouped into tasks to reduce the number of tests needed and to allow for easier access to the results. Key test parameters were discussed among the funding agencies and a total of 11 tasks were identified to measure the desired test parameters. The tasks are:

Task 1. Physical Design
Task 2. Electrical Output
Task 3. Durability
Task 4. In-Flight Aerodynamics
Task 5. Electrical Activity Post-impact
Task 6. Accuracy and Precision
Task 7. Temperature Effects
Task 8. Risk of Penetration
Task 9. Risk of Blunt Trauma
Task 10. Assessment of the XREP Training Round
Task 11. Physiological Effects (Swine model)

It is hoped the report allows decision makers, end users and other stake holders to easily review the characteristics key to their unique needs.

1.3 XREP Design Overview

The XREP is marketed as a less-lethal option for the military, law enforcement and corrections officers. The projectile is fired from a 12 gauge shotgun platform. The projectile is designed to be fired from either a smooth or rifled barrel. The round is spin stabilized in flight by three spring-loaded curved fins that deploy from the chassis as the round exits the muzzle. These fins convert the forward velocity of the round into circumferential spin to provide aerodynamic stability in-flight. The body of the XREP consists of two main sections: a nose section and a chassis section (Figure 1).

The nose section is connected to the front of the chassis section via mechanical fracture pins. These pins are designed to allow the chassis to separate when the nose section impacts the target. The nose section has four forward facing metal barbs that are designed to penetrate the skin of the target. The nose section also has two rearward facing metal barbs that are designed to penetrate into the hand of the target if he or she grabs the area where he or she was impacted.

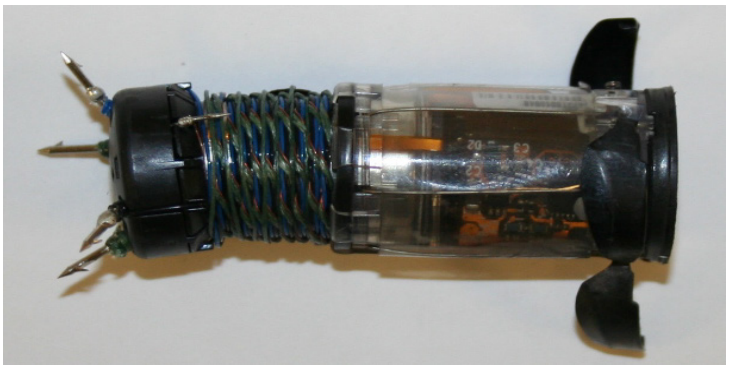

Figure 1 - XREP Device

The chassis section is designed to break away on impact and unspool a bare metal wire that electrically connects the nose barbs to the chassis electronics. The chassis section houses two batteries and the electronic circuitry of the round. The chassis also houses 6 metal "cholla" needles that are designed to spring out radially from the chassis upon impact (Figure 2).

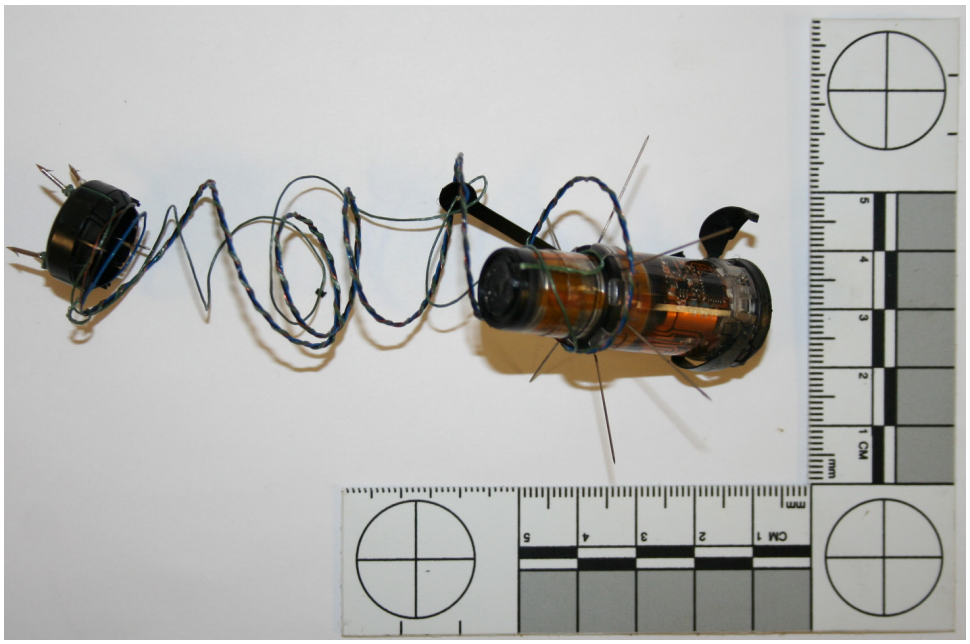

Figure 2 - XREP (nose detached)

The projectile is designed to utilize multiple methods to gain compliance from the target individual. The round has a kinetic effect that typically causes compliance through the transfer of kinetic energy when the round impacts the body. The primary mechanism for effect in a kinetic energy round is through pain compliance. The round is also designed to delivery electrical pulses through the metal sections. The electronics housed within the chassis are designed to incapacitate the target by delivering a pulsed voltage across; 1) the front barbs, 2) from the front to the rear barbs (if a part of the body engages them), 3) from the front barbs to the bare wire (if a part of the body engages it) and 4) from the front barbs to the "cholla" needles (if a part of the body engages them).

The training round is sold by TASER as a less expensive option for law enforcement officers to use for training purposes. The round is supposed to represent the aerodynamic characteristics of the XREP. The training round is also being sold as a kinetic energy projectile. The projectile utilizes the same spring-loaded tail fin stabilization (Figure 3 - XREP training round).

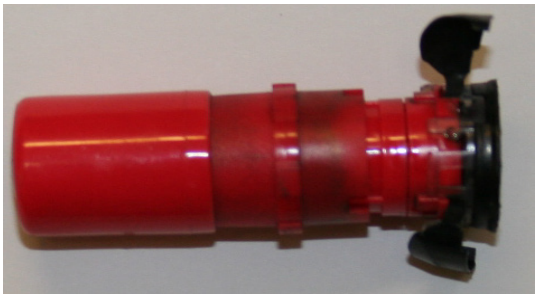

Figure 3 - XREP training round

2 Materials

2.1 Round Supply

At the time of testing the XREP device had experienced one major revision (version I to version II) and one smaller revision (version II to IIa). **All rounds tested for this report were XREP version IIa** and were supplied directly to WSU from TASER International. The rounds were shipped in four batches. The batch numbers and quantities shipped and dates are detailed below in the XREP inventory list (Table 1). The circuit board of the XREP has a unique six digit identifier which was documented for each round prior to testing. All of the batches shipped for testing in this effort are assumed to have been manufactured at the same time and are assumed to have no differences in performance.

Table 1 - XREP Inventory List

Batch #	Quantity	Date Received
1	32	9-8-10
2	100	9-21-10
3	50	9-24-10
4	115	2-4-11
Total	297	

2.2 Firing Platform

Two different platforms were used to fire the XREP device. A mounted X12 shotgun was used for all tasks that required the XREP to be fired with the exception of Task 5 (Electrical activity after impact). A universal receiver was used to fire the rounds for Task 5 because the X12 shotguns had been returned to TASER. It was determined that the differences in accuracy between these platforms was not a concern since velocity would likely be the primary cause of any potential failures and the velocity differences between the two platforms is very similar.

2.2.1 Mount Fired X12

The XREP projectile can be fired from a traditional smoothbore 12 gauge shotgun or the X12 TASER platform. The TASER X12 Less Lethal Shotgun is a re-engineered Mossberg 500 pump-action shotgun with “Radial Ammunition Key” to prevent the system from deploying lethal 12-gauge rounds. The X12 shotgun uses an 18.5 inch rifled barrel that TASER claims “optimizes the performance of the XREP, ensuring that an optimum spin rate is imparted upon the projectile as it exits the barrel”. Although the round can be fired from a traditional smoothbore barrel, TASER recommends using the X12 platform for best accuracy and range. For these reasons, the X12 platform was used for all ballistic testing [1].

The X12 was secured to a table mounted gun vise and was remotely fired using a computer-controlled, pneumatic firing system to allow the testing to be completely repeatable and user independent. The X12 was sighted using a laser bore site (SL-100, Concept Development Corporation, Fountain Hills, AZ). The X12 was re-sighted using the laser sight for each shot

(Figure 4). The X12 was cleaned after every ten shots and at the end of each test sequence so that subsequent test sequences were always started with a cleaned barrel.

Figure 4 - X12 Firing Platform

2.2.2 Universal Receiver

A table mounted universal receiver (HS Precision Model UR01 Rapid City, SD) was used to fire all rounds for the Task 5 testing (Figure 5). The receiver was fitted with an 18 inch smooth bore cylindrical barrel and a laser sight. The receiver was pneumatically driven and computer controlled to allow the testing to be completely repeatable and user independent. The receiver's laser sight was sighted in at each firing distance using a 12 gauge bore sight.

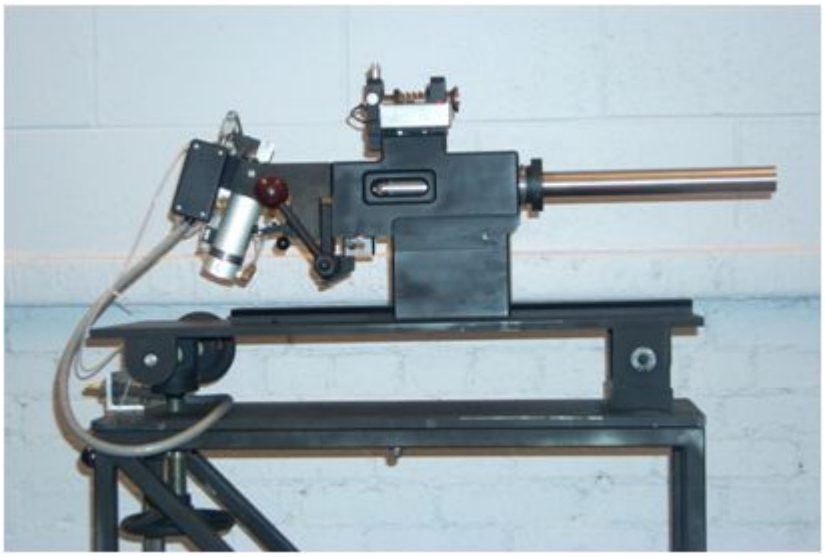

Figure 5 - Universal Receiver

2.3 High Speed Video

High-speed video (Redlake Inc., model HG 100K, Tucson AZ) was collected at 20,000 fps to determine the exact location of impact and to determine the in-flight characteristics and impact dynamics of the projectile for Tasks 4, 6-10. Video was collected at 5,000 fps to document target engagement for Task 5.

2.4 Velocity Measurements

The velocity of each round was recorded with three light screens (Oehler Research Inc., Model 57, Austin TX). Each screen has a row of LED emitters on the top and detectors on the bottom. The skyscreens were attached to an Oehler 35P chronograph (Figure 6). The front screen (placed 1 meter from the target) is 12 inches from the middle screen and 24 inches from the back screen. When a projectile crosses the front screen a voltage drop is sent to the chronograph and a timer begins. When the projectile crosses the middle screen, a second voltage drop is sent to the chronograph and the first timer stops and a second timer starts. When the projectile crosses the back screen, a third voltage drop is sent to the chronograph and the second timer stops. The chronograph knows the fixed distance between the screens and has the time of transit between screens. The velocity is calculated using Equation 1:

$$V = D / T$$

Equation 1

Where V is the calculated velocity, D is the fixed distance between the screens and T is the time as measured by the chronograph.

Figure 6 - Chronograph and Skyscreen

2.5 Rotary Torque Measurements

The magnitude of torque needed to separate the nose from the chassis was tested with a uni-axial test machine (Model 8500, Instron, Norwood MA, USA). A torque load cell (Model 11038, Sensor Developments Inc., Orion, MI, USA) was used to measure torque.

2.6 Electrical Output Measurements

The preliminary assessment of electrical output (Task 2) was contracted to Dr. Adler, Professor of Biomedical Engineering and Systems and Computer Engineering at Carlton University, Ottawa, Canada. The test materials used included an oscilloscope (Model 4224, Pico Technology, Eaton Socon, Cambridgeshire, UK), Pico Scope 6.5.78.5 software, calibrated 600 ohm loads, and a high voltage probe (Model 6015A, Tektronix Inc., Beaverton, Or, USA). The report prepared by Dr. Adler's group is included (Annex L). Final electrical assessments were conducted at Wayne State University using the same model oscilloscope, Pico Scope 6.5.13.15 software, a calibrated 600 ohm load (Model WOR10W1605, Wholesale Electronics Inc., Mitchell Sd, USA) and using a high voltage probe (Model 10076B, Agilent Technologies, Colorado Springs, Co, USA).

2.7 3-Rib Ballistic Impact Dummy

A biomechanical surrogate was recently developed and validated to determine the risk of injury due to blunt ballistic impacts [2-5]. The surrogate, or 3-Rib Ballistic Impact Dummy (3-RBID), was developed to provide a portable surrogate to evaluate non-lethal kinetic rounds in terms of risk of injury. Three BioSID ribs are joined to a spine box with a polyurethane sheet joining the ribs in the front (Figure 7). The impact surface measures 6.0 inches in height and 8.5 inches in width. A urethane foam pad is placed in front of the polyurethane sheet to achieve biofidelity.

A 50 pound mass is attached to the base of the 3-RBID to provide the appropriate mass of the thorax. The 3-RBID is placed on a Teflon coated table to allow for a low friction interface between the surrogate and table. A non-contact RibEye system is used to measure the location of each of the three ribs independently in three dimensions. The RibEye collects data at 20 kHz. Data collected from each rib is used to calculate the magnitude and velocity of rib deflection.

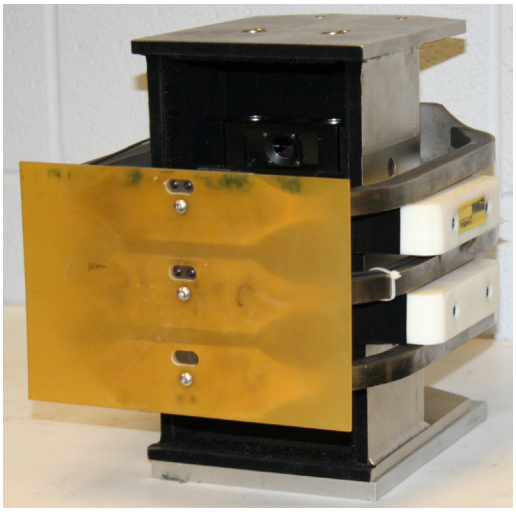

Figure 7 - 3 RBID

2.8 Penetration Surrogate

A biomechanical surrogate was recently developed and validated to determine the risk of injury due to penetrating ballistic impacts [6]. The surrogate was developed to provide repeatability and to evaluate non-lethal kinetic rounds in terms of risk of injury. The surrogate is comprised of two layers. The Laceration Assessment Layer (LAL) is sheepskin chamois and a close cell foam. The Penetration Assessment Layer (PAL) is 20%/wt ordinance gelatine (Figure 8). The impact surface measures 5.5 inches in height and 5.5 inches wide and it is approximately 14 inches long.

Figure 8 - Penetration Surrogate

3 Methodology

Tasks were completed with the goal of reducing the total number of rounds needed. For this reason, several rounds were used for more than one task. In some cases this meant rounds were measured (non-destructively for the first task) and then fired (for a second task), in other cases rounds were tested in such a way that each shot yielded data for multiple tasks.

The ballistic test facility was configured such that projectiles fired to test for accuracy at 5, 10 or 15 meters could also be recorded with high speed video while in flight (Figure 9). The in-flight aerodynamics of each projectile were measured at intermediate distances as the projectile traversed the distance from the muzzle to the target. Accuracy and precision were measured at the target distance; velocity was measured 1 meter from the target. At 5 meter testing, the proximal camera was placed 4 meters from the target (dashed line). At 10 and 15 meters, the proximal camera was placed 3 meters from the target. At 20 meters only a target camera was used.

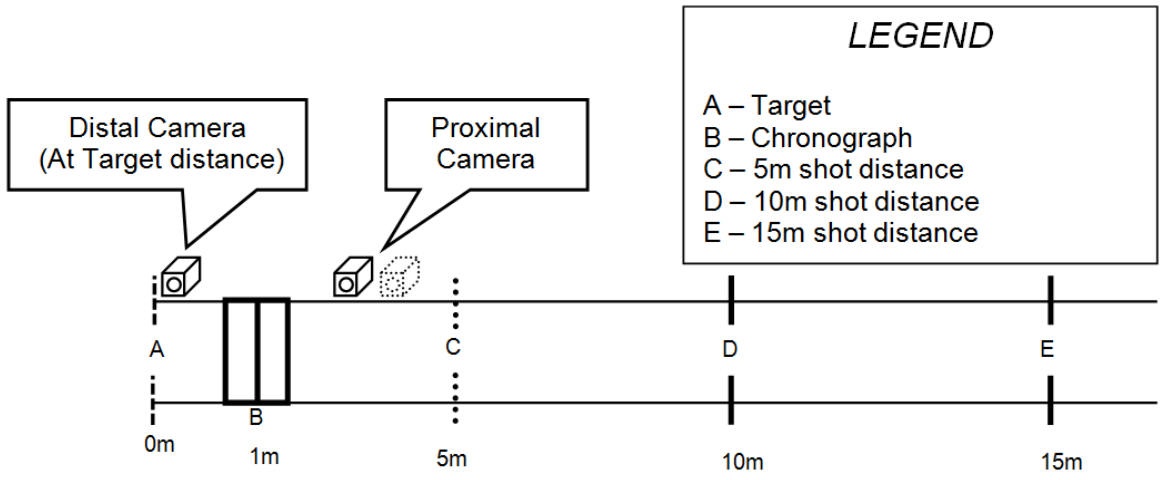

Figure 9 - Lab Schematic

3.1 Task 1 Physical Design

The assessment of physical characteristics included a characterization of the physical properties of the overall munition as well as the sub-munition pieces. For this task, the physical properties of ten rounds were measured and averaged. The properties assessed were overall dimensions and mass in addition to the dimensions and mass of the chassis and nose assemblies separately. Mass was measured using a digital balance (Ohaus, Model E0D120, Pine Brook Nj) and the physical dimensions were measured using digital calipers (Mitutoyo Corp., Model CD-8”C, Chicago Il). The wires connecting the nose and the chassis were cut as close to the nose as possible. The total mass and the mass of the chassis do not include the plastic wrap that contains the cholla barbs before the round separates. The total length measurement and the length of the nose

measurements included the length of the nose barbs. The total diameter was recorded at the largest point, i.e. the rear faring, the nose diameter was recorded at the nose frame, and the chassis diameter was recorded at the middle of the chassis. The average and standard deviation of these measurements were reported.

An assessment of the torque required to break the nose section free from the chassis was also performed. The breech section of an electrically inert XREP was secured to the base plate of a uni-axial test machine (Model 8500, Instron, Norwood Ma) and the nose was inserted into a custom fixture that held the four nose barbs. The nose section was rotated about the longitudinal axis of the chassis at a constant velocity of 0.5 degrees/sec. A digital output of the torque versus position was collected. The average and standard deviation of the peak torque and angle required to separate the two components was reported.

3.2 Task 2 Electrical Output

The assessment of the electrical output of the projectile included two separate tests to measure the electrical output of the most likely discharge modalities. These included discharge across the front barbs and discharge from a front barb to a rearward facing barb. The rear facing barbs, bare wire hand trap and cholla barbs are all part of the same circuit and thus do not all warrant testing.

Prior to data collection each XREP was removed from the shotgun shell by cutting away the section of the shell nearest the primer. The non-conductive tether that prevents electrical discharge in the shell was then cut and the XREP was removed from the shell. The exposed XREP was placed on an insulated bench top and secured for electrical output analysis. For measurements across the front barbs probes were connected to the barb that had a blue wire and to the barb that had a black wire. For measurements from the front to the rear barbs, probes were connected to the front barb that had a blue wire and to the rear facing barb on the opposite side (radially).

Electrical activity was measured using an oscilloscope (Model 4224, Pico Technology, Eaton Socon, Cambridgeshire, UK) which collected data at 1 Ms/sec using a high voltage probe (Model 10076B, Agilent Technologies, Colorado Springs, Co, USA). A 600 ohm, 10 watt resistor was placed in series between the front barb and the probe lead using a pair of alligator clips. The resistor was used to represent the load that a human body would create during exposure to the XREP [7, 8]. Data recorded during each exposure included peak waveform voltage, peak waveform current, waveform charge, PPS and duration. Peak voltage, current and charge values were measured for three discrete waveforms every second of the discharge. The PPS were measured for each second and the average for the entire duration was reported for each round. All results were averaged for the 5 rounds for each scenario. The data were analyzed using the statistical software package SPSS (Version 19.0, IBM corporation).

3.3 Task 3 Durability

The durability of the XREP was assessed by drop test at two different temperatures and in two different initial orientations. All rounds were dropped onto a smooth and level concrete surface. Twenty live rounds were tested at 23ºC (room temperature) and twenty live rounds were tested at -20ºC. Ten rounds at each temperature were dropped from an initial horizontal orientation and ten rounds at each temperature were dropped from an initial vertical orientation. Testing began

from an initial height of 1 meter. If breakage did not occur, then the height was increased by 50 centimeters and a new round was dropped. This incremental increase continued until a round broke. Breakage was considered to be a crack in the chassis, separation of the nose assembly from the chassis or any permanent deformation which may cause the round to malfunction. The average drop height at fracture and the standard deviation of the drop height for both temperatures and orientations was reported. Photographs of the rounds with an ABFO #2 photoscale were taken after the drop tests. If a round had been displaced relative to the shotgun casing, the software Image J (NIH, Research Services Branch) was used to measure the amount that the round had displaced.

The inherent accuracy of the drop tested round was assessed using the X12 mounted firing system. A paper target containing a bull's eye and one inch grid marks was mounted down range at distances of 5, 10, and 15 meters from the barrel. The X12 system was aimed using a laser bore sight (SL-100, Concept Development Corporation, Fountain Hills, Az) prior to each shot. After each round was loaded and aimed, the X12 was triggered via computer. Prior to impact, rounds traveled through 3 infrared light screens (Oehler Research Inc., Model 57, Austin, Tx) which calculated the velocity.

After each impact, the target was changed. Targets were used to record the impact information, including the data and time of impact, projectile velocity, and mass of the projectile. After each impact, key-testing information was recorded. X and Y coordinate data were measured from the point of impact to the axis origin using digital calipers. The accuracy data were analyzed using the statistical software package SPSS (Version 19.0, IBM corporation). Data were reported in terms of average X and Y offset as well as an overall circle of precision for each distance and compared to the un-dropped results of Task 6. The data were analyzed using the statistical software package SPSS (Version 19.0, IBM corporation).

3.4 Task 4 In-Flight Aerodynamics

The aerodynamics of the XREP round was studied using high speed video cameras (Redlake Inc., model HG 100K, Tucson AZ) recording at 20,000 FPS. Cameras were positioned at various distances from the barrel to record flight characteristics at a range of deployment distances. Rounds were fired at the target from 4 different distances (5, 10, 15 and 20 meters). At least ten rounds were fired at each distance. This allowed the overall aerodynamics to be recorded at a range of distances from the barrel. The aerodynamics were recorded at the muzzle, at impact as well as at 5, 7.5, 10, 12, 15 and 20 meters. Still images were analyzed for pitch using a software based image processing program (Image J, version 1.43u). Rotation data was measured by slowing down the high speed video to a point where the rotations were counted. Data recorded included attitude of the round (in degrees of pitch above or below horizontal) and rotations per second. . All data were analyzed with SPSS (Version 19.0, IBM corporation) for statistical significance and averages and standard deviations are reported.

3.5 Task 5 Electrical Activity Post-Impact

The post-impact electrical activity was assessed by firing electrically live XREPs at a human tissue surrogate. The surrogate (pork loin) was positioned on the mid-sagittal line of an

anthropomorphic test device which was suspended two meters from the muzzle. Electrical activity was measured using an oscilloscope (Model 4224, Pico Technology, Eaton Socon, Cambridgeshire, UK) which collected data at 1 Ms/sec using a high voltage probe (Model 10076B, Agilent Technologies, Colorado Springs, Co, USA). Two copper barbs were inserted into the lateral aspects of the pork loin at the point of aim and connected to the probe leads. After each round was loaded and aimed, the universal receiver was triggered via computer. Prior to impact, rounds traveled through 3 infrared light screens (Oehler Research Inc., Model 57, Austin Tx) which calculated the velocity.

After each impact, the round was allowed to fully discharge into the surrogate before it was recovered. The surrogate was repositioned after each test to allow for a clean impact site. The velocity of each round was recorded in addition to the duration and rate of electrical exposure.

3.6 Task 6 Accuracy and Precision

The inherent accuracy of the round was assessed using a fixed position firing system. The fixed position firing method utilized a table-mounted and pneumatically-triggered, X12 which was strapped into a damped gun vise for repeatable firing conditions. A paper target containing a bull's eye and one inch grid marks was mounted down range at distances of 5, 10, 15 and 20 and meters from the barrel. A minimum of ten rounds were fired at each distance. The X12 was aimed using a laser sight prior to each impact. Rounds traveled through 3 infrared light screens (Oehler Research Inc., Model 57, Austin Tx) which calculated the velocity.

After each impact the target paper was changed. For shots fired at 20 meters, 2 paper targets were combined to provide a target with enough vertical length to measure from the point of aim to the point of impact. After each impact, X and Y coordinate data were measured from the point of impact to the axis using digital calipers. The accuracy data were analyzed using the statistical software package SPSS (Version 19.0, IBM corporation). Data are reported in terms of average X and Y offset as well as an overall circle of precision for each distance.

3.7 Task 7 Temperature Effects

The effect of temperature on the accuracy, precision and aerodynamics of the XREP round were assessed. Temperature effects were determined by repeating the tests for accuracy and precision (Task 6) as well as recording the aerodynamics of the round (Task 4) at 50°C and -20°C. Rounds were stored in a temperature conditioning chamber at either 50°C or -20°C for at least 24 hours prior to being fired. Rounds were fired in a facility that was kept at 23°C so only one round was removed from the conditioning chamber at a time.

3.7.1 In-Flight Aerodynamics

The inherent accuracy of the round was assessed using the X12 mounted firing system. The aerodynamics of the XREP round were studied using two high speed video cameras (Redlake Inc., model HG 100K, Tucson Az) recording at 20,000 FPS each. Cameras were positioned at various distances from the barrel to record flight characteristics at a range of deployment distances. Rounds were fired at the target from 4 different distances (5, 10, 15 and 20 meters).

Ten rounds were fired at each distance. This protocol allowed the overall aerodynamics to be recorded at a range of distances from the barrel. Overall aerodynamics were recorded at the muzzle, at impact as well as at 5, 7.5, 10, 12, and 15 meters.

Data recorded included attitude of the round (in degrees of pitch above or below horizontal), rotations per second and velocity. All data were analyzed with SPSS (Version 19.0, IBM corporation) for statistical significance and averages and standard deviations are reported.

3.7.2 Accuracy and Precision

The inherent accuracy of the round was assessed using the X12 mounted firing system. A paper target containing a bull's eye and one inch grid marks was mounted down range at distances of 5, 10, 15 and 20 meters from the barrel. The X12 was aimed using a laser bore sight (SL-100, Concept Development Corporation, Fountain Hills, Az) prior to each impact. After each round was loaded and aimed, the X12 was triggered via computer. Prior to impact, rounds traveled through 3 infrared light screens (Oehler Research Inc., Model 57, Austin, Tx) which calculated the velocity.

After each impact the target paper was changed. Targets were used to record the impact information, including the date and time of impact, projectile velocity, and mass of the projectile. After each impact, key-testing information was recorded. X and Y coordinate data were measured from the point of impact to the axis using digital calipers. The accuracy data were analyzed using the statistical software package SPSS (Version 19.0, IBM corporation). Data are reported in terms of average X and Y offset as well as an overall circle of precision for each distance.

3.8 Task 8 Risk of Penetration

The skin penetration test protocol required the use of a combination of 20% ordnance gelatin, 0.60 cm foam, and a layer of natural chamois. The LAL, which consists of the foam and chamois, was placed on the front face (towards the projectile) of the gelatin. This layer represented the epidermis and dermis layers of the skin. The PAL consisted of a 5.5” x 5.5” x 14” block of 20 wt% ordnance gelatin stored at 10°C prior to testing. The LAL layer was secured to the PAL with adjustable elastic straps. The front face of the surrogate was positioned at a 0-degree angle of incidence. The PAL was cut to expose a flat surface free from damage for each subsequent test.

Penetration effects were assessed at 2 distances: 2 and 5 meters. Ten fair hit impacts were completed as part of each test distance. Test round velocities were calculated independently using three light screens and a chronograph (Oehler Research Inc., Models 57 and 35P, Austin, Tx). After completion of each test, the surrogate was visually inspected and evaluated for penetration. Test round masses were recorded using digital balance (Ohaus, model E0D120, Pine Brook, Nj).

3.9 Task 9 Risk of Blunt Trauma

The blunt trauma assessment was conducted to determine the probability of injury from the impact of the XREP projectile. This testing protocol required the use of the 3-RBID thoracic surrogate to measure the viscous criteria (VC) for each impact. The 3-RBID was positioned on a Teflon coated table to allow for a low friction interface between the surrogate and table. For the purposes of this testing, a non-contact displacement (Robert A. Denton Inc. model RibEye, Rochester Hills, Mi) system was integrated into the surrogate. This system allowed for deflection measurements to be made over a wide region of the sternum. Data were collected at 20,000 Hz. Data collected from each rib were used to obtain the magnitude and velocity of deflection. Test round masses were recorded using digital balance (Ohaus, model E0D120, Pine Brook Nj).

Blunt trauma effects were assessed at 2 meters. Test round velocities were calculated independently using three light screens and a chronograph (Oehler Research Inc., Models 57 and 35P, Austin TX). Ten "fair hit" impacts were completed. For each impact that fell within the specifications, the injury parameter of VC was determined. Based on previous research, it has been determined that a VC of 0.8 will result in a 50% chance of sustaining a thoracic skeletal injury at a level AIS $\geq$ 2. This injury level correlates to multiple rib fractures [3, 9].

3.10 Task 10 Training Round Evaluation

The accuracy and precision of the XREP training round was assessed to determine how well it represents the live XREP round. Both in-flight aerodynamics and the accuracy and precision were measured simultaneously to reduce the overall number of rounds needed.

3.10.1 In-Flight Aerodynamics

The aerodynamics of the XREP training projectile was studied using high speed video cameras (Redlake Inc., model HG 100K, Tucson Az) recording at 20,000 FPS. Cameras were positioned at various distances from the barrel to record flight characteristics at a range of deployment distances. Rounds were fired at the target from 4 different distances (5, 10, 15 and 20 meters). At least ten rounds were fired at each distance. This allowed the overall aerodynamics to be recorded at a range of distances from the barrel. The aerodynamics were recorded at the muzzle, at impact as well as at 5, 7.5, 10, 12, 15 and 20 meters (Figure 9). Still images were analyzed for pitch using a software based image processing program (Image J, version 1.43u). Rotation data were measured by slowing down the high speed video to a point where the rotations were counted. Data recorded included attitude of the round (in degrees of pitch above or below horizontal) and rotations per second. All data were analyzed with SPSS (Version 19.0, IBM corporation) for statistical significance and averages and standard deviations are reported.

3.10.2 Accuracy and Precision

The inherent accuracy of the round was assessed using a fixed position firing system. The fixed position firing method utilized a table-mounted and pneumatically-triggered, X12 which was strapped into a damped gun vise for repeatable firing conditions. A paper target containing a bull's eye and one inch grid marks was mounted down range at distances of 5, 10, 15 and 20 and meters from the barrel. A minimum of ten rounds were fired at each distance. The X12 was

aimed using a laser sight prior to each impact. Rounds traveled through 3 infrared light screens (Oehler Research Inc., Model 57, Austin Tx) which calculated the velocity.

After each impact the target paper was changed. For shots fired at 20 meters, 2 paper targets were combined to provide a target with enough vertical space to measure from the point of aim to the point of impact. After each impact, X and Y coordinate data were measured from the point of impact to the axis using digital calipers. Data are reported in terms of average X and Y offset as well as an overall circle of precision for each distance.

3.10.3 Comparison to XREP IIa

The results of both the aerodynamics and accuracy testing for the training round were compared to the results for the XREP IIa. A student's T-test was used to compare the results of the training round to the results of Tasks 4 and 6.

3.11 Task 11 Physiological Effects (Swine Model)

An anesthetised swine model was used to assess the effects of the XREP exposure on cardiac physiology. Five porcine sus scorfa (swine) specimens were used for this assessment. Dependent parameters assessed included: ECG traces, blood pressure, serum analysis, and gross pathologies. These values of mass were determined based scaling of previous research of porcine models representing the 50^{th} percentile male [10-12].

Prior to the commencement of Task 11 a test protocol was submitted to and approved by the Institutional Animal Care and Use Committee (IACUC) at Wayne State University. Testing was conducted in cooperation with the Surgical Research Services (SRS) and Division of Laboratory Animal Resources (DLAR) at Wayne State University. Full anesthesia and analgesia were used throughout the experiments with no resuscitation.

After a plane of surgical anesthesia was achieved, a Swan-Ganz catheter was used to monitor central venous pressure and mean arterial pressure. A 12 lead ECG was connected to the specimen for continuous monitoring. A cardiac physiologist reviewed and interpreted each ECG recording and documented any noted arrhythmias.

Exposures were applied to the specimen by attaching the nose probes to the midline of the thorax over the apex of the heart and a single cholla needle immediately inferior to the xiphoid process. The exposure was the standard pulse generated by the XREP during the normal application. Blood gases and electrolytes were measured before and after each exposure to monitor pH, PCO_2, PO_2,HCO_3, lactate, Na, K, hematocrit and hemoglobin levels. Heart rate, core body temperature and cardiac output were measured for signs of distress. Monitoring continued throughout the entire testing period which lasted four hours post exposure.

The specimen remained in a spine-horizontal position in an effort to prevent traumatic apnea. After all testing was completed; the specimens were euthanized according to the IACUC guidelines. Data are reported in terms of average blood gas and electrolyte levels as well as any anomalistic ECG data.

4 Results

4.1 Task 1 Physical Design

A total of 10 XREP rounds were evaluated. The average mass of the assembled projectile was 18.53 ± 0.03 g. The average masses of the nose and the chassis were 1.46 ± 0.01 g and 17.08 ± 0.03 g, respectively. The average diameters of the assembled projectile, nose, and chassis were 1.82 ± 0.01 cm, 1.90 ± 0.03 cm, and 1.63 ± 0.01 cm, respectively.

The average total length of the projectile was 5.87 ± 0.01 cm. The average lengths of the nose, chassis, front barbs, and cholla barbs were 1.88 ± 0.04 cm, 4.67 ± 0.03 cm, 0.77 ± 0.01 cm, and 1.97 ± 0.03 cm, respectively.

Six plastic shear pins are used to connect the nose of the XREP to the chassis. The average maximum torque required to separate the nose from the chassis was 0.597 ± 0.05 N*m. The average angle at maximum torque was 16.57 ± 3.79°. The nose of one round did not separate from the chassis and the test was stopped after 30° of rotation to protect the test equipment. All raw data and statistical values can be found in Annex A

Table 2 - Physical Parameter results

Variable	Average ± Standard Deviation
Total Mass	18.53 ± 0.03 g
Nose Mass	1.46 ± 0.01 g
Chassis Mass	17.08 ± 0.03 g
Total Diameter	1.82 ± 0.01 cm
Nose Diameter	1.90 ± 0.03 cm
Chassis Diameter	1.63 ± 0.01 cm
Total Length	5.87 ± 0.01 cm
Nose Length	1.88 ± 0.04 cm
Chassis Length	4.67 ± 0.03 cm
Front Barbs Length	0.77 ± 0.01 cm
Cholla Barbs Length	1.97 ± 0.03 cm
Maximum Separation Torque	0.60 ± 0.05 N*m
Angle at Max Torque	16.57 ± 3.79 °

4.2 Task 2 Electrical Output

A total of 10 rounds were used for this task. Five rounds were tested for electrical activity across the front nose barbs. The average peak voltage across the front barbs was 426.58 ± 3.13 volts. The average peak current across the front barbs was 0.72 ± 0.01 amps. The average charge per waveform across the front barbs was 71.98 ± 2.03 μC. The average PPS during the exposure across the front barbs was 18.48 ± 0.06. The average duration of the exposure across the front barbs was 19.39 ± 0.14 seconds. Five rounds were tested for electrical activity from the front

barb to a rear facing barb. The average peak voltage from the front barb to the rear facing barb was 427.13 ± 41.63 volts. The average peak current from the front barb to the rear facing barb was 0.72 ± 0.07 amps. The average charge per waveform from the front barb to the rear facing barb was 77.74 ± 5.39 μC. The average PPS during the exposure from the front barb to the rear facing barb was 18.62 ± 0.10. The average duration of the exposure from the front barb to the rear facing barb was 19.38 ± 0.13 seconds. The data from the two discharge paths were compared to each other using independent samples t-tests. The level of significance was $p \leq 0.05$ for all tests. Results are shown in Table 3.

Table 3 - Electrical output results

Discharge Path	Average Peak Voltage (V)	Average Peak Current (A)	Average Charge per Waveform (μC)	Average Pulses (s^{-1})	Average Total Duration (s)
Front-Front	426.58 ± 3.13	0.72 ± 0.01	71.98 ± 2.03	18.49 ± .06 †	19.39 ± 0.14
Front-Rear	427.13 ± 41.63	0.72 ± 0.07	77.74 ± 5.39	18.62 ± .11 †	19.38 ± 0.13

† indicates a statistical significance ($p \leq 0.05$) between two discharge paths

Electrical output testing results were compared using independent samples t-tests. Tests were run to determine if the differences in output variables peak voltage, peak current, average waveform charge, PPS and duration were statistically significant when measured between the front to front barbs and the front to rear barbs. Statistically significant differences were measured for average pulses per second. There were no statistically significant differences in peak voltage, peak current, PPS and duration between the two discharge paths. All raw data and statistical values can be found in Annex B.

4.3 Task 3 Durability

A total of 40 rounds were used to test durability, 20 rounds were tested at 23°C, and 20 rounds were tested at -20°C. The results of the drop test are tabulated in Table 4. The data from the drop tests were compared to each other using independent samples t-tests. The level of significance was $p \leq 0.05$ for all tests. After each drop test, the rounds were fired and velocity and accuracy data were collected and compared to Task 6 results shown in Table 5. One round missed the target, and therefore the accuracy data was unusable while errors with the velocity trap hardware resulted in lost velocity data for three rounds.

Drop testing results were compared using independent samples t-tests. Tests were run to determine if the differences in average drop height, breakage or slip amount were statistically significant when compared to drops performed at the same temperature with a different orientation (vertical compared to horizontal). Statistically significant differences were measured for drop height, breakage and slip amount for rounds drop tested when one orientation was compared to the other at both 23°C and -20°C. Tests were also run to determine if the differences in average drop height, breakage or slip amount were statistically significant when compared to drops performed at a different temperature (23°C compared to -20°C) with the same orientation. There were no statistically significant differences in average drop height, breakage or slip amount

for rounds dropped in the same orientation at different temperatures. All raw data and statistical values can be found in the

Table 4 - Drop testing results

Temperature (°C)	Orientation	Drop Height (m)	Breakage (%)	Slipped Distance (mm)
23	Horizontal	2.5 ± 0.7 †	0 †	0.0 ± 0.0 †
	Vertical	1.5 ± 0.2 †	90 †	0.6 ± 0.4 †
-20	Horizontal	2.5 ± 0.7 †	10 †	0.0 ± 0.1 †
	Vertical	1.5 ± 0.2 †	90 †	0.5 ± 0.3 †

† indicates a statistical significance ($p \leq 0.05$) between orientations at same temperature

For the statistical analysis of the velocity and accuracy data, the rounds dropped at 23°C and the rounds dropped at -20°C were compared to each other as well as the rounds fired in Task 6 using an ANOVA. If significant differences were measured with the ANOVA then the data were analyzed using post hoc tests; Fisher's least significant difference (LSD) tests if the data was parametric or Games-Howell tests if the data was nonparametric. The level of significance was $p \leq 0.05$ for all tests.

The effect of orientation (regardless of temperature) within distance groups was determined statistically (see Table 5). At 5 m, there was no statistically significant difference in velocity between any of the groups. There was no statistically significant difference in the X coordinate data between any groups. Rounds dropped both horizontally and vertically showed significantly more vertical drop than rounds tested for Task 6.

At 10 m, the rounds dropped vertically had a significantly higher velocity than rounds tested for Task 6. There was no statistically significant difference in the X coordinate data between any groups. Rounds dropped both horizontally and vertically showed significantly more vertical drop than rounds tested for Task 6.

At 15 m, the rounds dropped vertically had a significantly higher velocity than rounds tested for Task 6. There was no statistically significant difference in the X coordinate data between any groups. There was no statistically significant difference in the Y coordinate data between any groups.

Next, the effect of temperature (regardless of orientation) within distance groups was determined statistically (see Table 6). At 5 m, there was no statistically significant difference in velocity between any groups. There was no statistically significant difference in the X coordinate data between any groups. Rounds drop tested at both at 23°C and -20°C showed significantly more vertical drop than rounds tested for Task 6.

At 10 m, the rounds that were dropped tested at 23°C had a significantly higher velocity than rounds tested for Task 6. There was no statistically significant difference in the X coordinate data between any groups. Rounds drop tested at both at 23°C and -20°C showed significantly more vertical drop than rounds tested for Task 6.

At 15 m, there was no statistically significant difference in the velocity data between any groups. The rounds dropped at 23°C impacted significantly more left of the point of aim than rounds tested for Task 6 and the rounds dropped at -20°C. There was no statistically significant difference in the Y coordinate data between any groups.

Table 5 - Accuracy results for durability test - effect of drop orientation

Orientation	Distance (m)	Velocity (fps)	X Coordinate (cm)	Y Coordinate (cm)
Horizontal	5	225.9 ± 6.74	-0.87 ± 0.99	-2.97 ± 1.33
	10	214.8 ± 11.9	-0.38 ± 1.42	-12.93 ± 2.35
	15	210.3 ± 8.8	-0.40 ±3.45	-24.73 ± 2.63
Vertical	5	224.6 ± 12.5	0.17 ± 0.98	-3.09 ± 1.37
	10	222.2 ± 7.5 ‡	-1.56 ± 1.11	-10.69 ± 1.20
	15	216.4 ± 8.8 ‡	0.37 ± 3.39	-22.55 ± 3.73
Not Dropped (Task 6)	5	221.6 ± 8.5	0.63 ± 1.50	0.44 ± 1.98 †
	10	209.4 ± 7.3 ‡	-1.34 ± 2.14	-5.41 ± 2.21 †
	15	201.8 ± 15.0 ‡	0.93 ± 2.16	-18.70 ± 6.16

† indicates a statistical significance ($p \leq 0.05$) between all other orientations at the same distance

‡ indicates a statistical significance ($p \leq 0.05$) between two orientations at the same distance

Table 6 - Accuracy results for durability test - effect of temperature

Temperature (°C)	Distance (m)	Velocity (fps)	X Coordinate (cm)	Y Coordinate (cm)
-20	5	223.6 ±12.6	-0.16 ± 1.20	-3.16 ± 1.06
	10	212.6 ± 10.9	-1.70 ± 0.77	-12.42 ± 2.39
	15	208.3 ± 12.8	1.67 ± 3.11	-23.94 ± 2.83
23	5	226.9 ± 6.1	-0.54 ± 1.03	-2.90 ± 1.57
	10	222.7 ± 7.8 ‡	-0.43 ± 1.52	-11.13 ± 1.77
	15	217.0 ± 10.7	-2.38 ± 1.78 †	-23.22 ± 4.14
23 (Task 6)	5	221.6 ± 8.5	0.63 ± 1.51	0.44 ± 1.98 †
	10	209.4 ± 7.3 ‡	-1.34 ± 2.14	-5.41 ± 2.21 †
	15	201.8 ± 15.0	0.93 ± 2.16	-18.70 ± 6.16

† indicates a statistical significance ($p \leq 0.05$) between all other temperatures at the same distance

‡ indicates a statistical significance ($p \leq 0.05$) between two temperatures at the same distance

The mode of drop testing (horizontal initial orientation, vertical initial orientation, or not dropped) had mixed general effects on the velocity and accuracy data. Rounds dropped vertically had a significantly higher velocity than those rounds not dropped (Task 6). This was true at 10 m and 15 m, but not at 5 m. There were no significant general trends between modes for the X coordinate data. Rounds that were dropped tested from 5m and 10 m showed significantly more vertical drop than rounds that were not drop tested. At 15 m the difference was still present but no longer significant due to the standard deviation of Y coordinate data from Task 6.

The temperature at which the rounds were dropped did not generally affect the velocity or the X coordinate. However, rounds drop tested at -20°C showed significantly more vertical drop than rounds not drop tested., Rounds that were drop tested from 5 m and 10 m at 23°C also showed significantly more vertical drop than rounds that were not drop tested.

For this reason, several rounds were used for more than one task. In some cases this meant rounds were measured (non-destructively for the first task) and then fired (for a second task), in other cases rounds were tested in such a way that each shot yielded data for multiple tasks. All raw data and statistical values can be found in Annex C.

4.4 Task 4 In-Flight Aerodynamics

The aerodynamics of rounds fired at 5 10 and 15 meters were recorded by a proximal camera and by a target camera (0, 5, 7.5, 10, 12 and 15 meters respectively). The aerodynamics of rounds fired at 20 meters were recorded at the target distance.

Table 7 - Results of in-flight aerodynamics test

Distance (m)	Pitch (Deg)	Rotations (RPS)
0	0.1° ± 1.0°	126.0 ± 45.2 †
5	0.3° ± 4.0°	182.7 ± 46.4
7.5	-0.6° ± 0.9°	197.4 ± 25.3
10	-0.8° ± 1.1°	218.4 ± 16.8
12	-1.1° ± 4.1°	218.4 ± 53.9
15	1.0° ± 5.3°	218.9 ± 82.1
20	-0.4° ± 1.0°	278.5 ± 15.4 †

† indicate a statistical significance ($P \leq 0.05$) to all other distances

An ANOVA statistical analysis was performed to determine if statistical differences were present. A Least Square Difference (LSD) test was performed post hoc to determine which groups showed statistical differences. The rotations per second measured at 0 and 20 meters were significantly different from the rotations measured at all other distances. The rotational data follows an expected trend. As the projectile exits the barrel, the initial rotational velocity is due to the rifling of the X12 barrel that engages the projectile as it travels through the barrel. After the projectile exits the barrel and the fins have opened they begin to increase the rotational velocity. This trend is evident in the graph of the data (Figure 10). No statistically significant differences were found for the projectile pitch at any distance (Figure 11). The level of significance was $p \leq 0.05$ for all tests. All raw data and statistical values can be found in Annex D.

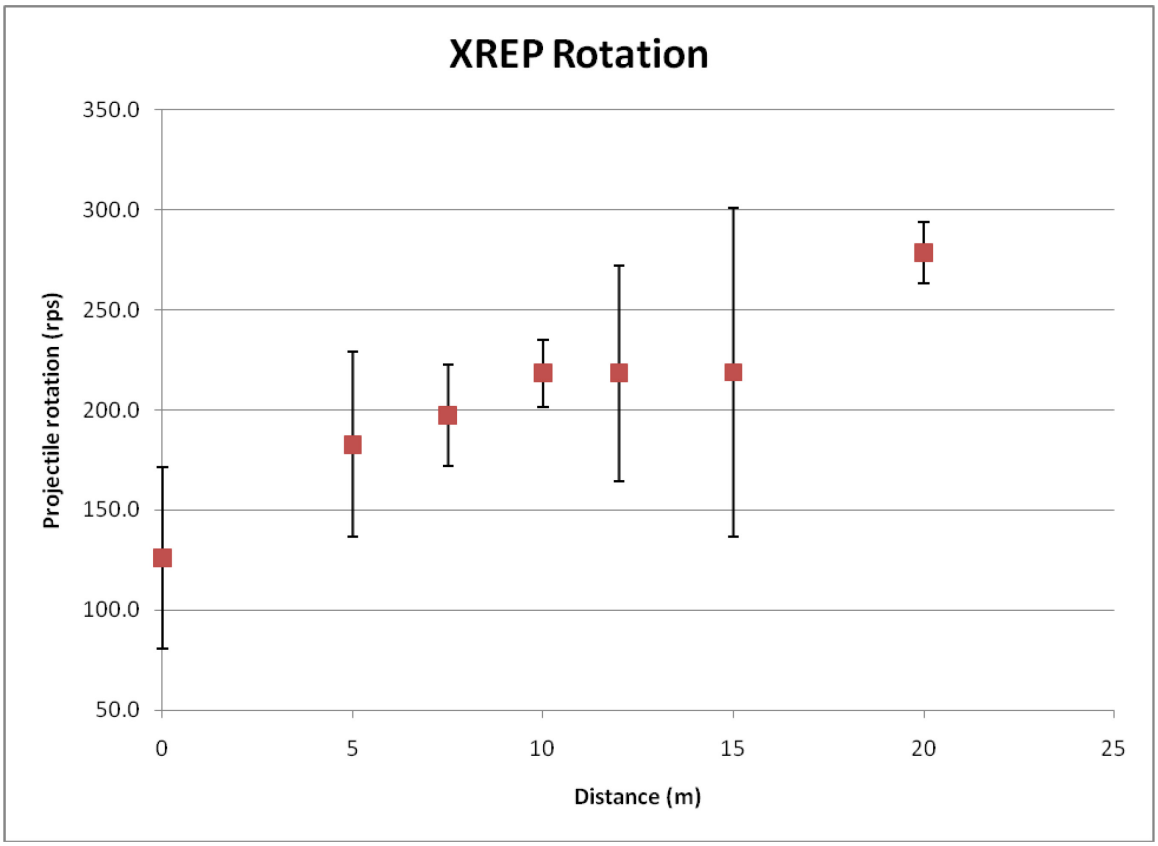

Figure 10 - XREP rotation versus distance

le

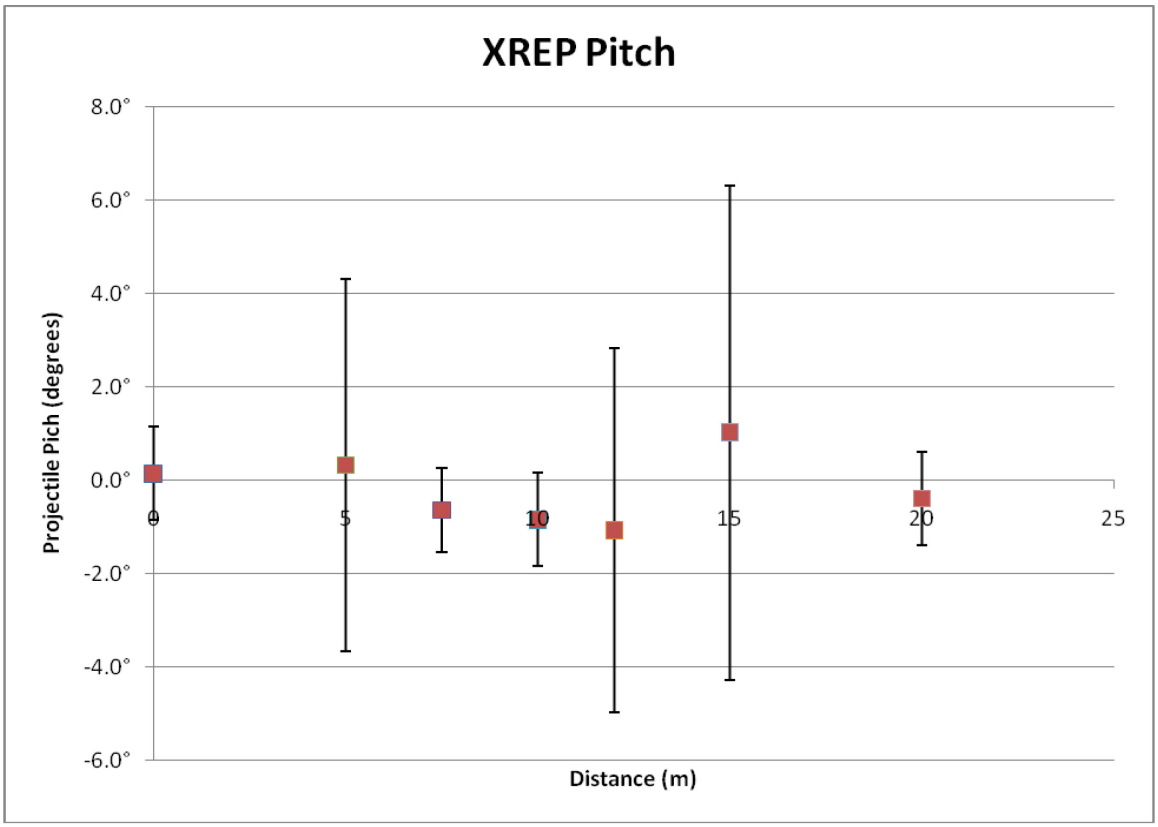

Figure 11 - XREP pitch versus distance

4.5 Task 5 Electrical Activity Post-Impact

A total of 19 rounds were tested for Task 5, results shown in Table 8 below. Triggering issues created incomplete data sets for 8 of the rounds and the oscilloscope failed to capture data for one round due to a probe falling out. None of the cholla barbs on any of the rounds deployed. The average exposure duration was 19.4 ± 0.4 seconds, and the average PPS was 18.1 ± 0.3 pps. The average velocity of the rounds was 223.7 ± 9.3 fps.

Table 8 - Post-Impact Electrical Activity Results

Variable	Average ± Standard Deviation
Exposure Duration	19.4 ± 0.4 s
Average Pulses per Second	18.1 ± 0.3 pps
Velocity	223.7 ± 9.3 fps

For all of the rounds tested electrically, the pulse train was interrupted by a short interval in which 1 – 4 pulses were missing. This cycle happened approximately once every 5 seconds. All raw data and statistical values can be found in Annex E.

4.6 Task 6 Accuracy and Precision

The average results for velocity and impact location are listed below in Table 9. The diameter of the circle of precision (COP) for the 10 rounds at 5 meters was 7.42 cm. The diameter of the COP for the 10 rounds fired at 10 meters was 8.88 cm. Precision dropped sharply at 15 meters and the diameter of the COP was 30.04 cm. The drop in precision was due two 2 rounds that were more than 2 standard deviations from the average. At 20 meters the diameter of the COP was 20.38 cm. The general trend of the rounds was downward and to the left of the point of aim with increasing distance.

Table 9 - Average values from accuracy testing

Distance (m)	Velocity (fps)	X Coordinate (cm)	Y Coordinate (cm)	COP Diameter (cm)
5	221.6 ± 8.5 †	0.63 ± 1.50	0.43 ± 1.98 †	7.42
10	209.4 ± 7.3 ‡	-1.36 ± 2.14	-5.40 ± 2.22 †	8.88
15	201.8 ± 15.0	-0.75 ± 4.84	-17.28 ± 5.43 †	30.04
20	200.2 ± 5.6 ‡	-11.86 ± 4.69 †	-51.37 ± 4.79 †	20.38

† indicates a statistical significance ($P \leq 0.05$) between all other distances
‡ indicates a statistical significance ($P \leq 0.05$) between two distances

The velocities at the 5 meter distance were significantly different from the velocities measured at all other distances. Additionally, the velocities measured at 10 meters were significantly different from the velocities measured at 20 meters. The velocity follows an expected trend that is due primarily to the drag created by the fins. The fins convert the forward velocity into rotational energy, slowing down the projectile. The X coordinate values for rounds fired at 20 meters were significantly different from rounds fired at all other distances. The Y coordinate values for rounds fired at each distance were significantly different from all other distances. The change in Y coordinate accuracy follows an expected trend due to gravitational forces. The projectile drops at a constant rate. The slower the projectile is traveling, the greater the amount of vertical drop as shown in the figure below (Figure 12). The level of significance was $p \leq 0.05$ for all tests. All raw data and statistical values can be found in Annex F.

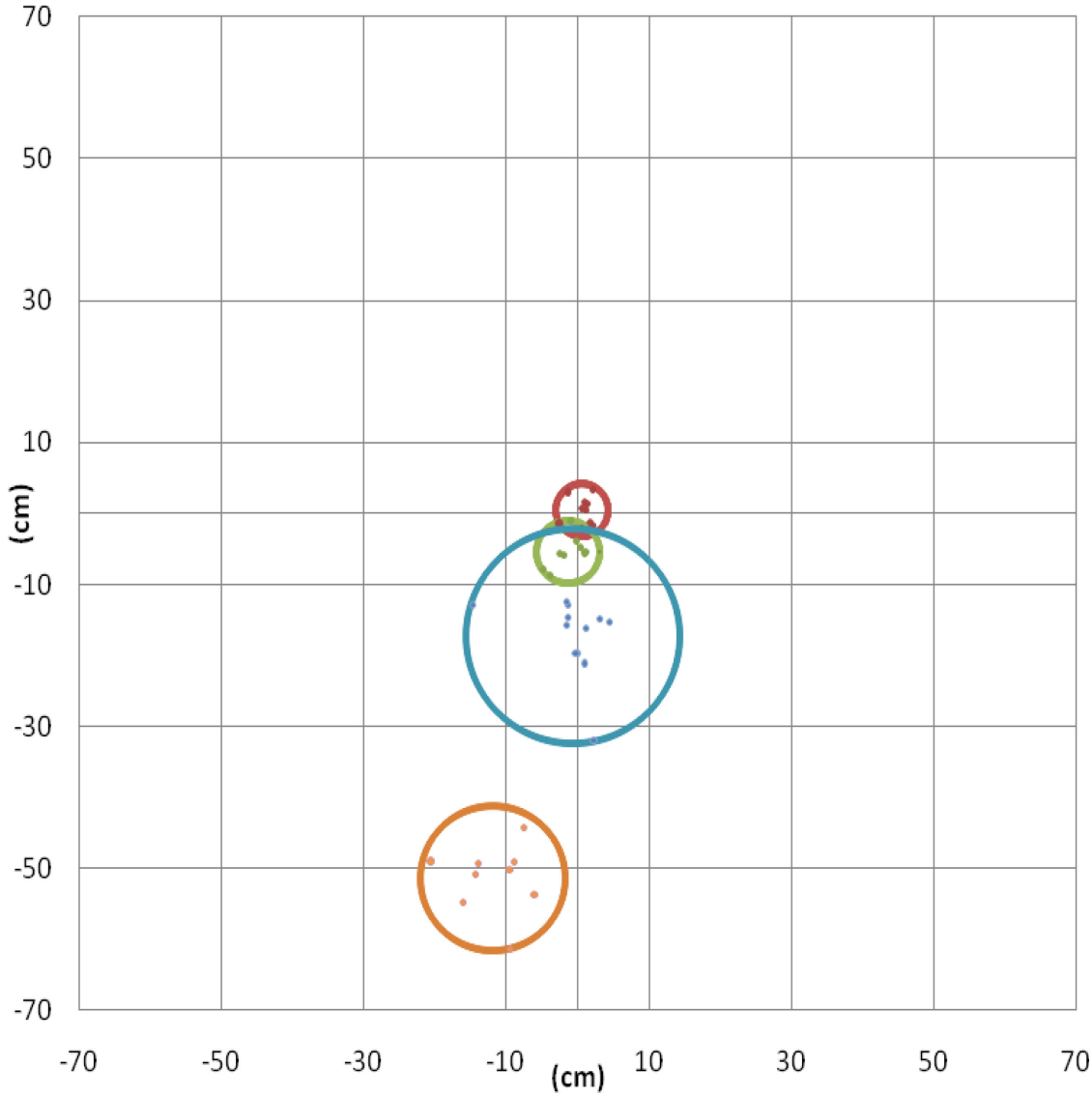

Figure 12 - XREP Accuracy and Precision

4.7 Task 7 Temperature Effects

A total of 108 XREP rounds were tested to determine the effects of temperature on accuracy and in-flight aerodynamics. Some rounds did not provide useful data, either due to a failure of the round—opening during flight or traveling out of range of the camera—or due to experimental errors—trigger error or data acquisition system error. Thirteen of these 108 XREPs opened during flight, causing the proximal and/or distal aerodynamics data to be unusable. In one of the thirteen cases, the velocity datum was unusable. In five of the thirteen cases, the accuracy data were unusable. In one of the thirteen cases, both the velocity and the accuracy data were unusable.

In an additional twelve of the 108 cases, the proximal and/or distal data were otherwise unusable. In one of the twelve cases, the velocity datum was also unusable. In a separate one of the twelve cases, the accuracy datum was unusable.

4.7.1 In-Flight Aerodynamics

The average results for pitch and rotation are listed below in Table 10. The rotational rate data for all temperatures are plotted in Figure 13 and the pitch data for all temperatures are plotted in Figure 14. For statistical comparisons, the data for the 50°C and the -20°C rounds were compared to the data for the rounds tested at room temperature 23°C in Task 6 using an ANOVA. If significant differences were measured with the ANOVA then the data were analyzed using post hoc tests; Fisher's LSD tests if the data was parametric or Games-Howell tests if the data was nonparametric. The level of significance was $p \leq 0.05$ for all tests.

First, the effect of distance within temperature groups was determined statistically. For the 50°C tests, the rotational rate as the round exited the muzzle (0 m), was significantly different that rotational rates at all other distances. The rotational rate at 5 m was different from rates at all other distances except 7.5 m. The rotational rate at 7.5 m was different from rates at all other distances except 5 m and 10 m. The rotational rate at 10 m was different from rates at all other distances except 7.5 m and 12 m. No other statistically significant differences were measured. As expected, the rotational rate increased as the distance from the muzzle increased. The pitch at 0 m was statistically higher than that at all other distances. The pitch values at 5 m, 7.5 m, and 12 m were statistically higher than that at 15 m. Additionally, the pitch at 7.5 m was statistically higher than that at 10 m and at 20 m. The general trend was an increasing downward pitch as distance increased

For the -20°C tests, the rotation values at 0 m were statistically different from rates at all other distances. The rotational rate at 5 m was different from rates at all other distances except 7.5 m. The rotational rate at 7.5 m was different from rates at all other distances except 5 m. The rotational rate at 10 m was different from rates at all other distances except 12 m. The rotational rate at 12 m was different from rates at all other distances except 10 m and 15 m. The rotation increased with increasing distance. There were no statistically significant differences between the pitch values at any distance.

Next, the effect of temperature within distance groups was determined statistically using an ANOVA. For the 0 m, 5 m and 7.5 m distances, the rotational rates at 50°C and -20°C were significantly lower that rate at 23°C. There were no statistical differences between the pitch values of different temperatures.

For the 10 m, 12 m and 15 m distances, there were no statistical differences between either the rotational rate nor the pitch values of different temperatures.

For the 20 m distance, the rotational rate at 50°C was significantly lower than rates at 23°C and 20°C. There were no statistical differences between the pitch values of different temperatures.

Table 10 - Results of in-flight aerodynamics test

Temperature (°C)	Distance (m)	Rotations (RPS)	Pitch (Deg)
50	0	61.6 ± 8.1 †	1.7 ± 1.9 †
	5	143.0 ± 15.6	-0.6 ± 0.6
	7.5	162.3 ± 24.9	0.5 ± 1.4
	10	201.8 ± 32.8 ^	-0.9 ± 1.4 #
	12	240.5 ± 14.6 ^#	-0.5 ± 0.9
	15	256.9 ± 19.5 ^#¥	-1.9 ± 0.9 ^#‡
	20	252.2 ± 21.1 ^#¥*	-1.3 ± 0.8 #
23	0	126.0 ± 45.2 *	0.1 ± 1.0
	5	182.7 ± 46.4 *	0.3 ± 4.0
	7.5	197.4 ± 25.3 *	-0.6 ± 0.9
	10	218.4 ± 16.8	-0.8 ± 1.1
	12	218.4 ± 53.9	-1.1 ± 4.1
	15	218.9 ± 82.1	1.0 ± 5.3
	20	278.5 ± 15.4	-0.4 ± 1.0
-20	0	66.9 ± 6.5 †	0.1 ± 3.4
	5	144.9 ± 8.9	-0.8 ± 1.1
	7.5	162.0 ± 14.5	0.2 ± 0.7
	10	200.7 ± 23.4 ^#	-1.2 ± 1.1
	12	224.8 ± 40.6 ^#	0.3 ± 2.3
	15	251.0 ± 31.7 ^#¥	-1.9 ± 3.9
	20	280.1 ± 17.7 ^#¥‡	-1.0 ± 0.8

^ statistical significance (p≦0.05) between 5 m at the same temperature

 # statistical significance (p≦0.05) between 7.5 m at the same temperature

¥ statistical significance (p≦0.05) between 10 m at the same temperature

‡ statistical significance (p≦0.05) between 12 m at the same temperature

† statistical significance (pP≦0.05) between all other distances at the same temperature

*** statistical significance (p≦0.05) between all other temperatures at the same distance**

For all three temperatures, the rotation of the round generally increased with distance. This is an expected trend because, at greater distances, the round's fins have a greater opportunity to turn forward velocity into rotational velocity. An exception to this trend is that, at 50°C, rotation decreased from 15 m to 20 m. Rotation did not show any general trends with respect to

temperature, except that the rotation at the lower distances (0 m, 5 m, 7.5 m) for 23°C was significantly higher than the rotation at the same distances at the other two temperatures.

The pitch does not show any general trends with respect to distance for any temperature. Furthermore, the pitch does not show any general trend with respect to temperature for any distance.

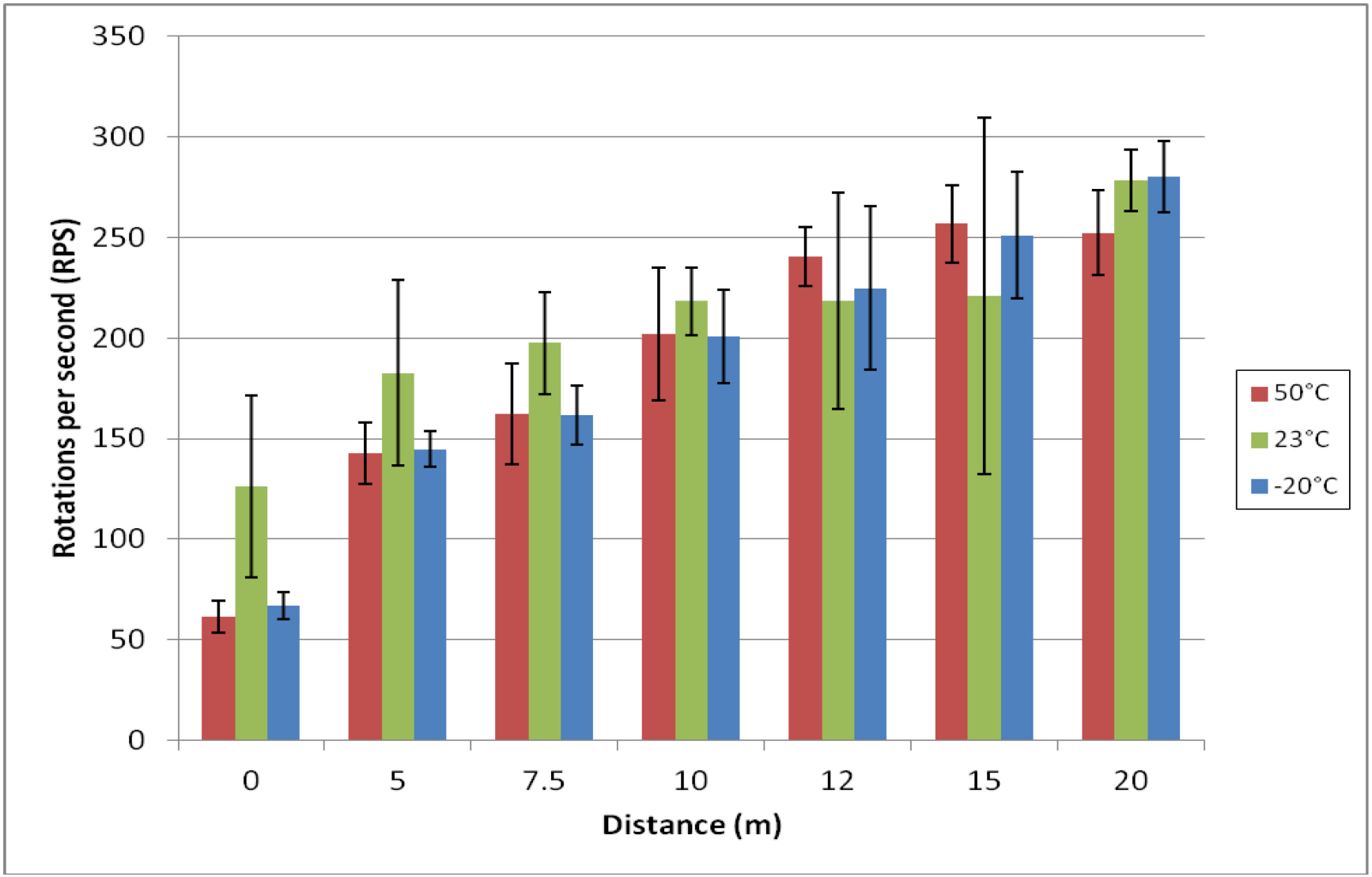

Figure 13 - XREP (50°C, 23°C and -20°C) Rotational Rates by Distance

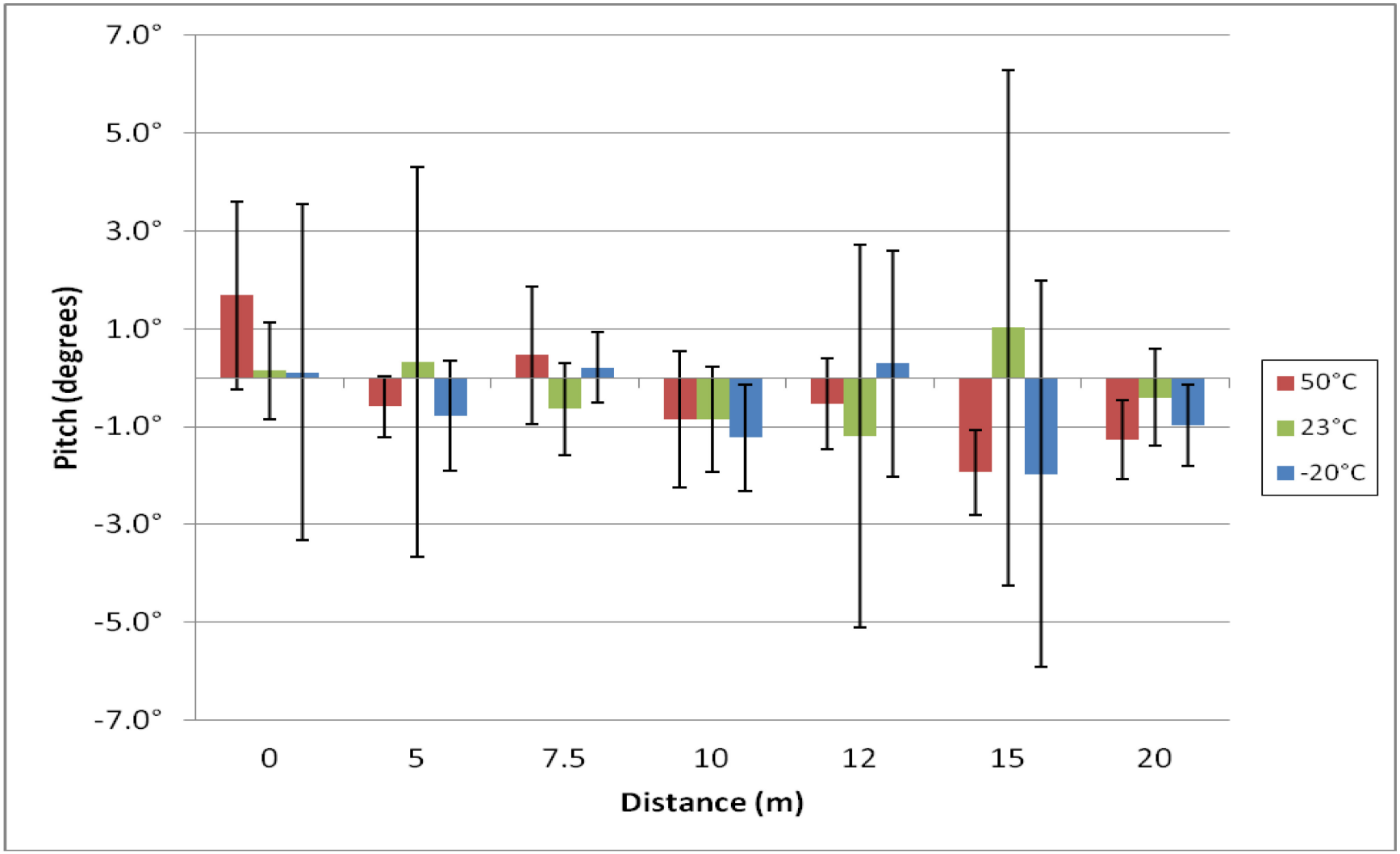

Figure 14 - XREP (50°C, 23°C and -20°C) Pitch by Distance

4.7.2 Accuracy and Precision

The average results for velocity and impact location are tabulated below in Table 11. The accuracy data were plotted for each temperature. Accuracy data for rounds fired at 50°C, 23°C (Task 6), and -20°C were plotted in Figure 15, Figure 16, and Figure 17, respectively. For the statistical analysis of the velocity and accuracy data, the results for the 50°C rounds and the -20°C rounds were compared to the rounds tested at room temperature 23°C in Task 6 using an ANOVA. If significant differences were measured with the ANOVA then the data were analyzed using post hoc tests; Fisher's LSD tests if the data was parametric or Games-Howell tests if the data was nonparametric. The level of significance was $p \leq 0.05$ for all tests.

First, the effect of distance within temperature groups was determined statistically. For the 50°C tests, the velocity at 20 m was statistically lower than velocities for all other distances. The X coordinate value at 20 m was significantly more left of the point of aim than all other distances. The differences in Y coordinate values at each distance were significantly different from all other distances. The vertical drop from the point of aim was lower for each consecutively longer distance.

For the -20°C tests, the velocities at 5 m and 10 m were both statistically higher than the velocities at 15m and 20 m. There was no statistically significant difference in the X coordinate data between any groups. The differences in Y coordinate values at each distance were significantly different from all other distances. The vertical drop from the point of aim was lower for each consecutively longer distance.

Next, the effect of temperature within distance groups was determined statistically. For the 5 m distance, there was no statistically significant difference between any of the measured variables.

For the 10 m distance, the velocity at 50°C was statistically higher than that at 23°C. The rounds tested at 50°C impacted significantly more right of the point of aim than rounds tested for Task 6 at 23°C. There was no statistically significant difference in the Y coordinate data between any groups.

For the 15 m distance, there was no statistically significant difference between any of the measured variables.

For the 20 m distance, there was no statistically significant difference between the velocity data. . The rounds tested at both 50°C and -20°C impacted significantly more right of the point of aim than rounds tested for Task 6 at 23°C. Rounds tested at both 50°C and -20°C showed significantly less vertical drop than rounds tested for Task 6 at 23°C.

For the 50°C tests, the diameter of the COP for the rounds fired at 5 meters was 6.95 cm. Precision improved at 10 meters and the diameter of the COP was 2.19 cm. The diameter of the COP was 6.64 cm. At 20 meters the diameter of the COP was 6.75 cm. The general trend of the rounds was downward with increasing distance.

For the -20°C tests, the diameter of the COP for the rounds fired at 5 meters was 8.01 cm. Precision improved at 10 meters and the diameter of the COP was 3.70 cm. The diameter of the COP was 14.59 cm. At 20 meters the diameter of the COP was 19.91 cm. The general trend of the rounds was downward and decreasing precision with increasing distance.

Table 11 - Accuracy results from temperature-tested XREPs

Temperature (°C)	Distance (m)	Velocity (fps)	X Coordinate (cm)	Y Coordinate (cm)	COP (cm)
50	5	223.7 ± 6.9	0.90 ± 2.59	-1.20 ± 0.95 †	6.95
	10	218.1 ± 6.1 ‡	1.64 ± 1.07 ‡	-5.98 ± 1.31 †	2.19
	15	211.9 ± 5.9	3.09 ± 3.47	-19.59 ± 3.51 †	6.64
	20	197.36 ± 25.9 †	-2.21 ± 2.95 †	-31.90 ± 3.12 †	6.75
23	5	221.6 ± 8.5	0.63 ± 1.50	0.43 ± 1.98	7.42
	10	209.4 ± 7.3 ‡	-1.34 ± 2.14 ‡	-5.41 ± 2.21	8.88
	15	201.8 ± 15.0	0.93 ± 2.15	-17.28 ± 5.43	30.04
	20	200.2 ± 5.6	-11.86 ± 4.69 *	-51.37 ± 4.79 *	20.38
-20	5	221.5 ± 7.3 ^	0.51 ± 2.44	-1.77 ± 2.96 †	8.01
	10	216.0 ± 8.6 ^	0.10 ± 2.12	-6.93 ± 1.33 †	3.70
	15	200.6 ± 15.4	1.54 ± 5.03	-17.91 ± 5.20 †	14.59
	20	193.3 ± 18.2	1.85 ± 7.13	-29.69 ± 10.23 †	19.91

† statistical significance ($p \leq 0.05$) between all other distances at the same temp.

^ statistical significance ($p \leq 0.05$) between this value and values at 15m & 20m at the same temp.

*** statistical significance ($p \leq 0.05$) between all other temperatures at the same distance**

‡ statistical significance ($p \leq 0.05$) between two temperatures at the same distance

The velocity at the target tends to decrease as the distance from the target increases. This is an expected trend that is due primarily to the drag created by the fins. The fins convert the forward velocity into rotational velocity, slowing down the projectile. The X coordinate values for rounds did not show a general trend dependant on the distance from the target. The Y coordinate values decreased as the distance from the target increased. The change in Y coordinate accuracy follows an expected trend due to gravitational forces. The projectile drops at a constant rate. The slower the projectile is traveling, the greater the amount of vertical drop as shown in the graphs on the following pages (Figure 15-Figure 17).

While some of the velocity values of the rounds decreased as temperature decreased, few of these trends were significant. Neither the X coordinate nor the Y coordinate values of the rounds showed significant trends dependent on temperature. Overall the rounds tested at 50°C showed smaller circles of precision indicating less deviation in both X and Y coordinates. All raw data and statistical values can be found in Annex G.

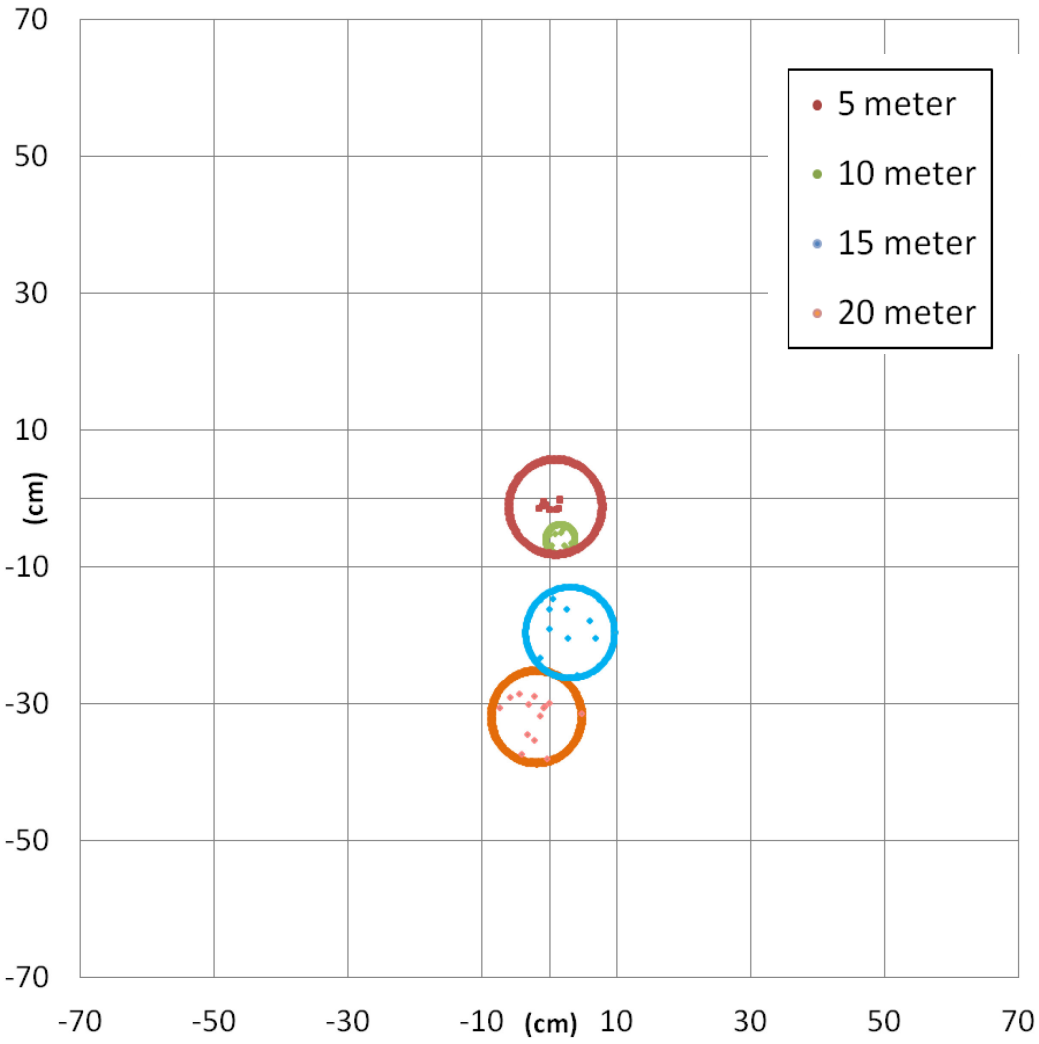

Figure 15 - XREP Accuracy and Precision at 50°C

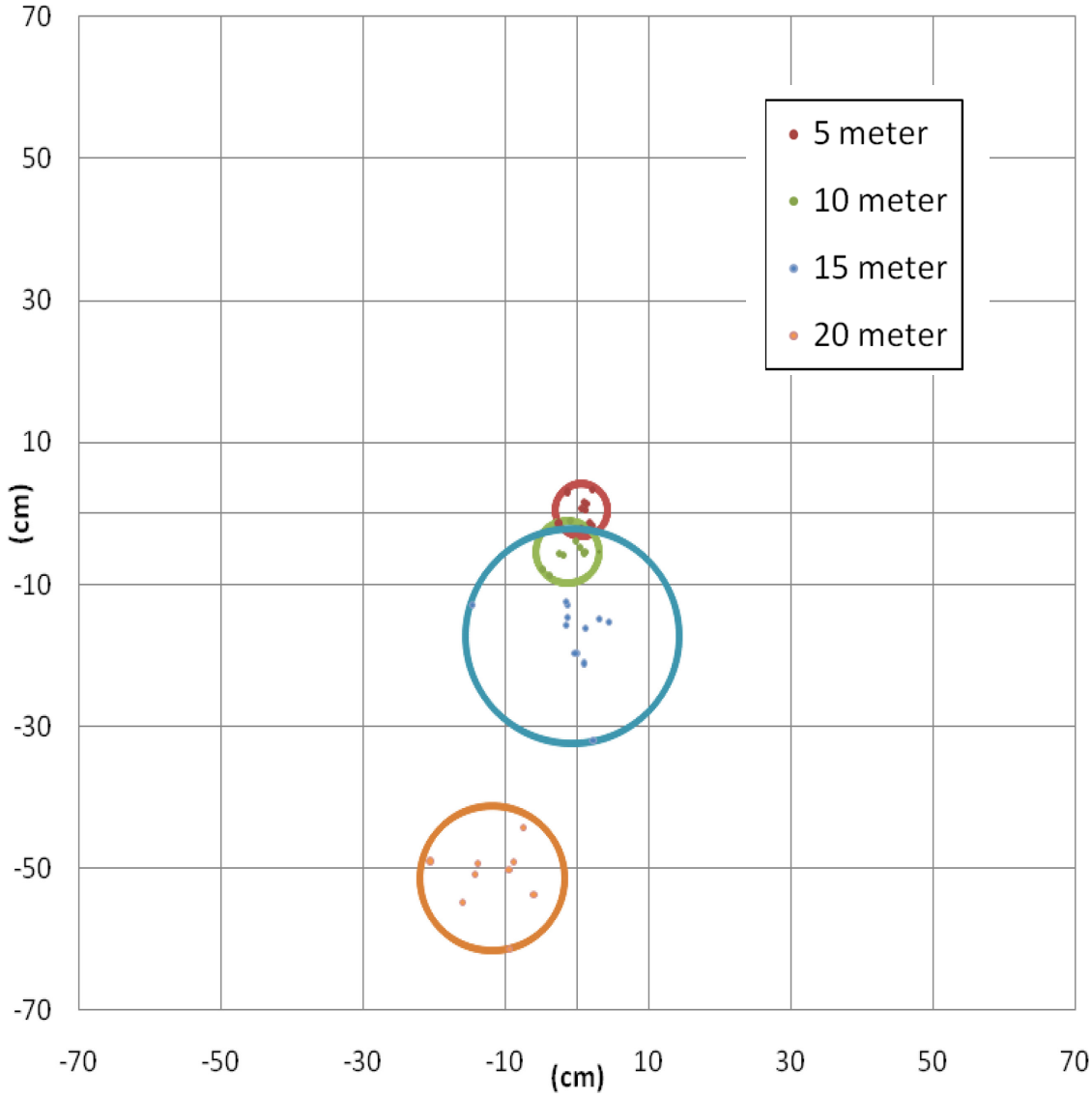

Figure 16 - XREP Accuracy and Precision at 23°C

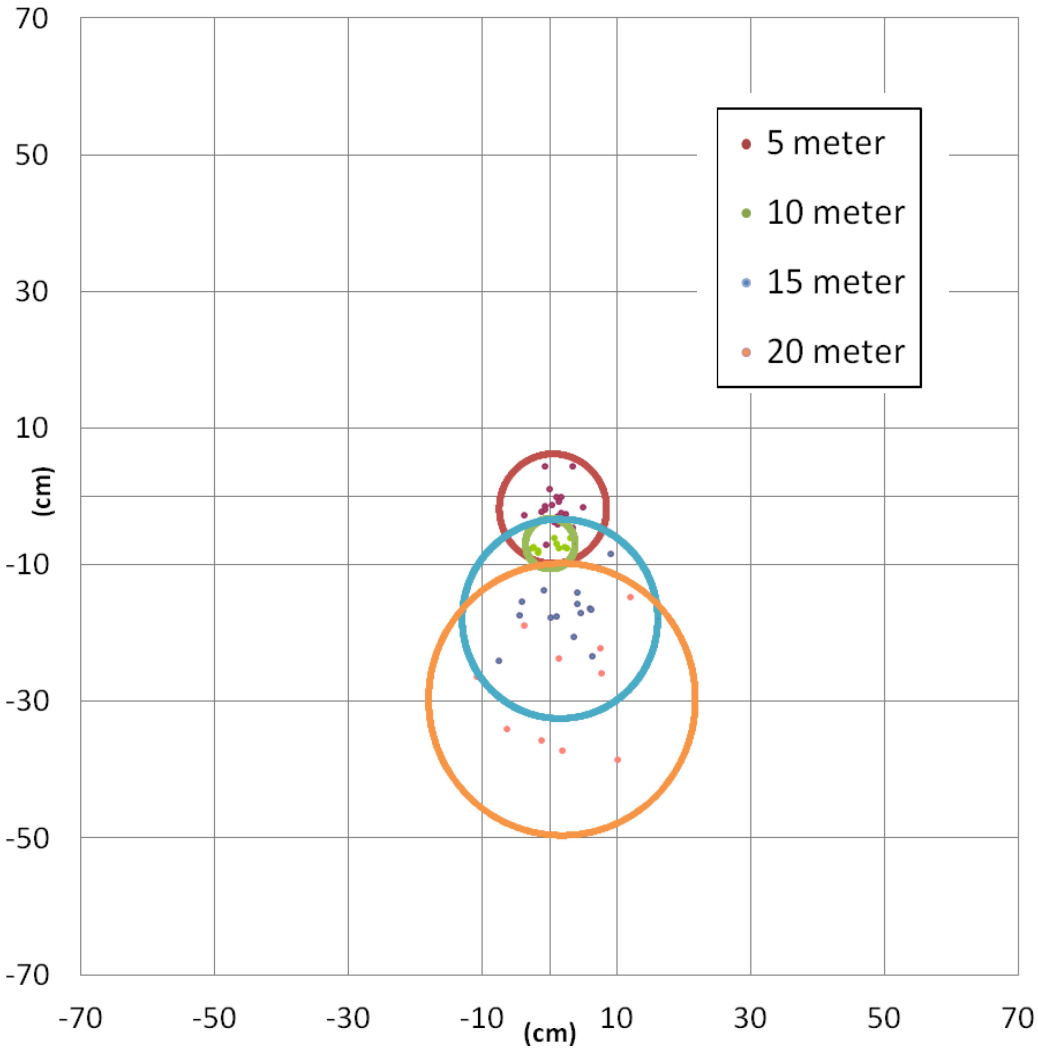

Figure 17 - XREP Accuracy and Precision at -20°C

4.8 Task 8 Risk of Penetration

Penetration testing may result in one of three outcomes (no injury, laceration of the LAL, perforation of the PAL). At 2 meters 100% of the rounds perforated the PAL. At 5 meters 90% of the rounds perforated the PAL. The design of the projectile is such that the chassis should separate from the nose section upon impact. Chassis separation occurred in 80% of the impacts at 2 meters and 60% at 5 meters. All raw data and statistical values can be found in Annex H.

Table 12 - Results of the penetration testing

Distance (m)	Velocity (fps)	Mass (g)	Chassis Separation	Outcome		
				No Injury	Laceration	Perforation
2	233.1 ± 13.0	18.54 ± 0.08	80%	0	0	10
5	236.1 ± 11.4	18.62 ± 0.07	60%	0	1	9

4.9 Task 9 Risk of Blunt Trauma

Blunt trauma testing was carried out at 2 meters to assess if there was a need to test at further distances. Based on the results of the 2 meter testing no additional testing was completed. The data displayed in table 3 show the average VC_{max} value is 0.0616 m/s. The maximum VC_{max} value recorded was 0.0754 indicating a minimal risk of injury by blunt trauma. The 10^{th} shot impacted in the center of the test surrogate but the top rib reported a VC_{max} value of 59.57. This data point was removed from analysis due to an error in the software. All raw data and statistical values can be found in Annex I.

Table 13 - Results from blunt trauma testing

Velocity (fps)	Mass (g)	Avg. Max. Deflection (mm)	VC_{max} (m/s)
230.4 ± 6.1	18.50 ± 0.06	6.21 ± 0.489	0.0616 ± 0.0127

4.10 Task 10 Assessment of XREP Training Round

In-Flight Aerodynamics
The aerodynamics of training rounds fired at 5 10 and 15 meters were recorded by a proximal camera and by a target camera (0, 5, 7.5, 10, 12 and 15 meters respectively). The aerodynamics of training rounds fired at 20 meters were recorded at the target distance.

Table 14 - Results of in-flight aerodynamics test

Distance (m)	Pitch (Deg)	Rotations (RPS)
0	-0.2° ± 3.9°	64.2 ± 45.2 †
5	-0.2° ± 3.4°	210.7 ± 15.6 †
7.5	-1.1° ± 0.9°	276.3 ± 33.9 †
10	0.7° ± 0.7°	313.0 ± 31.0 ‡
12	-2.1° ± 1.7°	321.6 ± 20.0 ‡,¥

15	0.0° ± 1.6°	341.0 ± 19.0 ¥,₮
20	-1.4° ± 1.2°	342.1 ± 9.4 ₮

† indicates a statistically significance difference (P≦0.05) to all other distances
‡, ₮, ¥ indicate a statistically significance difference (P≦0.05) between all groups except those marked

An ANOVA statistical analysis was performed to determine if statistical differences were present. A Fischer's LSD or Games Howell test was performed post hoc to determine which groups showed statistical differences. The rotations per second measured at 0, 5, and 7.5 meters were significantly different from the rotations measured at all other distances. The rotations per second at 10 meters were different from rotations measured at all other distances except 12 meters. The rotations per second at 12 meters were different from rotations measured at all other distances except 10 and 15 meters. The rotations per second at 15 meters were different from rotations measured at all other distances except 12 and 20 meters. Lastly, the rotations per second at 20 meters were different from rotations measured at all other distances except 15 meters. The rotational data follows an expected trend. As the projectile exits the barrel, the initial rotational velocity is due to the rifling of the X12 barrel that engages the projectile as it travels through the barrel. After the projectile exits the barrel and the fins have opened they begin to increase the rotational velocity (Figure 18). No statistical differences in pitch were present at any other distances (Figure 19). The level of significance was $p \leq 0.05$ for all tests.

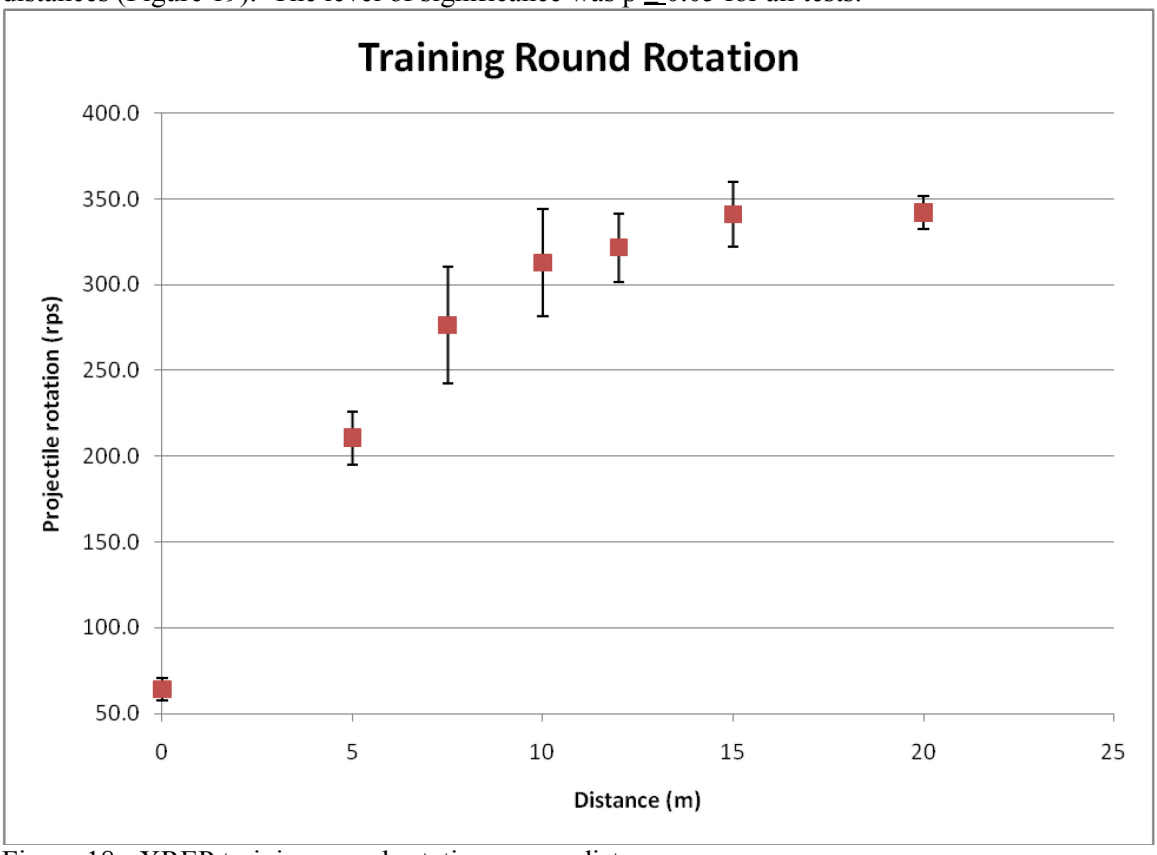

Figure 18 - XREP training round rotation versus distance

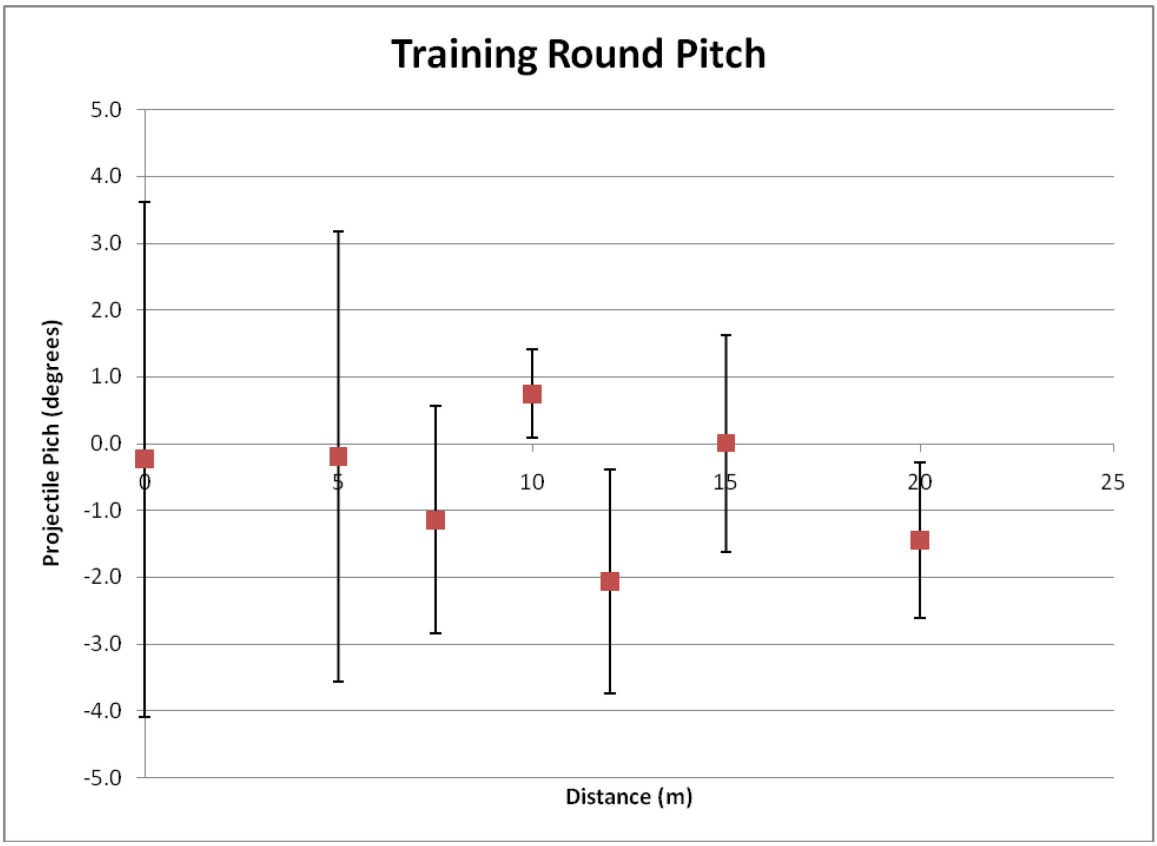

Figure 19 - XREP Training round pitch versus distance

4.10.1 Accuracy and Precision

The average results for velocity and impact location are listed below in Table 15. The diameter of the COP for the 10 rounds at 5 meters was 7.99 cm. The diameter of the COP for the 10 rounds fired at 10 meters was 17.03 cm. The diameter of the COP for the rounds at 15 meters was 28.94 cm and at 20 meters the diameter of the COP was 28.57 cm. The general trend of the rounds was downward and to the left of the point of aim with increasing distance.

Table 15 - Average values from accuracy testing

Distance (m)	Velocity (fps)	X Coordinate (cm)	Y Coordinate (cm)	COP Diameter (cm)
5	240.8 ± 10.5 †	-1.9 ± 1.1 ‡	-3.6 ± 1.7 †	7.99
10	231.8 ±11.6 ‡	-3.6 ± 1.6 ‡	-11.9 ± 3.9 †	17.03
15	228.2 ± 8.4 ‡	-7.5 ± 4.9 †	-23.5 ± 5.6 †	28.94
20	217.8 ± 10.4 †	-11.7 ± 4.8 †	-46.5 ± 5.6 †	28.57

† indicates a statistical significance (P≦0.05) to all other distances
‡ indicates a statistical significance (P≦0.05) between all groups except those marked

The velocities at the 5 and 20 meter distances were significantly different from the velocities measured at all other distances. Additionally, the velocities measured at 10 and 15 meters were significantly different from the velocities measured at all other distances except when compared to each other. The X coordinate values for rounds fired at 15 and 20 meters were significantly different from rounds fired at all other distances. Whereas the X coordinates measured at 5 and 10 meters were significantly different from the X coordinates measured at all other distances except when compared to each other. The Y coordinate values for rounds fired at each distance were significantly different from all other distances (Figure 20). The level of significance was $p \leq 0.05$ for all tests.

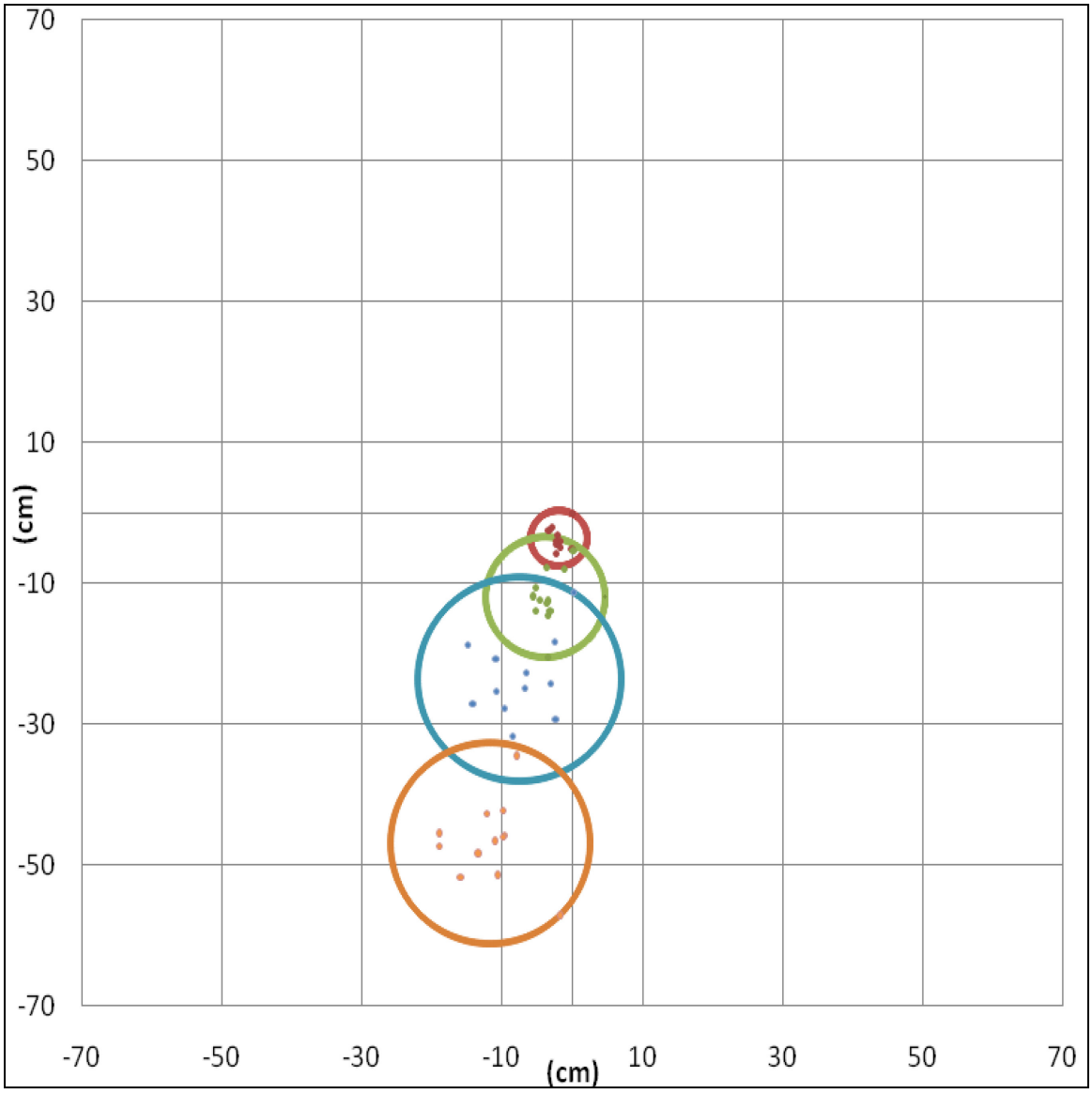

Figure 20 - XREP training round Accuracy and Precision

4.10.2 Comparison to XREP IIa

A student's T-test was used to compare the variables measured for the training round against the XREP IIa (Tasks 4 & 6). The variables that were compared were those measured for the assessment of accuracy, precision and in-flight aerodynamics. Table 16 shows the results of the comparisons. Statistically significant differences are shaded. Rotation was significantly different at all distances except 5 meters. Pitch was significantly different only at the 10 meter distance. Velocity was significantly different at all but the 15 meter distance. The X coordinate was significantly different at all distances but 20 meters and the Y coordinate was significantly different at all distances (Table 16). All raw data and statistical values can be found in Annex J.

Table 16 - Comparison of average values for the XREP IIa and the XREP training round

Distance (m)	Projectile	Velocity (fps)	X Coordinate (cm)	Y Coordinate (cm)	Pitch (Deg)	Rotations (RPS)
0	Trainer	N/A	N/A	N/A	-0.2° ± 3.9°	64.2 ± 45.2
	XREP	N/A	N/A	N/A	0.1° ± 1.0°	126.0 ± 45.2
	P-value	N/A	N/A	N/A	0.77161	0.00287
5	Trainer	240.8 ± 10.5	-1.9 ± 1.1	-3.6 ± 1.7	-0.2° ± 3.4°	210.7 ± 15.6
	XREP	221.6 ± 8.5	0.63 ± 1.5	0.43 ± 1.9	0.3° ± 4.0°	182.7 ± 46.4
	P-value	0.00028	0.00039	0.00012	0.75819	0.08703
7.5	Trainer	N/A	N/A	N/A	-1.1° ± 0.9°	276.3 ± 33.9
	XREP	N/A	N/A	N/A	-0.6° ± 0.9°	197.4 ± 25.3
	P-value	N/A	N/A	N/A	0.44231	0.00002
10	Trainer	231.8 ±11.6	-3.6 ± 1.6	-11.9 ± 3.9	0.7° ± 0.7°	313.0 ± 31.0
	XREP	208.6 ± 7.4	-1.17 ± 2.1	-5.46 ± 2.1	-0.8° ± 1.1°	218.4 ± 16.8
	P-value	0.00002	0.00686	0.00013	0.00104	0.00000
12	Trainer	N/A	N/A	N/A	-2.1° ± 1.7°	321.6 ± 20.0
	XREP	N/A	N/A	N/A	-1.2° ± 3.9°	218.4 ± 53.9
	P-value	N/A	N/A	N/A	0.51725	0.00002
15	Trainer	228.2 ± 8.4	-7.5 ± 4.9	-23.5 ± 5.6	0.0° ± 1.6°	341.0 ± 19.0
	XREP	197.0 ± 20.0	-0.44 ± 4.7	-16.94 ± 5.3	1.0° ± 5.3°	221.0 ± 88.6
	P-value	0.30419	0.00126	0.00640	0.54959	0.00044
20	Trainer	217.8 ± 10.4	-11.7 ± 4.8	-46.5 ± 5.6	-1.4° ± 1.2°	342.1 ± 9.4
	XREP	195.8 ± 14.9	-9.85 ± 7.7	-51.25 ± 4.5	-0.4° ± 1.0°	278.5 ± 15.4
	P-value	0.00060	0.50103	0.04578	0.06987	0.00000

4.11 Task 11 Physiological Effects (Swine Model)

A total of five specimens were used to measure the cardio-physiological effects of a single XREP exposure. The average mass of the specimens was 49.44 ± 4.46 Kg. All five specimens used for this task survived for the entire duration of the exposure and monitoring period. The average and standard deviations for the electrolyte levels are reported below in Table 17. Shaded areas indicate data that is outside of normal physiological ranges as reported by Hannon et al [13].

Table 17 - Average physiological levels during and after XREP exposure

		Baseline	Post-Exposure	1 hour	2 hour	3 hour	4 hour
PO2 (mmHg)	Avg.	315.40	318.60	345.60	388.80	369.40	336.20
	Std. Dev.	64.84	66.91	64.12	46.31	92.62	77.39
PCO2 (mmHg)	Avg.	46.88	79.60	48.18	45.74	44.14	44.28
	Std. Dev.	4.29	12.62	3.67	4.80	5.27	6.09
HCO3 (mMol/L)	Avg.	28.06	26.40	29.38	30.74	30.96	31.50
	Std. Dev.	2.72	3.11	4.30	2.75	3.33	3.17
pH	Avg.	7.39	7.13	7.39	7.44	7.45	7.46
	Std. Dev.	0.05	0.12	0.05	0.06	0.05	0.05
Lactate (mMol/L)	Avg.	0.60	7.90	1.09	0.50	0.54	0.51
	Std. Dev.	0.19	3.08	0.53	0.13	0.13	0.13
Potassium (mMol/L)	Avg.	4.18	4.62	4.56	4.56	4.56	4.58
	Std. Dev.	0.13	0.41	0.25	0.15	0.13	0.23
Sodium (mMol/L)	Avg.	139.40	142.20	138.40	137.80	136.40	137.80
	Std. Dev.	1.95	4.27	4.39	2.77	2.70	2.86
Hematocrit (% PCV)	Avg.	24.20	27.40	23.60	22.00	21.20	21.20
	Std. Dev.	2.86	3.05	3.21	1.41	1.48	0.84
Hemoglobin (g/dL)	Avg.	8.26	9.32	8.04	7.50	7.20	7.20
	Std. Dev.	0.98	1.05	1.11	0.49	0.49	0.30
Cardiac Output	Avg.	4.93	6.81	4.66	4.17	4.00	3.76
	Std. Dev.	0.51	1.90	0.70	0.78	0.54	0.64
Heart Rate (BPM)	Avg.	84.50	96.80	76.40	67.20	63.60	60.40
	Std. Dev.	23.33	21.02	19.71	13.70	8.65	4.88
Mean Arterial Pressure (mmHg)	Avg.	89.50	78.80	80.20	77.20	73.00	74.20
	Std. Dev.	16.26	8.93	6.30	5.45	6.20	5.26
Temperature (°C)	Avg.	38.00	38.31	37.94	37.75	37.64	37.76
	Std. Dev.	0.01	0.14	0.30	0.33	0.43	0.23

The ECG data from two of the specimens showed no abnormal electrical activity. An additional two specimens showed a few (less than five each) premature ventricular contractions. These abnormal events are not uncommon and are not a cause for concern. The fifth specimen developed an arterial arrhythmia approximately ten minutes after the XREP exposure. The arrhythmia appeared to be two competing p-waves, each controlling the heart rate switching from ~83 beats per minute (bmp) to about 98 bpm (Figure 21). The p-waves and heart rate alternated back and forth for approximately 4 minutes before the arrhythmia resolved. There were no other abnormalities with this specimen and the arrhythmia did not affect the duration of the experiment, the specimen was able to persist for the entire four hour monitoring period. All raw data and statistical values can be found in Annex K

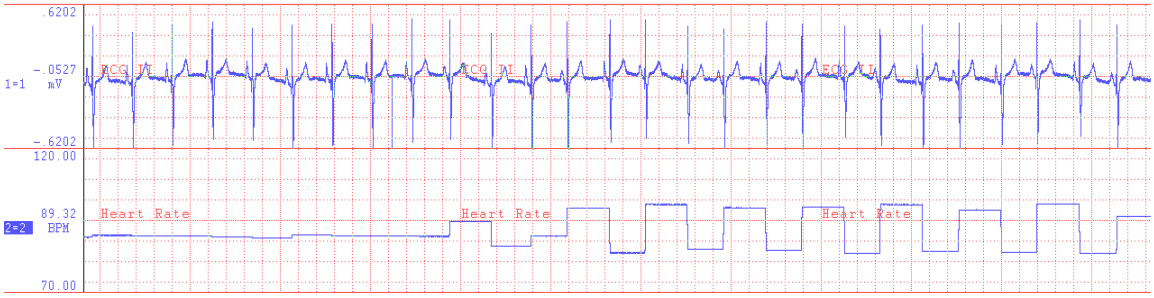

Figure 21 - ECG of onset of alternating P-waves and heart rate

5 Discussion

The XREP rounds shipped to WSU in four batches in the fall/winter of 2010/11 were sent as production rounds as TASER was "ramping up" the manufacturing process. TASER notified WSU that the XREP round may undergo further redesigns but that the current round was representative of the currently available production round.

The physical dimensions of the XREPs tested are within the manufacturers reported values [14] for length. The mass of the projectile was found to be 0.2 grams more than manufacturer's specification. One potential cause of this discrepancy may be the inclusion of the insulated tether that prevents the round from electrical discharge. This tether was included in the measurements for mass for safety reasons. Most measured physical variables had standard deviations of less than 1% indicating a repeatable manufacturing process. The mass of the projectile was found to be 0.2 grams more than manufacturer's specification.

The mechanism by which the nose separates from the chassis was changed in the current version. Previous versions of the projectile seem to have used fracture pins that separated when some pre-determined amount of compressive force or deflection was reached. The current version of the XREP uses a shearing fracture pin design. A ring with six pins is attached on the inside (nose) end of the chassis. These pins fracture when a pre-determined torque or amount of rotation is applied to the chassis while the nose is held in place. The average maximum torque and angle at which it was applied seem to have more variability based on the higher standard deviations (8% and 22%).

The electrical outputs of the XREPs tested are within the manufacturer's reported values [14] for pulse rate (PPS) and duration. The differences measured in pulses per second between the two discharge paths were statistically significant but both values are within the manufacturer's specified range of 18-22 pulses per second (Figure 22). The voltage of the projectile was found to be ~25 volts less than manufacturer's specification. One potential cause of this discrepancy may be the use of a 600 ohm resistor as opposed to the 2000 ohm resistor specified by the manufacturer. The 600 ohm resistor was used intentionally to allow for comparison of data collected on other ECDs which are typically tested with a 600 ohm load.

The shape of the XREP waveform is a simple triangular wave superimposed on a square wave (Figure 23). This simple shape allows for the relatively low sampling rate of 1 mega sample (10^6) per second. It should also be noted that the data shown in figures 15 and 16 was recorded with a 1:100 high voltage probe. The values in the figures are actually $1/100^{th}$ of the recorded values.

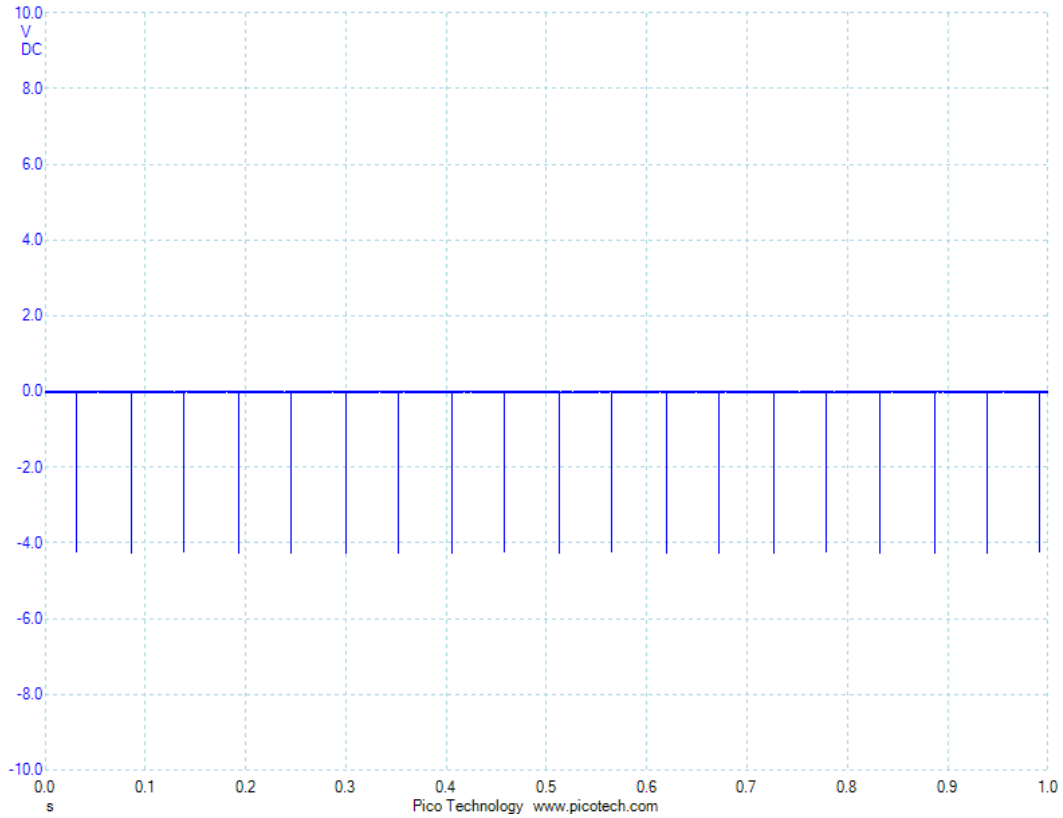

Figure 22 - Example of XREP pulse rate

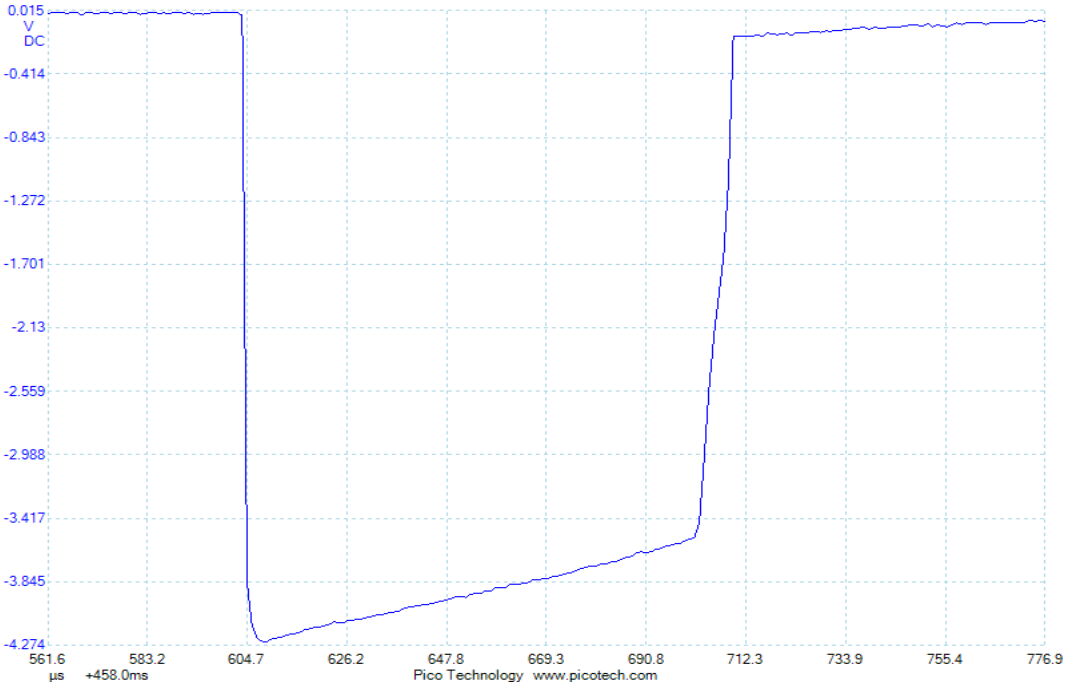

Figure 23 - Example of XREP waveform

Two of the rounds tested (rounds 4 and 5) in the front to rear discharge path showed lower peak voltages, lower currents, longer pulse durations and higher charge per waveform (although still with the manufacturer's specifications). The reason for these two anomalies is not readily apparent. The test setup remained constant and the rounds were all tested on the same day in the same environmental conditions. These data are listed in appendix B.

All of the XREPs tested electrically demonstrated an unexpected pattern of missing waveforms. After five seconds of electrical activity the XREP would skip (1-5) waveform(s). This pattern was very repeatable and would occur after every five second of electrical activity (Figure 27 in Appendix F). The reason for this behavior is not readily apparent although it may be due to some portion of the algorithm that is used in the XREP descending from an older ECD with a five second duration. Pulses per second were recorded by counting the number of waveforms for each of the 20 oscilloscope memory buffers (each buffer was 1 second in duration). Every fifth buffer would have fewer pulses due to the pattern of dropped pulses leading to a lower overall PPS value for each round.

Electrical out testing was initially sub-contracted to the University of Carleton in Ottawa, Ontario. Twenty rounds were shipped to the Ottawa police department for this testing. This group determined which probes were carrying the electrical signal and helped to define the appropriate test parameters to report. No output was measured for nine of the twenty rounds. Four of the rounds were believed to have previously been fired (perhaps during removal from the shell), three of the nine rounds were determined to be dead on arrival, 2 rounds were mis-configured (Probe was attached to the wrong front barb) during data collections. Due to insufficient data from the Carleton testing, WSU repeated the data collection. It should be noted that all of the rounds tested for Task 2 and Task 5 produced an electrical output. The final report from the Carleton University testing can be found in Appendix F.

Drop testing showed that dropping the XREP in a vertical orientation created significantly more damage that dropping the XREP horizontally, regardless of the temperature. Rounds dropped vertically were damaged at an average height of 1.5 meters which is well within a normal operational height. It is important to clarify that the damage noted (usually projectile motion relative to the cartridge) was visible upon inspection but did not affect the ability to fire the XREP.

The rounds tested for durability, regardless of drop orientation or temperature, showed significantly more vertical drop from the point of aim then the rounds tested in Task 6 which was used as a baseline measurement. This trend was true at all distances but only statistically significant for the 5 meter and 10 meter distances. One would expect the velocity to follow a similar trend, however, the opposite trend exists and velocity was higher for the Task 3 rounds. The same accuracy test methodology was followed for Task 3 and Task 6 but the testing was performed on different days and under potentially different atmospheric conditions.

The pitch of the round is stable at all distances and there was no statistically significant difference in pitch at any distance measured. The one caveat to the pitch is that the round did, on several occasions, separate from the chassis in flight and become unstable. During these instances it was not possible nor practical to measure the pitch or rotational rate. However, it should be noted that these rounds were not stable and tumbled in flight. Rounds separated in-flight in 4/46 (8.69%) of the shots.

There were several shots that did not produce a complete data set (missing velocity, video or accuracy data). These missing data were due to a variety of reasons. Velocity data is missing if the round impacted the chronograph ("hit chrono" in raw data), if the chronograph was not reset, if the chronograph failed to record the velocity ("error") or if the projectile had separated in flight ("Open"). In these instances, in-flight aerodynamics would still be measureable, as well as accuracy if the round did not impact the chronograph. Video data is missing if the round traveled above or below the field of view ("No video"), if the projectile broke open ("Open"), if the projectile impacted the chronograph ("Hit chrono"), or if the cameras did not trigger ("No video"). Accuracy data is missing if the round failed to impact the target paper either because it impacted the chronograph ("NA") or if the projectile had separated in flight ("Open").

The rounds tested for electrical activity after impact all showed signs of electrical activity even when the data set was incomplete. One interesting finding from this testing was that at 2 meters there were no separations of the nose from the chassis. The rounds penetrated into the pork material on every shot. A similar trend was previously reported for the Task 8 penetration testing at the same distance. This distance is less than the recommended firing range of 5 meters but represents a real-world worst-case scenario that an end-user may experience.

The accuracy and precision of the round at distances of 10 meters or less are similar to other kinetic energy rounds. At longer distances the round loses velocity most likely due to the drag created by the stabilizing fins. The loss of velocity causes a significant drop in accuracy and precision. Almost all rounds fired at 20 meters showed a trend to the lower left of the point of aim. This trend was significantly different than the X coordinate for any other distance. This leftward trend may be caused by the curved fins that deploy to stabilize the round from tumbling.

The rounds stored at 50°C were found to be more precise (smaller circle of precision) than rounds stored at 23°C or -20°C. Statistical analysis of these data was not possible due to the sample size, however, the differences are apparent visually in Figure 15-Figure 17. The reason for this difference is not readily apparent. The tests at 50°C and at -20°C were completed on the same days so atmospheric conditions were the same.

The rounds tested for velocity after storage at 50°C and at -20°C both followed the same trend reported in the Task 6 data: decreasing velocities at greater distances. The velocities for the 50°C rounds were significantly lower at 20 meters when compared to all other distances. The larger standard deviation in velocities for rounds stored at -20°C reduced the significance of the differences between each distance. The velocities were significantly lower for the -20°C rounds at 15 meters when compared to 5 and 10 meters and for the -20°C rounds at 20 meters when compared to 5 and 10 meters.

The rounds tested for accuracy after storage at 50°C and at -20°C both followed the same trend reported in the Task 6 Y coordinate data; statistically significant increasing vertical drop at greater distances. Rounds stored at -20°C and fired at 5 and 10 meters had significantly more vertical drop than the rounds stored at room temperature.

The rounds tested for accuracy after storage at 50°C and at -20°C did not follow the trend reported in the Task 6 X coordinate data. There was no trend to either the right of left for the rounds stored at either 50°C or -20°C. Rounds stored at 50°C and at -20°C and fired at 20 meters impacted significantly less left (nearer to the point of aim) than the rounds stored at room

temperature. Previously it was suggested that the reason for the leftward trend may have been due to the fin shape but the same fins did not cause the same leftward trend for the 50°C and at -20°C rounds. The reason for this trend is not readily apparent at this time although testing for Task 6 was completed on a different day and under potentially different atmospheric conditions.

There were several shots that did not produce a complete data set (missing velocity, video or accuracy data). These missing data were due to a variety of reasons. Velocity data is missing if the chronograph failed to record the velocity ("N/A"). In these instances, in-flight aerodynamics would still be measureable as well as accuracy. Video data is missing if the round traveled above or below the field of view ("OOV"), if the projectile broke open ("Open"), or if the cameras did not trigger ("NV"). Accuracy data is missing if the round failed to impact the target paper ("missed target") or if the projectile had separated in flight ("Open").

The rounds tested for pitch after storage at 50°C and at -20°C followed a similar trend reported in the Task 6 pitch data; the rounds were fairly stable in flight. Rounds stored at 50°C and measured as they left the muzzle had significantly more upward pitch than rounds measured at any other distance. Rounds stored at 50°C and measured at 15 meters had significantly more downward pitch than rounds measured at 5, 7.5 and 12 meters, however, no average pitch value at any temperature or distance was greater than ± 2°.

The rounds tested for rotation after storage at 50°C and at -20°C followed a similar trend reported in the Task 6 rotation data and the rotational rate increases at greater distances.

The one caveat to the pitch is that the round did, on several occasions, separate from the chassis in flight and become unstable. During these instances it was not possible nor practical to measure the pitch or rotational rate, however it should be noted that these rounds were not stable and tumbled in flight. Rounds separated in-flight in 12/108 (11.11%) of the shots. This is slightly more often than with the rounds tested in Task 6. Half of the twelve rounds that opened did so during the -20°C testing at 5 meters. There was no apparent reason for this anomaly.

The probability of injury testing performed on the XREP round indicated that the round has a low probability of causing a blunt thoracic injury. However, while kinetic energy rounds are generally fired at the thoracoabdominal region, if the round were to strike the head or neck, the risk of injury is much greater. The round showed a high likelihood of perforation at close ranges. It is difficult to surmise how much of the perforation is "by design" with penetration of the barbs into the skin. The penetration surrogate was developed with any perforation (invagination) of the PAL being classified as a penetration. This kinetic energy projectile is unlike others due to the barbed front which is needed for the NMI effect. Penetration testing at greater distances may provide additional insights into penetration risks at tactical distances.

The training round has a higher velocity at all distances and a greater vertical drop at all distances except the farthest distance of 20 meters. This could be due to the training round having a greater mass. The training round was shown to have statistically significant differences in most of the measured variables and may not represent the actual characteristics of the XREP IIa. Ultimately it will be up to the end user to determine if the differences shown in this work are merely statistical differences or functional differences that will affect their training and preparedness.

The differences that exist between the physiological data collected for this study and the normal physiological values fall into two main categories; differences due to the exposure (parameters that moved outside of normal values after the exposure) and differences due to the population (parameters that remained outside of the normal range for the entirety of the experiment). Differences due to the exposure are similar to data presented by others for swine that are exposed to conducted energy device [10-12]. Differences for the duration of the experiment may be due to differences in the size of the animals used for this study and what are reported by Hannon et al. [13]. The values reported in this report are similar to differences reported previously for the same size animal [15].

5.1 Potential Sources of Error

The assumption that all batches have identical properties is based on information provided by the supplier. Each projectile has a unique six digit identifier and these numbers do not seem to be lined to the batch in any way. If the batches do differ in some way then this would be a source of potential error.

Physical parameters were measure with digital calipers with a limited resolution. The accuracy of the recorded values were limited by the resolution and as such are a source of potential error.

The torque and angular data were collected with a custom fixture that engaged the four front barbs. This fixture was built to accept the front barbs into four holes and these holes needed to be of a sufficient diameter to accept the barbed part as well as the shaft. This design allowed for a small about of motion (~1º) between the nose and fixture and may be a source of potential error.

The electrical activity was recorded using a computer based oscilloscope. One shortcoming of this device is that some amount of the waveform (~50 ms) is "lost" while the software switches memory buffers. This means that it was possible that some waveforms were missed and the recorded duration of the XREP discharge is missing some amount of time (~1 second). These are two known sources of error.

The resistance of the 600 ohm resistor was checked before and after each test to ensure that the values were consistent, however, the resistance may have varied during the exposure which would be a source of potential error.

Accuracy data was collected using paper targets. The exact center point of the impact was difficult to determine in some cases because the paper targets were torn. In these cases, the targets were re-assembled which would be a source of potential error.

Care was taken to ensure that pitch and rotation were measured at the same point in the video for each round but this was not possible on every video and this may be been a source of potential error.

Variations in the temperature and humidity in the lab could also be a potential source of error. The thermostat in the lab is set to a fixed temperature but the lab is a large space and temperature gradients are possible. The ventilation system used to remove lead from the air provides a laminar flow but also creates a potential source of error.

The penetration surrogate utilizes ballistic ordnance gelatin which is determined, in part, by the molecular weight of the collagen fibers. This molecular weight is likely a range of weights and could be a potential source of error. The preparation of the ordnance gelatin requires thoroughly mixing several kilograms of powdered gelatin into distilled water. Any heterogeneity in the mixture could be a possible source of error. The penetration surrogate is calibrated before and after it is used to ensure it has the proper resistance to penetration however temperature fluctuations could provide a source of error in the testing.

Measurements recorded with three rib surrogate used for blunt injury assessment could vary slightly depending on exact impact location. If a round impacted in between the ribs of the surrogate this could provide a source of potential error. This situation is representative of the actual outcome one would expect if the projectile impacted between a target's ribs.

Measurements taken on live animals provide an instantaneous value of a potentially dynamic metric. Changes in physiological parameters of interest occur continuously and as such each measurement only represents a "snapshot" of the whole picture. If changes in key parameters occur outside the window of measurement then those changes may go unnoticed. This would be a potential source of error.

Heart rate and mean arterial pressure measurements were taken after the blood draws for electrolyte and blood gas measurements (which were taken at exactly 1 hour intervals). The amount of time for the hemodynamics to return to pre-blood draw levels was not constant and as such this is a known source of error.

6 Conclusions

The XREP represents an impressive step forward in conducted energy devices. The ability to deploy a conducted energy device at a greater distance allows law enforcement and military personnel the ability to incapacitate a dangerous subject before they are close enough to do harm. The XREP round appears to have similar aerodynamics to other kinetic energy rounds at distances of less than 10 meters. The significant changes between the point of aim and point of impact create a specific set of challenges for training. The XREP training round appears to have several significant differences to the XREP. The injury data shows minimal risk of blunt trauma with the XREP but a very high risk of penetrating injury at close range. Additional testing at greater ranges would help to better define the risk of injury at tactical distances.

This report represents a full characterization of the TI XREP device. This device is not without merit but end-users and decision makers need to assess all aspects of the XREP testing to determine if the XREP meets their specific needs. This assessment was conducted to provide the end-user with the knowledge to make an informed decision. Wayne State University neither endorses nor condemns the XREP. It is recommended that the end-user take the above information in compliment with their existing knowledge and experience.

This page intentionally left blank.

References

1. TASER®. *TASER® X12™ by Mossberg®.* 2011 [cited 2011 03-02-2011]; Available from: http://www.taser.com/products/law/Pages/TASERX12.aspx.

2. Bir, C., D. Viano, and A. King, *Development of biomechanical response corridors of the thorax to blunt ballistic impacts.* J Biomech, 2004. **37**(1): p. 73-9.

3. Bir, C.A., *The Evaluation of Blunt Ballistic Impacts of the Thorax*, in *Mechanical Engineering*. 2000, Wayne State University: Detroit. p. 164.

4. Bir, C.A. and D.C. Viano, *Biomechanical predictor of commotio cordis in high-speed chest impact.* Journal of Trauma-Injury Infection and Critical Care, 1999. **47**(3): p. 468-473.

5. Bir, C. and D.C. Viano, *Design and injury assessment criteria for blunt ballistic impacts.* Journal of Trauma-Injury Infection and Critical Care, 2004. **57**(6): p. 1218-24.

6. Bir, C.A., S.J. Stewart, and M. Wilhelm, *Skin penetration assessment of less lethal kinetic energy munitions.* J Forensic Sci, 2005. **50**(6): p. 1426-9.

7. TASER®. *Response by Magne Nerheim, Taser International vice-president of research and development*. 2008 [cited 2011 11-20-2011]; Available from: http://www.cbc.ca/news/pdf/taser-reponse-to-cbc.pdf.

8. TASER®, *Taser® X26E Series Electronic Control Device Specification (Law Enforcement X26)*, Research&Development, Editor. 2009.

9. Gennarelli, T.A. and E. Wodzin, *The Abbreviated Injury Scale 2005. Update 2008.* 2008, Des Plaines, IL: American Association for Automotive Medicine (AAAM).

10. Jauchem, J.R., et al., *Acidosis, lactate, electrolytes, muscle enzymes, and other factors in the blood of Sus scrofa following repeated TASER exposures.* Forensic Sci Int, 2006. **161**(1): p. 20-30.

11. Dennis, A.J., et al., *Acute effects of TASER X26 discharges in a swine model.* Journal of Trauma-Injury Infection and Critical Care, 2007. **63**(3): p. 581-90.

12. Walter, R.J., et al., *TASER X26 discharges in swine produce potentially fatal ventricular arrhythmias.* Acad Emerg Med, 2008. **15**(1): p. 66-73.

13. Hannon, J.P., C.A. Bossone, and C.E. Wade, *Normal physiological values for conscious pigs used in biomedical research.* Lab Anim Sci, 1990. **40**(3): p. 293-8.

14. TASER®, *TASER® XREP™ Electronic Control Device (ECD) Specifications*, Research&Development, Editor. 2009.

15. Esquivel, A.O., et al., *The physiologic effects of a conducted electrical weapon in swine.* Ann Emerg Med, 2007. **50**(5): p. 576-83.

16. Viano, D.C. and I.V. Lau, *A viscous tolerance criterion for soft tissue injury assessment.* J Biomech, 1988. **21**(5): p. 387-99.

Annex A Task 1 Data

A.1 Physical Design Raw Data

Round #	Mass			Diameter		
	Total (g)	Nose (g)	Chassis (g)	Total (cm)	Nose (cm)	Chassis (cm)
1	18.50	1.46	17.04	1.82	1.89	1.63
2	18.52	1.45	17.09	1.82	1.92	1.63
3	18.57	1.48	17.10	1.81	1.90	1.63
4	18.55	1.45	17.10	1.81	1.91	1.64
5	18.49	1.45	17.04	1.82	1.87	1.63
6	18.52	1.46	17.06	1.82	1.89	1.65
7	18.53	1.45	17.08	1.83	1.89	1.63
8	18.56	1.45	17.11	1.82	1.95	1.63
9	18.52	1.45	17.07	1.83	1.96	1.63
10	18.57	1.46	17.10	1.81	1.86	1.63
Average	**18.53**	**1.46**	**17.08**	**1.82**	**1.90**	**1.63**
Stnd. Dev	**0.03**	**0.01**	**0.03**	**0.01**	**0.03**	**0.01**

Table A 1 - Mass and Diameters

Round #	Length				
	Total (cm)	Nose (cm)	Chassis (cm)	Front Barbs (cm)	Cholla Barbs (cm)
1	5.88	1.96	4.71	0.76	2.01
2	5.88	1.91	4.66	0.77	1.97
3	5.87	1.87	4.64	0.77	1.93
4	5.86	1.87	4.68	0.76	1.93
5	5.86	1.82	4.66	0.77	1.99
6	5.89	1.90	4.68	0.78	1.94
7	5.86	1.84	4.71	0.78	1.98
8	5.88	1.84	4.65	0.77	1.99
9	5.86	1.90	4.63	0.76	2.03
10	5.88	1.92	4.66	0.77	1.97
Average	**5.87**	**1.88**	**4.67**	**0.77**	**1.97**
Stnd. Dev	**0.01**	**0.04**	**0.03**	**0.01**	**0.03**

Table A 2 – Segment Lengths

Round #	Max. Shear Torque (N*m)	Angle @ Max Torque (°)
1	0.66	17.55
2	0.60	did not fail
3	0.67	17.48
4	0.55	15.78
5	0.64	21.37
6	0.60	13.78
7	0.54	10.44
8	0.57	16.99
9	0.61	22.37
10	0.53	13.38
Average	**0.597**	**16.57**
Stnd. Dev	**0.049**	**3.79**

Table A 3 - Maximum torque and angle at separation

Annex B Task 2 Data

B.1 Electrical Output Raw Data

Discharge Path	Average Buffer Peak Voltage (v)	Average Buffer Peak Current (a)	Average Waveform Charge (μC)	Average Pulse Rate PPS
Front to Front	425.483	0.719	74.221	18.429
Front to Front	423.332	0.716	71.713	18.450
Front to Front	428.649	0.725	69.073	18.550
Front to Front	424.501	0.718	71.308	18.550
Front to Front	430.938	0.729	73.567	18.450
Average	**426.581**	**0.722**	**71.976**	**18.486**
Standard Deviation	**3.137**	**0.005**	**2.032**	**0.059**
Front to Rear	458.541	0.776	76.476	18.571
Front to Rear	458.450	0.776	71.846	18.804
Front to Rear	455.548	0.771	73.881	18.571
Front to Rear	380.461	0.649	81.710	18.600
Front to Rear	382.637	0.651	84.765	18.550
Average	**427.127**	**0.724**	**77.735**	**18.619**
Standard Deviation	**41.632**	**0.068**	**5.393**	**0.105**

B.2 Electrical Output Statistical Analysis - Independent Samples t-Tests of Discharge Paths

Independent Samples Test

		Levene's Test for Equality of Variances		t-test for Equality of Means						
									95% Confidence Interval of the Difference	
		F	Sig.	t	df	Sig. (2-tailed)	Mean Difference	Std. Error Difference	Lower	Upper
Voltage	Equal variances assumed	78.822	.000	-.029	8	.977	-.54682	18.67115	-43.60256	42.50893
	Equal variances not assumed			-.029	4.045	.978	-.54682	18.67115	-52.15757	51.06393
Current	Equal variances assumed	78.509	.000	-.088	8	.932	-.00270	.03059	-.07323	.06783
	Equal variances not assumed			-.088	4.050	.934	-.00270	.03059	-.08721	.08181
Charge	Equal variances assumed	6.788	.031	-2.234	8	.056	-5.75910	2.57737	-11.70251	.18432
	Equal variances not assumed			-2.234	5.113	.075	-5.75910	2.57737	-12.34045	.82226
PPS	Equal variances assumed	.578	.469	-2.482	8	.038	-.13369	.05386	-.25789	-.00949
	Equal variances not assumed			-2.482	6.325	.046	-.13369	.05386	-.26385	-.00353
Duration	Equal variances assumed	.059	.814	.117	8	.909	.01000	.08515	-.18635	.20635
	Equal variances not assumed			.117	7.865	.909	.01000	.08515	-.18694	.20694

Annex C Task 3 Data

C.1 Durability Raw Data

Round #	Drop Height (m)	Outcome	Slipped (mm)	Velocity (fps)	Distance (m)	X Coordinate (cm)	Y Coordinate (cm)
Test Temperature: 23 °C							
Test Orientation: Horizontal							
1	1.0	No Breakage	0.0	223.0	5.0	-2.1	-1.6
2	1.5	No Breakage	0.0	232.0	10.0	2.2	-9.8
3	2.0	No Breakage	0.0	218.0	15.0	-2.0	-26.0
4	2.5	No Breakage	0.0	225.0	5.0	-0.2	-1.1
5	3.0	No Breakage	0.0	221.0	10.0	-0.1	-12.1
6	3.0	No Breakage	0.0	198.0	15.0	missed target	missed target
7	3.0	No Breakage	0.0	223.0	5.0	0.0	-2.3
8	3.0	No Breakage	0.0	219.0	10.0	-0.7	-13.8
9	3.0	No Breakage	0.0	222.0	15.0	-3.3	-23.5
10	3.0	No Breakage	0.0	239.0	5.0	-0.8	-3.6
Average	**2.5**		**0.0**	**222.0**		**-0.8**	**-10.4**
Stnd. Dev	**0.7**		**0.0**	**10.6**		**1.6**	**9.4**
Test Temperature: 23 °C **Test Orientation: Vertical**							
11	1.0	No Breakage	0.0	222.0	10.0	-0.6	-10.9
12	1.5	Slipped	0.6	222.0	15.0	-4.1	-25.2
13	1.5	Slipped	1.4	222.0	5.0	-0.8	-2.9
14	1.5	Slipped	0.5	209.0	10.0	-0.2	-11.5
15	1.5	Slipped	0.6	229.0	15.0	-3.0	-16.0
16	1.5	Slipped	0.3	225.0	5.0	-1.1	-5.9
17	1.5	Slipped	0.7	231.0	10.0	-3.0	-11.6
18	1.5	Slipped	0.4	213.0	15.0	0.5	-25.4
19	1.5	Slipped	0.6	225.0	10.0	-0.6	-8.2
20	1.5	Slipped	0.4	231.0	5.0	1.2	-2.9
Average	**1.5**		**0.6**	**222.9**		**-1.2**	**-12.0**
Stnd. Dev	**0.2**		**0.4**	**7.2**		**1.7**	**8.1**

Test Temperature: -20 °C							
Test Orientation: Horizontal							
21	1.0	No Breakage	0.0	209.0	15.0	-4.4	-24.5
22	1.5	No Breakage	0.0	217.0	5.0	-2.4	-4.2
23	2.0	No Breakage	0.0	207.0	10.0	-2.1	-12.9
24	2.5	No Breakage	0.0	204.0	15.0	4.4	-29.2
25	3.0	No Breakage	0.0	228.0	5.0	0.0	-3.4
26	3.0	Notch	0.0	212.0	10.0	-0.8	-12.1
27	3.0	No Breakage	0.0	no velocity	15.0	2.6	-21.5
28	3.0	No Breakage	0.0	226.0	5.0	-0.6	-4.6
29	3.0	No Breakage	0.0	198.0	10.0	-0.8	-16.9
30	3.0	Slipped	0.4	211.0	15.0	0.3	-23.7
Average	**2.5**		**0.0**	**212.4**		**-0.4**	**-15.3**
Stnd. Dev	**0.7**		**0.1**	**9.8**		**2.5**	**9.3**
Test Temperature: -20 °C							
Test Orientation: Vertical							
31	1.0	No Breakage	0.0	241.0	5.0	0.6	-2.2
32	1.5	Slipped	0.3	226.0	10.0	-1.6	-10.2
33	1.5	Slipped	0.3	no velocity	15.0	3.7	-20.2
34	1.5	Slipped	0.4	229.0	5.0	1.2	-2.1
35	1.5	Slipped	0.4	no velocity	10.0	-2.3	-10.9
36	1.5	Slipped	0.5	208.0	15.0	4.2	-24.1
37	1.5	Slipped	0.4	224.0	5.0	0.7	-2.0
38	1.5	Slipped	1.3	220.0	10.0	-2.6	-11.5
39	1.5	Slipped	0.5	210.0	15.0	0.9	-24.4
40	1.5	Slipped	0.5	200.0	5.0	-0.6	-3.6
Average	**1.5**		**0.5**	**219.8**		**0.4**	**-11.1**
Stnd. Dev	**0.2**		**0.3**	**13.2**		**2.3**	**9.0**

C.2 Durability Statistical Analysis – Independent Samples t-test of Drop Height, Outcome and Slip Distance

C.2.1 Orientation = Horizontal

Independent Samples Test

		Levene's Test for Equality of Variances		t-test for Equality of Means						
									95% CI of the Difference	
		F	Sig.	t	df	Sig. (2-tailed)	Mean Difference	Std. Error Difference	Lower	Upper
Drop_Height	Equal variances assumed	.000	1.000	.000	18	1.000	.00000	.33333	-.70031	.70031
	Equal variances not assumed			.000	18.000	1.000	.00000	.33333	-.70031	.70031
Outcome	Equal variances assumed	5.062	.037	-1.000	18	.331	-.10000	.10000	-.31009	.11009
	Equal variances not assumed			-1.000	9.000	.343	-.10000	.10000	-.32622	.12622
Slip_Amount	Equal variances assumed	5.062	.037	-1.000	18	.331	-.04000	.04000	-.12404	.04404
	Equal variances not assumed			-1.000	9.000	.343	-.04000	.04000	-.13049	.05049

C.2.2 Orientation = Vertical

Independent Samples Test

		Levene's Test for Equality of Variances		t-test for Equality of Means						
									95% Confidence Interval of the Difference	
		F	Sig.	t	df	Sig. (2-tailed)	Mean Difference	Std. Error Difference	Lower	Upper
Drop_Height	Equal variances assumed	.000	1.000	.000	18	1.000	.00000	.07071	-.14856	.14856
	Equal variances not assumed			.000	18.000	1.000	.00000	.07071	-.14856	.14856
Outcome	Equal variances assumed	.000	1.000	.000	18	1.000	.00000	.14142	-.29712	.29712
	Equal variances not assumed			.000	18.000	1.000	.00000	.14142	-.29712	.29712
Slip_Amount	Equal variances assumed	.104	.751	.582	18	.568	.09000	.15452	-.23464	.41464
	Equal variances not assumed			.582	17.873	.568	.09000	.15452	-.23481	.41481

C.2.3 Temperature = -20°C

Independent Samples Test

		Levene's Test for Equality of Variances		t-test for Equality of Means						
									95% Confidence Interval of the Difference	
		F	Sig.	t	df	Sig. (2-tailed)	Mean Difference	Std. Error Difference	Lower	Upper
Drop_Height	Equal variances assumed	15.161	.001	4.358	18	.000	1.05000	.24095	.54379	1.55621
	Equal variances not assumed			4.358	9.808	.001	1.05000	.24095	.51171	1.58829
Outcome	Equal variances assumed	.000	1.000	-5.657	18	.000	-.80000	.14142	-1.09712	-.50288
	Equal variances not assumed			-5.657	18.000	.000	-.80000	.14142	-1.09712	-.50288
Slip_Amount	Equal variances assumed	1.832	.193	-3.752	18	.001	-.42000	.11195	-.65520	-.18480
	Equal variances not assumed			-3.752	11.579	.003	-.42000	.11195	-.66491	-.17509

C.2.4 Temperature = 23°C

Independent Samples Test

		Levene's Test for Equality of Variances		t-test for Equality of Means						
									95% Confidence Interval of the Difference	
		F	Sig.	t	df	Sig. (2-tailed)	Mean Difference	Std. Error Difference	Lower	Upper
Drop_Height	Equal variances assumed	15.161	.001	4.358	18	.000	1.05000	.24095	.54379	1.55621
	Equal variances not assumed			4.358	9.808	.001	1.05000	.24095	.51171	1.58829
Outcome	Equal variances assumed	5.063	.037	-9.000	18	.000	-.90000	.10000	-1.11009	-.68991
	Equal variances not assumed			-9.000	9.000	.000	-.90000	.10000	-1.12622	-.67378
Slip_Amount	Equal variances assumed	7.486	.014	-4.834	18	.000	-.55000	.11377	-.78903	-.31097
	Equal variances not assumed			-4.834	9.000	.001	-.55000	.11377	-.80737	-.29263

C.3 Durability Statistical Analysis – ANOVA for Orientation vs. Velocity, X and Y Coordinates

C.3.1 Distance = 5 meters

ANOVA

		Sum of Squares	df	Mean Square	F	Sig.
Velocity	Between Groups	81.987	2	40.993	.462	.637
	Within Groups	1864.971	21	88.808		
	Total	1946.958	23			
X	Between Groups	9.397	2	4.699	3.092	.067
	Within Groups	31.914	21	1.520		
	Total	41.311	23			
Y	Between Groups	70.024	2	35.012	12.886	.000
	Within Groups	57.058	21	2.717		
	Total	127.083	23			

Test of Homogeneity of Variances

	Levene Statistic	df1	df2	Sig.
Velocity	.563	2	21	.578
X	.360	2	21	.702
Y	1.524	2	21	.241

Multiple Comparisons

Dependent Variable		(I) Orientation	(J) Orientation	Mean Difference (I-J)	Std. Error	Sig.	95% CI Lower Bound	95% CI Upper Bound
Y	LSD	Vertical	Horizontal	-.11429	.88108	.898	-1.9466	1.7180
			None	-3.52071*	.81232	.000	-5.2100	-1.8314
		Horizontal	Vertical	.11429	.88108	.898	-1.7180	1.9466
			None	-3.40643*	.81232	.000	-5.0957	-1.7171
		None	Vertical	3.52071*	.81232	.000	1.8314	5.2100
			Horizontal	3.40643*	.81232	.000	1.7171	5.0957

C.3.2 Distance = 10 meters

ANOVA

		Sum of Squares	df	Mean Square	F	Sig.
Velocity	Between Groups	583.063	2	291.532	3.722	.044
	Within Groups	1409.889	18	78.327		
	Total	1992.952	20			
X	Between Groups	5.027	2	2.514	.883	.430
	Within Groups	54.088	19	2.847		
	Total	59.115	21			
Y	Between Groups	228.202	2	114.101	28.748	.000
	Within Groups	75.411	19	3.969		
	Total	303.613	21			

Test of Homogeneity of Variances

	Levene Statistic	df1	df2	Sig.
Velocity	1.192	2	18	.326
X	2.306	2	19	.127
Y	.613	2	19	.552

Multiple Comparisons

Dependent Variable		(I) Orientation	(J) Orientation	Mean Difference (I-J)	Std. Error	Sig.	95% Lower Bound
Velocity	LSD	Vertical	Horizontal	7.33333	5.10970	.168	-3.4018
			None	12.72222*	4.66450	.014	2.9225
		Horizontal	Vertical	-7.33333	5.10970	.168	-18.0684
			None	5.38889	4.66450	.263	-4.4109
		None	Vertical	-12.72222*	4.66450	.014	-22.5220
			Horizontal	-5.38889	4.66450	.263	-15.1886
Y	LSD	Vertical	Horizontal	2.24762	1.10838	.057	-.0722
			None	-5.27460*	1.00399	.000	-7.3760
		Horizontal	Vertical	-2.24762	1.10838	.057	-4.5675
			None	-7.52222*	1.05000	.000	-9.7199
		None	Vertical	5.27460*	1.00399	.000	3.1732
			Horizontal	7.52222*	1.05000	.000	5.3245

C.3.3 Distance = 15 meters

ANOVA

		Sum of Squares	df	Mean Square	F	Sig.
Velocity	Between Groups	696.072	2	348.036	2.455	.118
	Within Groups	2268.033	16	141.752		
	Total	2964.105	18			
X	Between Groups	6.099	2	3.050	.347	.712
	Within Groups	149.415	17	8.789		
	Total	155.514	19			
Y	Between Groups	131.576	2	65.788	3.027	.075
	Within Groups	369.494	17	21.735		
	Total	501.070	19			

C.4 Durability Statistical Analysis – ANOVA for Temperature vs. Velocity, X and Y Coordinates

C.4.1 Distance = 5 meters

ANOVA

		Sum of Squares	df	Mean Square	F	Sig.
Velocity	Between Groups	113.987	2	56.993	.653	.531
	Within Groups	1832.971	21	87.284		
	Total	1946.958	23			
X	Between Groups	6.112	2	3.056	1.823	.186
	Within Groups	35.199	21	1.676		
	Total	41.311	23			
Y	Between Groups	70.210	2	35.105	12.962	.000
	Within Groups	56.873	21	2.708		
	Total	127.083	23			

Test of Homogeneity of Variances

	Levene Statistic	df1	df2	Sig.
Velocity	.811	2	21	.458
X	.320	2	21	.730
Y	1.637	2	21	.219

Multiple Comparisons

Dependent Variable		(I) Temperature	(J) Temperature	Mean Difference (I-J)	Std. Error	Sig.	95% CI Lower Bound	95% CI Upper Bound
Y	LSD	Room Temp T6	Room Temp T3	3.33500*	.81099	.000	1.6484	5.0216
			-20 T3	3.59214*	.81099	.000	1.9056	5.2787
		Room Temp T3	Room Temp T6	-3.33500*	.81099	.000	-5.0216	-1.6484
			-20 T3	.25714	.87965	.773	-1.5722	2.0865
		-20 T3	Room Temp T6	-3.59214*	.81099	.000	-5.2787	-1.9056
			Room Temp T3	-.25714	.87965	.773	-2.0865	1.5722

C.4.2 Distance = 10 meters

ANOVA

		Sum of Squares	df	Mean Square	F	Sig.
Velocity	Between Groups	720.102	2	360.051	5.092	.018
	Within Groups	1272.851	18	70.714		
	Total	1992.952	20			
X	Between Groups	5.798	2	2.899	1.033	.375
	Within Groups	53.317	19	2.806		
	Total	59.115	21			
Y	Between Groups	217.242	2	108.621	23.894	.000
	Within Groups	86.372	19	4.546		
	Total	303.613	21			

Test of Homogeneity of Variances

	Levene Statistic	df1	df2	Sig.
Velocity	.617	2	18	.550
X	2.944	2	19	.077
Y	.111	2	19	.896

Multiple Comparisons

Dependent Variable		(I) Temperature	(J) Temperature	Mean Difference (I-J)	Std. Error	Sig.	95% Confidence Interval	
							Lower Bound	Upper Bound
Velocity	LSD	Room Temp T6	Room Temp T3	-13.26984*	4.23782	.006	-22.1732	-4.3665
			-20 T3	-3.15556	4.69040	.510	-13.0097	6.6986
		Room Temp T3	Room Temp T6	13.26984*	4.23782	.006	4.3665	22.1732
			-20 T3	10.11429	4.92390	.055	-.2304	20.4590
		-20 T3	Room Temp T6	3.15556	4.69040	.510	-6.6986	13.0097
			Room Temp T3	-10.11429	4.92390	.055	-20.4590	.2304
Y	LSD	Room Temp T6	Room Temp T3	5.71746*	1.07448	.000	3.4685	7.9664
			-20 T3	7.00556*	1.12372	.000	4.6536	9.3575
		Room Temp T3	Room Temp T6	-5.71746*	1.07448	.000	-7.9664	-3.4685
			-20 T3	1.28810	1.18619	.291	-1.1946	3.7708
		-20 T3	Room Temp T6	-7.00556*	1.12372	.000	-9.3575	-4.6536
			Room Temp T3	-1.28810	1.18619	.291	-3.7708	1.1946

C.4.3 Distance = 15 meters

ANOVA

		Sum of Squares	df	Mean Square	F	Sig.
Velocity	Between Groups	797.405	2	398.703	2.944	.082
	Within Groups	2166.700	16	135.419		
	Total	2964.105	18			
X	Between Groups	52.210	2	26.105	4.296	.031
	Within Groups	103.303	17	6.077		
	Total	155.514	19			
Y	Between Groups	118.800	2	59.400	2.642	.100
	Within Groups	382.271	17	22.487		
	Total	501.070	19			

Test of Homogeneity of Variances

	Levene Statistic	df1	df2	Sig.
Velocity	4.910	2	16	.022
X	.882	2	17	.432
Y	1.264	2	17	.308

Multiple Comparisons

Dependent Variable		(I) Temperature	(J) Temperature	Mean Difference (I-J)	Std. Error	Sig.	95% Confidence Interval	
							Lower Bound	Upper Bound
X	LSD	Room Temp T6	Room Temp T3	3.31375*	1.40532	.031	.3488	6.2787
			-20 T3	-.73768	1.27581	.571	-3.4294	1.9540
		Room Temp T3	Room Temp T6	-3.31375*	1.40532	.031	-6.2787	-.3488
			-20 T3	-4.05143*	1.44341	.012	-7.0968	-1.0061
		-20 T3	Room Temp T6	.73768	1.27581	.571	-1.9540	3.4294
			Room Temp T3	4.05143*	1.44341	.012	1.0061	7.0968

Annex D Task 4 Data

D.1 In-Flight Aerodynamics Raw Data

Round #	Proximal			Distal		
	Pitch (Deg)	Distance (m)	Rotations (RPS)	Pitch (Deg)	Distance (m)	Rotations (RPS)
1	0.0°	0	76	0.0°	5	290
2	0.0°	0	71	0.0°	5	133
3	0.0°	0	74	1.4°	5	142
4	0.0°	0	90	-1.4°	5	179
5	-1.9°	0	167	1.4°	5	161
6	1.4°	0	171	-1.5°	5	173
7	0.0°	0	185	-2.5°	5	200
8	0.0°	0	126	-1.7°	5	161
9	1.9°	0	133	10.8°	5	227
10	0.0°	0	167	-3.2°	5	161
Average	**0.1°**	**0.0**	**126.0**	**0.3°**	**5.0**	**182.7**
Stnd. Dev	**1.0°**	**0.0**	**45.2**	**4.0°**	**0.0**	**46.4**
11	0.9°	7.5	250	-1.5°	10	227
12	-1.0°	7.5	217	-0.8°	10	238
13	-1.0°	7.5	167	0.0°	10	200
14	0.0°	7.5	192	0.7°	10	238
15	0.0°	7.5	179	-0.7°	10	227
16	Open	7.5	Open	Open	10	Open
17	-1.9°	7.5	185	-0.9°	10	208
18	-1.9°	7.5	208	-2.9°	10	227
19	-0.9°	7.5	179	-1.7°	10	192
20	0.0°	7.5	200	0.0°	10	208
Average	**-0.6°**	**7.5**	**197.4**	**-0.8°**	**10.0**	**218.4**
Stnd. Dev	**0.9°**	**0.0**	**25.3**	**1.1°**	**0.0**	**16.8**
21	-2.8°	12	227	-1.3°	15	200
22	-1.8°	12	217	2.3°	15	208
23	No Video	12	No Video	No Video	15	No Video
24	-2.8°	12	250	-1.9°	15	263
25	1.7°	12	238	No Video	15	No Video
26	-1.0°	12	250	-1.6°	15	294
27	Open	12	Open	Open	15	Open
28	-4.7°	12	227	-2.5°	15	250

29	-0.9°	12	238	-1.4°	15	250
30	8.8°	12	156	12.3°	15	98
31	-7.4°	12	83	8.8°	15	63
32	-1.0°	12	278	-1.9°	15	313
33	0.0°	12	238	-2.6°	15	250
Average	**-1.1°**	**12.0**	**218.4**	**1.0°**	**15.0**	**218.9**
Stnd. Dev	**4.1°**	**0.0**	**53.9**	**5.3°**	**0.0**	**82.1**
34				No Video	20	No Video
35				0.00°	20	290
36				-1.59°	20	303
37				-0.60°	20	290
38				-1.51°	20	267
39				Open	20	Open
40				0.00°	20	267
41				Hit Chrono	20	Hit Chrono
42				0.00°	20	290
43				-1.04°	20	256
44				0.00°	20	278
45				1.47°	20	267
46				Open	20	Open
Average				**-0.4°**	**20.0**	**278.5**
Stnd. Dev				**1.0°**	**0.0**	**15.4**

D.2 In-Flight Aerodynamics Statistical Analysis

ANOVA

		Sum of Squares	df	Mean Square	F	Sig.
Rotation	Between Groups	122232.115	6	20372.019	9.213	.000
	Within Groups	134877.768	61	2211.111		
	Total	257109.882	67			
Pitch	Between Groups	33.419	6	5.570	.574	.749
	Within Groups	591.682	61	9.700		
	Total	625.102	67			

Test of Homogeneity of Variances

	Levene Statistic	df1	df2	Sig.
Rotation	3.421	6	61	.006
Pitch	3.990	6	61	.002

Multiple Comparisons

LSD

Dependent Variable	(I) Distance	(J) Distance	Mean Difference (I-J)	Std. Error	Sig.	95% Confidence Interval	
						Lower Bound	Upper Bound
Rotation	.0	5.0	-56.7000*	21.0291	.009	-98.750	-14.650
		7.5	-71.4444*	21.6053	.002	-114.647	-28.242
		10.0	-92.3333*	21.6053	.000	-135.536	-49.131
		12.0	-92.3636*	20.5456	.000	-133.447	-51.280
		15.0	-92.9000*	21.0291	.000	-134.950	-50.850
		20.0	-152.6667*	21.6053	.000	-195.869	-109.464
	5.0	.0	56.7000*	21.0291	.009	14.650	98.750
		7.5	-14.7444	21.6053	.498	-57.947	28.458
		10.0	-35.6333	21.6053	.104	-78.836	7.569
		12.0	-35.6636	20.5456	.088	-76.747	5.420
		15.0	-36.2000	21.0291	.090	-78.250	5.850
		20.0	-95.9667*	21.6053	.000	-139.169	-52.764

	7.5	.0	71.4444*	21.6053	.002	28.242	114.647
		5.0	14.7444	21.6053	.498	-28.458	57.947
		10.0	-20.8889	22.1666	.350	-65.214	23.436
		12.0	-20.9192	21.1350	.326	-63.181	21.343
		15.0	-21.4556	21.6053	.325	-64.658	21.747
		20.0	-81.2222*	22.1666	.001	-125.547	-36.897
	10.0	.0	92.3333*	21.6053	.000	49.131	135.536
		5.0	35.6333	21.6053	.104	-7.569	78.836
		7.5	20.8889	22.1666	.350	-23.436	65.214
		12.0	-.0303	21.1350	.999	-42.292	42.232
		15.0	-.5667	21.6053	.979	-43.769	42.636
		20.0	-60.3333*	22.1666	.008	-104.658	-16.008
	12.0	.0	92.3636*	20.5456	.000	51.280	133.447
		5.0	35.6636	20.5456	.088	-5.420	76.747
		7.5	20.9192	21.1350	.326	-21.343	63.181
		10.0	.0303	21.1350	.999	-42.232	42.292
		15.0	-.5364	20.5456	.979	-41.620	40.547
		20.0	-60.3030*	21.1350	.006	-102.565	-18.041
	15.0	.0	92.9000*	21.0291	.000	50.850	134.950
		5.0	36.2000	21.0291	.090	-5.850	78.250
		7.5	21.4556	21.6053	.325	-21.747	64.658
		10.0	.5667	21.6053	.979	-42.636	43.769
		12.0	.5364	20.5456	.979	-40.547	41.620
		20.0	-59.7667*	21.6053	.007	-102.969	-16.564
	20.0	.0	152.6667*	21.6053	.000	109.464	195.869
		5.0	95.9667*	21.6053	.000	52.764	139.169
		7.5	81.2222*	22.1666	.001	36.897	125.547
		10.0	60.3333*	22.1666	.008	16.008	104.658
		12.0	60.3030*	21.1350	.006	18.041	102.565
		15.0	59.7667*	21.6053	.007	16.564	102.969

Annex E Task 5 Data

E.1 In-Flight Aerodynamics Statistical Analysis

Round #	Number of Cholla Barbs Engaged	NMI Duration (s)	Average PRF (PPS)	Velocity (fps)
1	0	no data	no data	243
2	0	no data	no data	214
3	0	no data	no data	222
4	0	no data	no data	231
5	0	no data	no data	N/A
6	0	no data	no data	237
7	0	19.5	17.8	211
8	0	19.6	18.2	228
9	0	19.7	18.2	235
10	0	no data	no data	225
11	0	no data	no data	219
12	0	19.4	17.6	233
13	0	19.6	17.6	223
14	0	19.3	18.4	215
15	0	no data	no data	216
16	0	19.4	18.2	213
17	0	18.2	18.5	223
18	0	19.4	18.1	213
19	0	19.5	18.1	225
Average	**0.0**	**19.4**	**18.1**	**223.7**
Stnd. Dev	**0.0**	**0.4**	**0.3**	**9.3**

Annex F Task 6 Data

F.1 Accuracy and Precision Raw Data

Round #	Target Distance (m)	Velocity (fps)	X Coordinate (cm)	Y Coordinate (cm)
1	5	221	2.07	-1.66
2	5	224	1.25	1.33
3	5	217	-2.61	-1.37
4	5	235	-1.32	3.02
5	5	216	0.52	-2.17
6	5	227	1.09	0.57
7	5	218	0.97	1.64
8	5	208	1.67	-1.24
9	5	216	2.08	3.43
10	5	234	0.57	0.80
Average	5	221.6	0.63	0.43
Stnd. Dev		8.5	1.50	1.98
11	10	212	-2.5	-5.6
12	10	211	1.1	-5.5
13	10	212	-3.9	-8.7
14	10	199	-4.9	-7.8
15	10	212	0.3	-4.7
16	10	Open	Open	Open
17	10	216	-0.2	-3.9
18	10	209	-2.0	-5.8
19	10	196	1.0	-5.7
20	10	218	-1.0	-1.0
Average		208.6	-1.36	-5.40
Stnd. Dev		7.4	2.14	2.22
21	15	Error	-1.52	-15.80
22	15	Error	-1.35	-12.90
23	15	186	2.23	-32.00
24	15	220	-1.60	-12.53
25	15	200	0.90	-21.10
26	15	214	0.00	-19.60
27	15	Open	Open	Open
28	15	190	3.17	-14.80

29	15	199	4.39	-15.38
30	15	184	-0.30	-19.59
31	15	Error	-14.80	-12.84
32	15	221	-1.32	-14.59
33	15	Error	1.16	-16.17
Average		201.8	-0.75	-17.28
Stnd. Dev		15.0	4.84	5.43
34	20	Hit chrono	NA	NA
35	20	203	-14.02	-49.27
36	20	205	-8.85	-49.008
37	20	197	-9.59	-50.25
38	20	192	-6.10	-53.72
39	20	Open	Open	Open
40	20	197	-20.63	-48.95
41	20	Hit chrono	NA	NA
42	20	211	-14.30	-50.89
43	20	201	-9.57	-61.30
44	20	197	-16.06	-54.72
45	20	199	-7.62	-44.24
46	20	Open	Open	Open
Average		200.22	-11.86	-51.37
Stnd. Dev		5.56	4.69	4.79

F.2 Accuracy and Precision Statistical Analysis

ANOVA

		Sum of Squares	df	Mean Square	F	Sig.
Velocity	Between Groups	2701.961	3	900.654	9.967	.000
	Within Groups	2891.678	32	90.365		
	Total	5593.639	35			
X	Between Groups	986.419	3	328.806	39.685	.000
	Within Groups	265.133	32	8.285		
	Total	1251.552	35			
Y	Between Groups	14850.025	3	4950.008	302.691	.000
	Within Groups	523.307	32	16.353		
	Total	15373.332	35			

Test of Homogeneity of Variances

	Levene Statistic	df1	df2	Sig.
Velocity	4.506	3	32	.010
X	6.972	3	32	.001
Y	2.603	3	32	.069

Multiple Comparisons

LSD

Dependent Variable	(I) Distance	(J) Distance	Mean Difference (I-J)	Std. Error	Sig.	95% Confidence Interval	
						Lower Bound	Upper Bound
Velocity	5.00	10.00	12.15556*	4.36773	.009	3.2588	21.0523
		15.00	19.85000*	4.50911	.000	10.6652	29.0348
		20.00	21.37778*	4.36773	.000	12.4810	30.2745
	10.00	5.00	-12.15556*	4.36773	.009	-21.0523	-3.2588
		15.00	7.69444	4.61911	.106	-1.7144	17.1033
		20.00	9.22222*	4.48119	.048	.0943	18.3501
	15.00	5.00	-19.85000*	4.50911	.000	-29.0348	-10.6652
		10.00	-7.69444	4.61911	.106	-17.1033	1.7144
		20.00	1.52778	4.61911	.743	-7.8810	10.9366

	20.00	5.00	-21.37778*	4.36773	.000	-30.2745	-12.4810
		10.00	-9.22222*	4.48119	.048	-18.3501	-.0943
		15.00	-1.52778	4.61911	.743	-10.9366	7.8810
X	5.00	10.00	1.97344	1.32255	.145	-.7205	4.6674
		15.00	-.30475	1.36536	.825	-3.0859	2.4764
		20.00	12.48900*	1.32255	.000	9.7951	15.1829
	10.00	5.00	-1.97344	1.32255	.145	-4.6674	.7205
		15.00	-2.27819	1.39867	.113	-5.1272	.5708
		20.00	10.51556*	1.35691	.000	7.7516	13.2795
	15.00	5.00	.30475	1.36536	.825	-2.4764	3.0859
		10.00	2.27819	1.39867	.113	-.5708	5.1272
		20.00	12.79375*	1.39867	.000	9.9448	15.6427
	20.00	5.00	-12.48900*	1.32255	.000	-15.1829	-9.7951
		10.00	-10.51556*	1.35691	.000	-13.2795	-7.7516
		15.00	-12.79375*	1.39867	.000	-15.6427	-9.9448
Y	5.00	10.00	5.84611*	1.85806	.004	2.0614	9.6308
		15.00	19.13375*	1.91820	.000	15.2265	23.0410
		20.00	51.80700*	1.85806	.000	48.0223	55.5917
	10.00	5.00	-5.84611*	1.85806	.004	-9.6308	-2.0614
		15.00	13.28764*	1.96499	.000	9.2851	17.2902
		20.00	45.96089*	1.90633	.000	42.0778	49.8439
	15.00	5.00	-19.13375*	1.91820	.000	-23.0410	-15.2265
		10.00	-13.28764*	1.96499	.000	-17.2902	-9.2851
		20.00	32.67325*	1.96499	.000	28.6707	36.6758
	20.00	5.00	-51.80700*	1.85806	.000	-55.5917	-48.0223
		10.00	-45.96089*	1.90633	.000	-49.8439	-42.0778
		15.00	-32.67325*	1.96499	.000	-36.6758	-28.6707

Annex G Task 7 Data

G.1 Temperature Effects Raw Data

Round #	Temperature (◦C)	Target Distance (m)	Velocity (fps)	X Coordinate (cm)	Y Coordinate (cm)
1	50	5	225	7.50	-3.39
2	50	5	228	1.52	-0.30
3	50	5	233	-0.80	-0.40
4	50	5	231	-1.50	-1.40
5	50	5	227	-1.08	-1.10
6	50	5	213	1.09	-1.54
7	50	5	219	1.60	0.00
8	50	5	227	-0.60	-0.90
9	50	5	214	0.00	-1.60
10	50	5	220	1.30	-1.40
Average			**223.7**	**0.90**	**-1.20**
Stnd. Dev			**6.9**	**2.59**	**0.95**
11	-20	5	234	2.45	-2.59
12	-20	5	222	-0.68	-1.40
13	-20	5	214	-5.81	-6.70
14	-20	5	224	1.70	-2.40
15	-20	5	209	3.47	-4.54
16	-20	5	230	1.63	0.00
17	-20	5	231	open	open
18	-20	5	215	open	open
19	-20	5	N/A	open	open
20	-20	5	229	1.05	0.00
21	-20	5	227	open	open
22	-20	5	216	1.30	-0.70
23	-20	5	230	0.00	1.12
24	-20	5	211	0.30	-1.24
25	-20	5	213	-0.64	-1.83
26(NV)	-20	5	225	-3.80	-2.80
27(NV)	-20	5	228	1.20	-4.00
28(NV)	-20	5	217	open	open
29(NV)	-20	5	218	open	open
30(NV)	-20	5	217	-0.70	4.50
31(NV)	-20	5	219	1.20	-2.90
32(NV)	-20	5	223	-1.20	-2.20
Average			**221.5**	**0.09**	**-1.73**
Stnd. Dev			**7.3**	**2.31**	**2.53**

33	50	10	230	2.10	-4.56
34	50	10	210	0.80	-8.00
35	50	10	215	0.40	-6.80
36	50	10	225	3.20	-6.50
37	50	10	221	0.90	-5.10
38	50	10	218	2.80	-7.40
39	50	10	213	2.30	-6.90
40	50	10	216	0.00	-5.40
41	50	10	220	1.70	-5.00
42	50	10	213	2.20	-4.10
Average			**218.1**	**1.64**	**-5.98**
Stnd. Dev			**6.1**	**1.07**	**1.31**
43	-20	10	221	-1.70	-8.20
44	-20	10	220	-2.50	-7.40
45	-20	10	225	-2.60	-7.60
46	-20	10	194	open	open
47	-20	10	221	-1.70	-7.90
48	-20	10	216	0.60	-6.10
49	-20	10	211	1.40	-7.60
50	-20	10	223	-1.30	-3.50
51	-20	10	211	2.60	-7.60
52	-20	10	219	1.00	-6.90
53	-20	10	215	2.20	-7.40
Average			**216.0**	**-0.20**	**-7.02**
Stnd. Dev			**8.6**	**1.97**	**1.36**
54	50	15	218	6.80	-20.50
55	50	15	218	0.57	-14.70
56	50	15	218	-1.46	-23.31
57	50	15	209	0.00	-16.20
58	50	15	206	4.19	-25.90
59	50	15	209	9.31	-21.90
60	50	15	214	0.00	-19.00
61	50	15	213	2.66	-16.20
62	50	15	200	5.95	-17.80
63	50	15	214	2.79	-20.40
Average			**211.9**	**3.08**	**-19.59**
Stnd. Dev			**5.9**	**3.47**	**3.51**
64	-20	15	205	-5.30	-30.80
65(OOV)	-20	15	175	OOV	OOV
66	-20	15	211	4.20	-14.10
67	-20	15	205	0.10	-17.70
68	-20	15	197	9.16	-8.36
69	-20	15	215	4.56	-16.97

70	-20	15	173	open	open
71	-20	15	204	6.30	-23.40
72	-20	15	190	-7.50	-24.00
73(OOV)	-20	15	167	open	open
74	-20	15	211	6.20	-16.50
75	-20	15	206	3.55	-20.50
76(NV)	-20	15	205	-4.50	-17.40
77	-20	15	218	-0.80	-13.80
78	-20	15	208	4.20	-15.80
79	-20	15	206	-4.10	-15.40
80	-20	15	215	1.00	-17.50
Average			**200.6**	**1.22**	**-18.02**
Stnd. Dev			**15.4**	**5.06**	**5.38**
81(OOV)	50	20	212	-0.70	-30.40
82(NV)	50	20	196	-3.20	-34.50
83	50	20	199	-2.20	-35.40
84(NV)	50	20	201	-4.10	-37.30
85(NV)	50	20	212	-4.40	-28.50
86	50	20	205	-0.30	-38.00
87	50	20	201	-3.10	-30.10
88	50	20	204	0.00	-30.00
89	50	20	215	-0.80	-30.60
90	50	20	200	-7.40	-30.60
91	50	20	201	-2.30	-28.90
92	50	20	211	4.80	-31.40
93	50	20	196	-1.40	-31.80
94	50	20	open	open	open
95	50	20	110	-5.90	-29.10
Average			**204.1**	**-1.93**	**-31.90**
Stnd. Dev			**6.4**	**2.87**	**3.12**
96(OOV)	-20	20	N/A	12.00	-14.70
97(NV)	-20	20	194	7.60	-22.20
98	-20	20	197	-1.20	-35.70
99	-20	20	193	1.90	-37.20
100	-20	20	148	open	open
101	-20	20	210	-3.80	-18.80
102	-20	20	193	-10.90	-26.30
103	-20	20	205	1.90	-49.60
104	-20	20	202	-6.30	-34.00
105	-20	20	170	open	open
106	-20	20	210	1.30	-23.70
107	-20	20	209	7.70	-25.90
108	-20	20	188	10.10	-38.50

Average	**193.3**	**1.85**	**-29.69**
Stnd. Dev	**18.2**	**7.13**	**10.23**

G.2 Temperature Effects Statistical Analysis – ANOVA of Temperature vs. Velocity, X, and Y

G.2.1 Temperature = -20°C

ANOVA

		Sum of Squares	df	Mean Square	F	Sig.
Velocity	Between Groups	16558.641	3	5519.547	7.322	.000
	Within Groups	43722.197	58	753.831		
	Total	60280.839	61			
X	Between Groups	19.442	3	6.481	.358	.784
	Within Groups	1032.688	57	18.117		
	Total	1052.130	60			
Y	Between Groups	4850.826	3	1616.942	25.137	.000
	Within Groups	3666.476	57	64.324		
	Total	8517.302	60			

Test of Homogeneity of Variances

	Levene Statistic	df1	df2	Sig.
Velocity	5.217	3	58	.003
X	5.606	3	57	.002
Y	9.754	3	57	.000

Multiple Comparisons

Dependent Variable		(I) Distance	(J) Distance	Mean Difference (I-J)	Std. Error	Sig.	95% CI	
							Lower Bound	Upper Bound
Velocity	Games-Howell	5 m	10 m	5.52381	3.04439	.300	-3.0939	14.1415
			15 m	20.87675*	4.05797	.000	9.5999	32.1536
			20 m	43.13919	15.71450	.072	-3.3738	89.6522
		10 m	5 m	-5.52381	3.04439	.300	-14.1415	3.0939
			15 m	15.35294*	4.54459	.012	2.8735	27.8324
			20 m	37.61538	15.84713	.133	-9.0702	84.3010
		15 m	5 m	-20.87675*	4.05797	.000	-32.1536	-9.5999
			10 m	-15.35294*	4.54459	.012	-27.8324	-2.8735
			20 m	22.26244	16.07266	.529	-24.7322	69.2571
		20 m	5 m	-43.13919	15.71450	.072	-89.6522	3.3738
			10 m	-37.61538	15.84713	.133	-84.3010	9.0702
			15 m	-22.26244	16.07266	.529	-69.2571	24.7322
Y	Games-Howell	5 m	10 m	5.15727*	.77323	.000	3.0474	7.2672
			15 m	14.03588*	1.97734	.000	8.5018	19.5699
			20 m	23.35308*	4.08745	.000	11.3101	35.3960
		10 m	5 m	-5.15727*	.77323	.000	-7.2672	-3.0474
			15 m	8.87861*	1.90607	.001	3.4751	14.2822
			20 m	18.19580*	4.05345	.003	6.1962	30.1955
		15 m	5 m	-14.03588*	1.97734	.000	-19.5699	-8.5018
			10 m	-8.87861*	1.90607	.001	-14.2822	-3.4751
			20 m	9.31719	4.44324	.194	-3.3065	21.9409
		20 m	5 m	-23.35308*	4.08745	.000	-35.3960	-11.3101
			10 m	-18.19580*	4.05345	.003	-30.1955	-6.1962
			15 m	-9.31719	4.44324	.194	-21.9409	3.3065

G.2.2 Temperature = 50°C

ANOVA

		Sum of Squares	df	Mean Square	F	Sig.
Velocity	Between Groups	4725.068	3	1575.023	6.437	.001
	Within Groups	9787.114	40	244.678		
	Total	14512.182	43			
X	Between Groups	184.572	3	61.524	8.414	.000
	Within Groups	292.470	40	7.312		
	Total	477.043	43			
Y	Between Groups	6860.515	3	2286.838	350.633	.000
	Within Groups	260.881	40	6.522		
	Total	7121.396	43			

Test of Homogeneity of Variances

	Levene Statistic	df1	df2	Sig.
Velocity	1.172	3	40	.333
X	2.234	3	40	.099
Y	6.067	3	40	.002

Multiple Comparisons

Dependent Variable		(I) Distance	(J) Distance	Mean Difference (I-J)	Std. Error	Sig.	95% CI Lower Bound	95% CI Upper Bound
Velocity	LSD	5 m	10 m	5.60000	6.99540	.428	-8.5382	19.7382
			15 m	11.80000	6.99540	.099	-2.3382	25.9382
			20 m	26.34286*	6.47648	.000	13.2534	39.4323
		10 m	5 m	-5.60000	6.99540	.428	-19.7382	8.5382
			15 m	6.20000	6.99540	.381	-7.9382	20.3382
			20 m	20.74286*	6.47648	.003	7.6534	33.8323
		15 m	5 m	-11.80000	6.99540	.099	-25.9382	2.3382
			10 m	-6.20000	6.99540	.381	-20.3382	7.9382
			20 m	14.54286*	6.47648	.030	1.4534	27.6323
		20 m	5 m	-26.34286*	6.47648	.000	-39.4323	-13.2534
			10 m	-20.74286*	6.47648	.003	-33.8323	-7.6534
			15 m	-14.54286*	6.47648	.030	-27.6323	-1.4534
X	LSD	5 m	10 m	-.74000	1.20928	.544	-3.1840	1.7040
			15 m	-2.19000	1.20928	.078	-4.6340	.2540
			20 m	3.11429*	1.11957	.008	.8515	5.3770
		10 m	5 m	.74000	1.20928	.544	-1.7040	3.1840
			15 m	-1.45000	1.20928	.238	-3.8940	.9940
			20 m	3.85429*	1.11957	.001	1.5915	6.1170
		15 m	5 m	2.19000	1.20928	.078	-.2540	4.6340
			10 m	1.45000	1.20928	.238	-.9940	3.8940
			20 m	5.30429*	1.11957	.000	3.0415	7.5670
		20 m	5 m	-3.11429*	1.11957	.008	-5.3770	-.8515
			10 m	-3.85429*	1.11957	.001	-6.1170	-1.5915
			15 m	-5.30429*	1.11957	.000	-7.5670	-3.0415
Y	Games-Howell	5 m	10 m	4.78100*	.51112	.000	3.3228	6.2392
			15 m	18.39100*	1.14971	.000	14.8928	21.8892
			20 m	30.70100*	.88620	.000	28.1690	33.2330
		10 m	5 m	-4.78100*	.51112	.000	-6.2392	-3.3228
			15 m	13.61000*	1.18437	.000	10.0685	17.1515
			20 m	25.92000*	.93072	.000	23.2973	28.5427
		15 m	5 m	-18.39100*	1.14971	.000	-21.8892	-14.8928
			10 m	-13.61000*	1.18437	.000	-17.1515	-10.0685
			20 m	12.31000*	1.38810	.000	8.3878	16.2322
		20 m	5 m	-30.70100*	.88620	.000	-33.2330	-28.1690
			10 m	-25.92000*	.93072	.000	-28.5427	-23.2973
			15 m	-12.31000*	1.38810	.000	-16.2322	-8.3878

G.3 Temperature Effects Statistical Analysis – ANOVA of Distance vs. Velocity, X, and Y

G.3.1 Distance = 5 meters

ANOVA

		Sum of Squares	df	Mean Square	F	Sig.
Velocity	Between Groups	35.042	2	17.521	.311	.735
	Within Groups	2143.738	38	56.414		
	Total	2178.780	40			
X	Between Groups	1.015	2	.507	.097	.908
	Within Groups	194.183	37	5.248		
	Total	195.198	39			
Y	Between Groups	32.615	2	16.308	2.879	.069
	Within Groups	209.594	37	5.665		
	Total	242.209	39			

G.3.2 Distance = 10 meters

ANOVA

		Sum of Squares	df	Mean Square	F	Sig.
Velocity	Between Groups	382.744	2	191.372	3.442	.047
	Within Groups	1501.122	27	55.597		
	Total	1883.867	29			
X	Between Groups	42.302	2	21.151	6.230	.006
	Within Groups	91.666	27	3.395		
	Total	133.968	29			
Y	Between Groups	11.847	2	5.923	2.218	.128
	Within Groups	72.107	27	2.671		
	Total	83.954	29			

Test of Homogeneity of Variances[a]

	Levene Statistic	df1	df2	Sig.
Velocity	.187	2	27	.830
X	4.567	2	27	.020
Y	.631	2	27	.540

Multiple Comparisons

Dependent Variable		(I) Temperature	(J) Temperature	Mean Difference (I-J)	Std. Error	Sig.	95% CI Lower Bound	95% CI Upper Bound
Velocity	Games-Howell	-20.00	23.00	6.55556	3.56017	.185	-2.5326	15.6437
			50 C	-2.10000	3.22896	.795	-10.3416	6.1416
		23.00	-20.00	-6.55556	3.56017	.185	-15.6437	2.5326
			50 C	-8.65556*	3.10587	.034	-16.6870	-.6241
		50 C	-20.00	2.10000	3.22896	.795	-6.1416	10.3416
			23.00	8.65556*	3.10587	.034	.6241	16.6870
X	Games-Howell	-20.00	23.00	1.44444	.95693	.311	-1.0083	3.8972
			50 C	-1.54000	.72234	.117	-3.4157	.3357
		23.00	-20.00	-1.44444	.95693	.311	-3.8972	1.0083
			50 C	-2.98444*	.78812	.007	-5.1002	-.8687
		50 C	-20.00	1.54000	.72234	.117	-.3357	3.4157
			23.00	2.98444*	.78812	.007	.8687	5.1002

G.3.3 Distance = 15 meters

ANOVA

		Sum of Squares	df	Mean Square	F	Sig.
Velocity	Between Groups	855.261	2	427.630	2.414	.106
	Within Groups	5668.282	32	177.134		
	Total	6523.543	34			
X	Between Groups	23.464	2	11.732	.709	.500
	Within Groups	496.488	30	16.550		
	Total	519.952	32			
Y	Between Groups	16.947	2	8.474	.337	.717
	Within Groups	754.552	30	25.152		
	Total	771.499	32			

G.3.4 Distance = 20 meters

ANOVA

		Sum of Squares	df	Mean Square	F	Sig.
Velocity	Between Groups	260.523	2	130.262	.330	.721
	Within Groups	12615.020	32	394.219		
	Total	12875.543	34			
X	Between Groups	966.390	2	483.195	18.771	.000
	Within Groups	797.969	31	25.741		
	Total	1764.359	33			
Y	Between Groups	2796.014	2	1398.007	31.954	.000
	Within Groups	1356.277	31	43.751		
	Total	4152.291	33			

Test of Homogeneity of Variances

	Levene Statistic	df1	df2	Sig.
Velocity	.911	2	32	.412
X	4.042	2	31	.028
Y	9.856	2	31	.000

Multiple Comparisons

Dependent Variable		(I) Temperature	(J) Temperature	Mean Difference (I-J)	Std. Error	Sig.	95% CI Lower Bound	95% CI Upper Bound
X	Games-Howell	-20.00	23.00	13.70545*	2.65851	.000	6.8969	20.5141
			50 C	4.05974	2.29102	.218	-2.0075	10.1270
		23.00	-20.00	-13.70545*	2.65851	.000	-20.5141	-6.8969
			50 C	-9.64571*	1.75042	.000	-14.3096	-4.9818
		50 C	-20.00	-4.05974	2.29102	.218	-10.1270	2.0075
			23.00	9.64571*	1.75042	.000	4.9818	14.3096
Y	Games-Howell	-20.00	23.00	21.68131*	3.47276	.000	12.6449	30.7177
			50 C	2.20909	3.19476	.773	-6.3676	10.7858
		23.00	-20.00	-21.68131*	3.47276	.000	-30.7177	-12.6449
			50 C	-19.47222*	1.80108	.000	-24.2568	-14.6876
		50 C	-20.00	-2.20909	3.19476	.773	-10.7858	6.3676
			23.00	19.47222*	1.80108	.000	14.6876	24.2568

G.4 Temperature Effects Statistical Analysis – ANOVA of Temperature vs. Pitch and Rotation

G.4.1 Temperature = -20 °C

ANOVA

		Sum of Squares	df	Mean Square	F	Sig.
Rotation	Between Groups	305707.939	6	50951.323	86.665	.000
	Within Groups	37626.456	64	587.913		
	Total	343334.394	70			
Pitch	Between Groups	43.417	6	7.236	1.361	.244
	Within Groups	340.381	64	5.318		
	Total	383.798	70			

Test of Homogeneity of Variances

	Levene Statistic	df1	df2	Sig.
Rotation	4.000	6	64	.002
Pitch	1.944	6	64	.087

Multiple Comparisons

Dependent Variable		(I) Distance	(J) Distance	Mean Difference (I-J)	Std. Error	Sig.	95% CI Lower Bound	95% CI Upper Bound
Rotation	Games-Howell	.0	5.0	-78.0000*	3.5116	.000	-89.735	-66.265
			7.5	-95.1000*	5.0143	.000	-112.529	-77.671
			10.0	-133.8000*	7.6934	.000	-161.465	-106.135
			12.0	-157.9333*	11.9006	.000	-199.785	-116.081
			15.0	-184.1000*	10.2409	.000	-221.401	-146.799
			20.0	-213.2111*	6.2357	.000	-235.833	-190.590
		5.0	.0	78.0000*	3.5116	.000	66.265	89.735
			7.5	-17.1000	5.3861	.072	-35.301	1.101
			10.0	-55.8000*	7.9408	.000	-83.760	-27.840
			12.0	-79.9333*	12.0619	.000	-121.981	-37.886
			15.0	-106.1000*	10.4280	.000	-143.555	-68.645
			20.0	-135.2111*	6.5384	.000	-158.227	-112.195
		7.5	.0	95.1000*	5.0143	.000	77.671	112.529
			5.0	17.1000	5.3861	.072	-1.101	35.301
			10.0	-38.7000*	8.7102	.007	-68.155	-9.245
			12.0	-62.8333*	12.5818	.003	-105.705	-19.961
			15.0	-89.0000*	11.0252	.000	-127.278	-50.722
			20.0	-118.1111*	7.4540	.000	-143.194	-93.028
		10.0	.0	133.8000*	7.6934	.000	106.135	161.465
			5.0	55.8000*	7.9408	.000	27.840	83.760
			7.5	38.7000*	8.7102	.007	9.245	68.155
			12.0	-24.1333	13.8690	.600	-69.952	21.686
			15.0	-50.3000*	12.4740	.013	-91.929	-8.671
			20.0	-79.4111*	9.4661	.000	-111.011	-47.811
		12.0	.0	157.9333*	11.9006	.000	116.081	199.785
			5.0	79.9333*	12.0619	.000	37.886	121.981
			7.5	62.8333*	12.5818	.003	19.961	105.705
			10.0	24.1333	13.8690	.600	-21.686	69.952
			15.0	-26.1667	15.4284	.626	-76.583	24.250
			20.0	-55.2778*	13.1165	.010	-99.296	-11.260

15.0	.0	184.1000*	10.2409	.000	146.799	221.401
	5.0	106.1000*	10.4280	.000	68.645	143.555
	7.5	89.0000*	11.0252	.000	50.722	127.278
	10.0	50.3000*	12.4740	.013	8.671	91.929
	12.0	26.1667	15.4284	.626	-24.250	76.583
	20.0	-29.1111	11.6317	.228	-68.685	10.463
20.0	.0	213.2111*	6.2357	.000	190.590	235.833
	5.0	135.2111*	6.5384	.000	112.195	158.227
	7.5	118.1111*	7.4540	.000	93.028	143.194
	10.0	79.4111*	9.4661	.000	47.811	111.011
	12.0	55.2778*	13.1165	.010	11.260	99.296
	15.0	29.1111	11.6317	.228	-10.463	68.685

G.4.2 Temperature = 50 °C

ANOVA

		Sum of Squares	df	Mean Square	F	Sig.
Rotation	Between Groups	302687.886	6	50447.981	115.250	.000
	Within Groups	27139.100	62	437.727		
	Total	329826.986	68			
Pitch	Between Groups	84.345	6	14.058	9.510	.000
	Within Groups	91.649	62	1.478		
	Total	175.995	68			

Test of Homogeneity of Variances

	Levene Statistic	df1	df2	Sig.
Rotation	2.271	6	62	.048
Pitch	1.825	6	62	.109

Multiple Comparisons

Dependent Variable		(I) Distance	(J) Distance	Mean Difference (I-J)	Std. Error	Sig.	95% CI Lower Bound	95% CI Upper Bound
Rotation	Games-Howell	.0	5.0	-81.4000*	5.7902	.000	-101.736	-61.064
			7.5	-100.7000*	8.2667	.000	-130.144	-71.256
			10.0	-140.2000*	10.6958	.000	-178.879	-101.521
			12.0	-178.9000*	5.2840	.000	-196.930	-160.870
			15.0	-195.3000*	6.6677	.000	-218.624	-171.976
			20.0	-190.6000*	7.1554	.000	-215.793	-165.407
		5.0	.0	81.4000*	5.7902	.000	61.064	101.736
			7.5	-19.3000	9.4181	.426	-51.060	12.460
			10.0	-58.8000*	11.6087	.003	-98.826	-18.774
			12.0	-97.5000*	6.9486	.000	-120.703	-74.297
			15.0	-113.9000*	8.0512	.000	-140.724	-87.076
			20.0	-109.2000*	8.4594	.000	-137.464	-80.936
		7.5	.0	100.7000*	8.2667	.000	71.256	130.144
			5.0	19.3000	9.4181	.426	-12.460	51.060
			10.0	-39.5000	13.0221	.088	-82.896	3.896
			12.0	-78.2000*	9.1157	.000	-109.151	-47.249
			15.0	-94.6000*	9.9816	.000	-127.801	-61.399
			20.0	-89.9000*	10.3138	.000	-124.083	-55.717
		10.0	.0	140.2000*	10.6958	.000	101.521	178.879
			5.0	58.8000*	11.6087	.003	18.774	98.826
			7.5	39.5000	13.0221	.088	-3.896	82.896
			12.0	-38.7000	11.3647	.057	-78.239	.839
			15.0	-55.1000*	12.0704	.006	-96.054	-14.146
			20.0	-50.4000*	12.3465	.013	-92.010	-8.790
		12.0	.0	178.9000*	5.2840	.000	160.870	196.930
			5.0	97.5000*	6.9486	.000	74.297	120.703
			7.5	78.2000*	9.1157	.000	47.249	109.151
			10.0	38.7000	11.3647	.057	-.839	78.239
			15.0	-16.4000	7.6952	.380	-42.056	9.256

			20.0	-11.7000	8.1214	.773	-38.922	15.522
		15.0						
			.0	195.3000*	6.6677	.000	171.976	218.624
			5.0	113.9000*	8.0512	.000	87.076	140.724
			7.5	94.6000*	9.9816	.000	61.399	127.801
			10.0	55.1000*	12.0704	.006	14.146	96.054
			12.0	16.4000	7.6952	.380	-9.256	42.056
			20.0	4.7000	9.0826	.998	-25.336	34.736
		20.0	.0	190.6000*	7.1554	.000	165.407	215.793
			5.0	109.2000*	8.4594	.000	80.936	137.464
			7.5	89.9000*	10.3138	.000	55.717	124.083
			10.0	50.4000*	12.3465	.013	8.790	92.010
			12.0	11.7000	8.1214	.773	-15.522	38.922
			15.0	-4.7000	9.0826	.998	-34.736	25.336
Pitch	LSD	.0	5.0	2.27867*	.55863	.000	1.1620	3.3954
			7.5	1.22400*	.54373	.028	.1371	2.3109
			10.0	2.54000*	.54373	.000	1.4531	3.6269
			12.0	2.20700*	.54373	.000	1.1201	3.2939
			15.0	3.61900*	.54373	.000	2.5321	4.7059
			20.0	2.94700*	.54373	.000	1.8601	4.0339
		5.0	.0	-2.27867*	.55863	.000	-3.3954	-1.1620
			7.5	-1.05467	.55863	.064	-2.1714	.0620
			10.0	.26133	.55863	.642	-.8554	1.3780
			12.0	-.07167	.55863	.898	-1.1884	1.0450
			15.0	1.34033*	.55863	.019	.2236	2.4570
			20.0	.66833	.55863	.236	-.4484	1.7850
		7.5	.0	-1.22400*	.54373	.028	-2.3109	-.1371
			5.0	1.05467	.55863	.064	-.0620	2.1714
			10.0	1.31600*	.54373	.018	.2291	2.4029
			12.0	.98300	.54373	.075	-.1039	2.0699
			15.0	2.39500*	.54373	.000	1.3081	3.4819
			20.0	1.72300*	.54373	.002	.6361	2.8099
		10.0						
			.0	-2.54000*	.54373	.000	-3.6269	-1.4531

		5.0	-.26133	.55863	.642	-1.3780	.8554
		7.5	-1.31600*	.54373	.018	-2.4029	-.2291
		12.0	-.33300	.54373	.542	-1.4199	.7539
		15.0	1.07900	.54373	.052	-.0079	2.1659
		20.0	.40700	.54373	.457	-.6799	1.4939
	12.0	.0	-2.20700*	.54373	.000	-3.2939	-1.1201
		5.0	.07167	.55863	.898	-1.0450	1.1884
		7.5	-.98300	.54373	.075	-2.0699	.1039
		10.0	.33300	.54373	.542	-.7539	1.4199
		15.0	1.41200*	.54373	.012	.3251	2.4989
		20.0	.74000	.54373	.178	-.3469	1.8269
	15.0	.0	-3.61900*	.54373	.000	-4.7059	-2.5321
		5.0	-1.34033*	.55863	.019	-2.4570	-.2236
		7.5	-2.39500*	.54373	.000	-3.4819	-1.3081
		10.0	-1.07900	.54373	.052	-2.1659	.0079
		12.0	-1.41200*	.54373	.012	-2.4989	-.3251
		20.0	-.67200	.54373	.221	-1.7589	.4149
	20.0	.0	-2.94700*	.54373	.000	-4.0339	-1.8601
		5.0	-.66833	.55863	.236	-1.7850	.4484
		7.5	-1.72300*	.54373	.002	-2.8099	-.6361
		10.0	-.40700	.54373	.457	-1.4939	.6799
		12.0	-.74000	.54373	.178	-1.8269	.3469
		15.0	.67200	.54373	.221	-.4149	1.7589

G.5 Temperature Effects Statistical Analysis – ANOVA of Distance vs. Pitch and Rotation

G.5.1 Distance = 0 meters

ANOVA

		Sum of Squares	df	Mean Square	F	Sig.
Rotation	Between Groups	25560.867	2	12780.433	17.773	.000
	Within Groups	19415.300	27	719.085		
	Total	44976.167	29			
Pitch	Between Groups	16.155	2	8.078	1.469	.248
	Within Groups	148.514	27	5.501		
	Total	164.670	29			

Test of Homogeneity of Variances

	Levene Statistic	df1	df2	Sig.
Rotation	25.241	2	27	.000
Pitch	2.702	2	27	.085

Multiple Comparisons

Dependent Variable		(I) Temperature	(J) Temperature	Mean Difference (I-J)	Std. Error	Sig.	95% CI Lower Bound	95% CI Upper Bound
Rotation	Games -Howell	-20.00	23.00	-59.1000*	14.4618	.006	-99.184	-19.016
			50.00	5.3000	3.2885	.268	-3.128	13.728
		23.00	-20.00	59.1000*	14.4618	.006	19.016	99.184
			50.00	64.4000*	14.5428	.004	24.244	104.556
		50.00	-20.00	-5.3000	3.2885	.268	-13.728	3.128
			23.00	-64.4000*	14.5428	.004	-104.556	-24.244

G.5.2 Distance = 5 meters

ANOVA

		Sum of Squares	df	Mean Square	F	Sig.
Rotation	Between Groups	9829.552	2	4914.776	5.784	.008
	Within Groups	22091.000	26	849.654		
	Total	31920.552	28			
Pitch	Between Groups	6.922	2	3.461	.572	.572
	Within Groups	157.432	26	6.055		
	Total	164.354	28			

Test of Homogeneity of Variances

	Levene Statistic	df1	df2	Sig.
Rotation	5.858	2	26	.008
Pitch	3.672	2	26	.039

Multiple Comparisons

Dependent Variable		(I) Temperature	(J) Temperature	Mean Difference (I-J)	Std. Error	Sig.	95% CI Lower Bound	95% CI Upper Bound
Rotation	Games-Howell	-20.00	23.00	-37.8000	14.9633	.072	-79.046	3.446
			50.00	1.9000	5.9197	.945	-13.804	17.604
		23.00	-20.00	37.8000	14.9633	.072	-3.446	79.046
			50.00	39.7000	15.5803	.064	-2.274	81.674
		50.00	-20.00	-1.9000	5.9197	.945	-17.604	13.804
			23.00	-39.7000	15.5803	.064	-81.674	2.274

G.5.3 Distance = 10 meters

ANOVA

		Sum of Squares	df	Mean Square	F	Sig.
Rotation	Between Groups	7732.367	2	3866.184	8.045	.002
	Within Groups	12494.322	26	480.551		
	Total	20226.690	28			
Pitch	Between Groups	6.239	2	3.119	2.758	.082
	Within Groups	29.411	26	1.131		
	Total	35.650	28			

Test of Homogeneity of Variances

	Levene Statistic	df1	df2	Sig.
Rotation	1.189	2	26	.321
Pitch	1.969	2	26	.160

Multiple Comparisons

Dependent Variable		(I) Temperature	(J) Temperature	Mean Difference (I-J)	Std. Error	Sig.	95% CI Lower Bound	95% CI Upper Bound
Rotation	LSD	-20.00	23.00	-35.4444*	10.0722	.002	-56.148	-14.741
			50.00	-.3000	9.8036	.976	-20.452	19.852
		23.00	-20.00	35.4444*	10.0722	.002	14.741	56.148
			50.00	35.1444*	10.0722	.002	14.441	55.848
		50.00	-20.00	.3000	9.8036	.976	-19.852	20.452
			23.00	-35.1444*	10.0722	.002	-55.848	-14.441

G.5.4 Distance = 12 meters

ANOVA

		Sum of Squares	df	Mean Square	F	Sig.
Rotation	Between Groups	1817.472	2	908.736	1.399	.265
	Within Groups	16891.700	26	649.681		
	Total	18709.172	28			
Pitch	Between Groups	.854	2	.427	.299	.744
	Within Groups	37.159	26	1.429		
	Total	38.012	28			

G.5.5 Distance = 15 meters

ANOVA

		Sum of Squares	df	Mean Square	F	Sig.
Rotation	Between Groups	2693.348	2	1346.674	.822	.449
	Within Groups	49134.712	30	1637.824		
	Total	51828.061	32			
Pitch	Between Groups	10.948	2	5.474	.705	.502
	Within Groups	232.796	30	7.760		
	Total	243.744	32			

G.5.6 Distance = 20 meters

ANOVA

		Sum of Squares	df	Mean Square	F	Sig.
Rotation	Between Groups	4761.618	2	2380.809	7.077	.004
	Within Groups	8410.489	25	336.420		
	Total	13172.107	27			
Pitch	Between Groups	3.958	2	1.979	2.638	.091
	Within Groups	18.753	25	.750		
	Total	22.711	27			

Test of Homogeneity of Variances

	Levene Statistic	df1	df2	Sig.
Rotation	.392	2	25	.680
Pitch	.104	2	25	.901

Multiple Comparisons

Dependent Variable		(I) Temperature	(J) Temperature	Mean Difference (I-J)	Std. Error	Sig.	95% CI Lower Bound	95% CI Upper Bound
Rotation	LSD	-20.00	23.00	1.4444	8.6464	.869	-16.363	19.252
			50.00	27.9111*	8.4274	.003	10.554	45.268
		23.00	-20.00	-1.4444	8.6464	.869	-19.252	16.363
			50.00	26.4667*	8.4274	.004	9.110	43.823
		50.00	-20.00	-27.9111*	8.4274	.003	-45.268	-10.554
			23.00	-26.4667*	8.4274	.004	-43.823	-9.110

Annex H Task 8 Data

H.1 Risk of Penetration Raw Data

Round #	Distance to Target (m)	Velocity (fps)	Mass (Kg)	Outcome	Chassis separation
1	2	222	0.01849	Perforation	yes
2	2	error	0.01860	Perforation	no
3	2	244	0.01847	Perforation	yes
4	2	229	0.01849	Perforation	yes
5	2	241	0.01859	Perforation	yes
6	2	misfire	N/A	N/A	N/A
7	2	250	0.01840	perforation	yes
8	2	227	0.01865	perforation	yes
9	2	225	0.01863	perforation	yes
10	2	225	0.01851	perforation	yes
11	2	241	0.01857	perforation	no
12	2	255	0.01857	perforation	no
Average		235.9	18.54273	100%	80%
Stnd. Dev		11.7	0.076432		
1	5	228.0	0.01869	perforation	no
2	5	230.0	0.01869	perforation	no
3	5	233.0	0.01862	perforation	yes
4	5	240.0	0.01861	laceration	yes
5	5	230.0	0.01864	perforation	yes
6	5	223.0	0.01868	perforation	no
7	5	231.0	0.01858	perforation	yes
8	5	error	0.01860	perforation	yes
9	5	225.0	0.01863	perforation	yes
10	5	225.0	0.01845	perforation	yes
11	5	218.0	0.01859	Perforation	no
Average		228.3	0.01862	90%	60%
Stnd. Dev		6.0	0.067568		

Annex I Task 9 Data

I.1 Risk of Blunt Trauma Raw Data

Round #	Distance to Target (m)	Velocity (fps)	Mass (Kg)	Max. Disp. (mm)	Vc_{Max}
1	2	225.0	0.01856	0.033	0.0717
2	2	233.0	0.01856	0.035	0.0754
3	2	230.0	0.01854	0.037	0.0730
4	2	236.0	0.01843	0.035	0.0732
5	2	231.0	0.01845	0.032	0.0511
6	2	226.0	0.01852	0.032	0.0511
7	2	225.0	0.01843	0.030	0.0416
8	2	229.0	0.01851	0.038	0.0665
9	2	244.0	0.01859	0.038	0.0665
10	2	225.0	0.01850	0.035	0.0462
Average		230.4	0.01851	0.035	0.0616
Stnd. Dev		6.1	0.00056	0.003	0.0127

Annex J Task 10 Data

J.1 Training Round Raw Data

Round #	Target Distance (m)	Velocity (fps)	Pitch (Deg)	Distance (m)	Rotations (RPS)	Pitch (Deg)	Distance (m)	Rotations (RPS)	X Coordinate (cm)	Y Coordinate (cm)
1	5	229	-3.2°	1	64	-0.6°	5	208	-1.72	-3.97
2	5	237	-5.3°	1	60	-1.8°	5	190	-0.09	-5.02
3	5	258	-3.6°	1	N/A	-1.2°	5	196	-2.37	-5.74
4	5	231	-5.3°	1	74	-1.3°	5	185	-1.70	-4.91
5	5	254	4.8°	1	N/A	8.4°	5	208	-0.06	-0.05
6	5	248	0.5°	1	71	-2.5°	5	230	-2.40	-4.00
7	5	241	0.5°	1	58	-3.0°	5	222	-2.20	-3.15
8	5	229	1.6°	1	56	-1.8°	5	222	-2.90	-2.09
9	5	234	4.3°	1	N/A	-0.6°	5	222	-2.35	-4.48
10	5	247	3.3°	1	67	2.5°	5	222	-3.39	-2.44
Average		240.8	-0.2°	1.0	64.2	-0.2°	5.0	210.7	-1.92	-3.58
Stnd. Dev		10.5	3.9°	0.0	6.8	3.4°	0.0	15.6	1.09	1.69
11	10	255		7.5	No Video		10	No Video	-3.54	-14.50
12	10	219	-1.7°	7.5	267	0.0°	10	303	-3.20	-13.83
13	10	227	-1.2°	7.5	278	0.8°	10	317	-5.21	-13.91
14	10	217	2.8°	7.5	230	0.7°	10	267	-1.17	-7.99
15	10	239	-3.5°	7.5	290	2.0°	10	317	-3.69	-7.67
16	10	221	-2.2°	7.5	247	1.4°	10	290	-3.52	-12.44
17	10	223	-0.6°	7.5	247	0.6°	10	267	0.08	-5.39
18	10	230	-0.6°	7.5	238		10	NA	-3.54	-20.48
19	10	237	-2.3°	7.5	317	0.0°	10	351	-5.61	-11.79

20	10	240	0.0°	7.5	290	1.3°	10	333	-3.71	-12.69
21	10	245	-2.8°	7.5	333	0.0°	10	351	-5.19	-10.57
22	10	228	-0.6°	7.5	303	0.7°	10	333	-4.64	-12.35
Average		231.8	-1.1°	7.5	276.3	0.7°	10.0	313.0	-3.80	-11.97
Stnd. Dev		11.6	1.7°	0.0	33.9	0.7°	0.0	31.0	1.65	3.89
23	15	219		12		0.0°	15	351	-10.91	-25.37
24	15	216		12			15		-2.46	-18.31
25	15	239		12			15		-6.55	-22.64
26	15	220	-4.2°	12	333	-3.9°	15	333	-8.52	-31.68
27	15	227	-2.2°	12	333	-0.7°	15	370	-2.41	-29.32
28	15	232		12		-1.6°	15	317	-15.00	-18.74
29	15	223	1.3°	12	303	1.7°	15	333	n/a	n/a
30	15	228	-1.3°	12	333	0.8°	15	351	-14.23	-27.04
31	15	233		12			15		0.24	-11.29
32	15	222	-2.9°	12	333	0.0°	15	333	-10.94	-20.74
33	15	172	0.0°	12	303	0.9°	15		n/a	n/a
34	15	227	-3.0°	12	303	1.4°	15	317	-3.16	-24.19
35	15	67	-2.0°	12	290		15		n/a	n/a
36	15	230	-3.0°	12	333	1.4°	15	333	-9.66	-27.81
37	15	245	-3.4°	12	351	0.0°	15	370	-6.74	-24.87
Average		213.3	-2.1°	12.0	321.6	0.0°	15.0	341.1	-7.53	-23.50
Stnd. Dev		43.6	1.7°	0.0	20.0	1.6°	0.0	19.0	4.88	5.60
38	20	243					20	351	-7.97	-34.43
39	20	226				0.0°	20	333	-19.01	-47.33
40	20	221				0.0°	20	351	-19.04	-45.40
41	20	213				-2.3°	20	333	-10.58	-51.34
42	20	217				-1.2°	20		-9.82	-42.21
43	20	221					20	333	-1.75	-57.06

44	20	203				-2.73	20	333	-9.77	-45.78
45	20	Error					20		NA	NA
46	20	212				-1.245	20	351	-9.83	-45.95
47	20	Error					20		NA	NA
48	20	206				-2.6°	20	351	-15.99	-51.71
49	20	212				-1.145	20	370	-10.97	-46.49
50	20	217				-1.3	20	351	-12.17	-42.58
51	20	223				0	20	370	-13.46	-48.28
Average		217.8				-1.4°	20.0	342.1	-11.70	-46.80
Stnd. Dev		10.4				1.2°	0.0	9.4	4.81	6.40

J.2 Training Round Statistical Analysis

J.2.1 ANOVA of In-flight Characteristics

ANOVA

		Sum of Squares	df	Mean Square	F	Sig.
Pitch	Between Groups	54.402	6	9.067	1.784	.116
	Within Groups	330.445	65	5.084		
	Total	384.847	71			
Rotations	Between Groups	484194.641	6	80699.107	157.899	.000
	Within Groups	31175.874	61	511.080		
	Total	515370.515	67			

Test of Homogeneity of Variances

	Levene Statistic	df1	df2	Sig.
Pitch	5.186	6	65	.000
Rotations	4.354	6	61	.001

Multiple Comparisons

Dependent Variable		(I) Distance	(J) Distance	Mean Difference (I-J)	Std. Error	Sig.	95% Confidence Interval	
							Lower Bound	Upper Bound
Rotations	Games-Howell	1	5	-146.21429*	5.56619	.000	-165.4284	-127.0002
			8	-212.07792*	10.48491	.000	-249.2155	-174.9404
			10	-248.61429*	10.09225	.000	-285.0330	-212.1956
			12	-257.21429*	6.77940	.000	-281.0339	-233.3947
			15	-276.51429*	6.56211	.000	-299.5063	-253.5223
			20	-283.31429*	5.25813	.000	-301.3715	-265.2571
		5	1	146.21429*	5.56619	.000	127.0002	165.4284
			8	-65.86364*	11.30908	.001	-104.3225	-27.4048
			10	-102.40000*	10.94603	.000	-140.0531	-64.7469
			12	-111.00000*	7.99514	.000	-137.5860	-84.4140
			15	-130.30000*	7.81174	.000	-156.2293	-104.3707
			20	-137.10000*	6.75352	.000	-159.4300	-114.7700
		8	1	212.07792*	10.48491	.000	174.9404	249.2155
			5	65.86364*	11.30908	.001	27.4048	104.3225
			10	-36.53636	14.09846	.183	-82.8440	9.7713
			12	-45.13636*	11.95296	.021	-85.0695	-5.2032
			15	-64.43636*	11.83107	.001	-104.0685	-24.8043
			20	-71.23636*	11.16069	.000	-109.4016	-33.0711
		10	1	248.61429*	10.09225	.000	212.1956	285.0330
			5	102.40000*	10.94603	.000	64.7469	140.0531
			8	36.53636	14.09846	.183	-9.7713	82.8440
			12	-8.60000	11.61005	.987	-47.7286	30.5286
			15	-27.90000	11.48453	.252	-66.7247	10.9247
			20	-34.70000	10.79264	.076	-72.0654	2.6654
		12	1	257.21429*	6.77940	.000	233.3947	281.0339
			5	111.00000*	7.99514	.000	84.4140	137.5860

		8	45.13636*	11.95296	.021	5.2032	85.0695
		10	8.60000	11.61005	.987	-30.5286	47.7286
		15	-19.30000	8.71786	.336	-48.1121	9.5121
		20	-26.10000*	7.78382	.049	-52.0917	-.1083
	15	1	276.51429*	6.56211	.000	253.5223	299.5063
		5	130.30000*	7.81174	.000	104.3707	156.2293
		8	64.43636*	11.83107	.001	24.8043	104.0685
		10	27.90000	11.48453	.252	-10.9247	66.7247
		12	19.30000	8.71786	.336	-9.5121	48.1121
		20	-6.80000	7.59532	.968	-32.1043	18.5043
	20	1	283.31429*	5.25813	.000	265.2571	301.3715
		5	137.10000*	6.75352	.000	114.7700	159.4300
		8	71.23636*	11.16069	.000	33.0711	109.4016
		10	34.70000	10.79264	.076	-2.6654	72.0654
		12	26.10000*	7.78382	.049	.1083	52.0917
		15	6.80000	7.59532	.968	-18.5043	32.1043

J.2.2 ANOVA of Accuracy and Precision

ANOVA

		Sum of Squares	df	Mean Square	F	Sig.
Velocity	Between Groups	2986.751	3	995.584	9.390	.000
	Within Groups	4453.183	42	106.028		
	Total	7439.935	45			
X	Between Groups	648.304	3	216.101	16.286	.000
	Within Groups	557.319	42	13.269		
	Total	1205.623	45			
Y	Between Groups	11855.003	3	3951.668	187.635	.000
	Within Groups	884.537	42	21.060		
	Total	12739.540	45			

Test of Homogeneity of Variances

	Levene Statistic	df1	df2	Sig.
Velocity	.690	3	42	.563
X	6.666	3	42	.001
Y	2.094	3	42	.115

Multiple Comparisons

Dependent Variable		(I) Distance	(J) Distance	Mean Difference (I-J)	Std. Error	Sig.	95% Confidence Interval Lower Bound	95% Confidence Interval Upper Bound
Velocity	LSD	5.00	10.00	9.05000*	4.40891	.046	.1525	17.9475
			15.00	12.63333*	4.40891	.006	3.7358	21.5309
			20.00	22.96667*	4.40891	.000	14.0691	31.8642
		10.00	5.00	-9.05000*	4.40891	.046	-17.9475	-.1525
			15.00	3.58333	4.20373	.399	-4.9001	12.0668
			20.00	13.91667*	4.20373	.002	5.4332	22.4001
		15.00	5.00	-12.63333*	4.40891	.006	-21.5309	-3.7358
			10.00	-3.58333	4.20373	.399	-12.0668	4.9001
			20.00	10.33333*	4.20373	.018	1.8499	18.8168
		20.00	5.00	-22.96667*	4.40891	.000	-31.8642	-14.0691
			10.00	-13.91667*	4.20373	.002	-22.4001	-5.4332
			15.00	-10.33333*	4.20373	.018	-18.8168	-1.8499
X	Games-Howell	5.00	10.00	1.66033*	.58770	.048	.0089	3.3117
			15.00	5.61033*	1.45109	.010	1.3180	9.9027
			20.00	9.77867*	1.43074	.000	5.5485	14.0089
		10.00	5.00	-1.66033*	.58770	.048	-3.3117	-.0089
			15.00	3.95000	1.48760	.080	-.3953	8.2953
			20.00	8.11833*	1.46776	.000	3.8341	12.4026
		15.00	5.00	-5.61033*	1.45109	.010	-9.9027	-1.3180
			10.00	-3.95000	1.48760	.080	-8.2953	.3953
			20.00	4.16833	1.97853	.182	-1.3258	9.6625
		20.00	5.00	-9.77867*	1.43074	.000	-14.0089	-5.5485
			10.00	-8.11833*	1.46776	.000	-12.4026	-3.8341
			15.00	-4.16833	1.97853	.182	-9.6625	1.3258
Y	LSD	5.00	10.00	8.38250*	1.96496	.000	4.4170	12.3480
			15.00	19.91500*	1.96496	.000	15.9495	23.8805
			20.00	42.96167*	1.96496	.000	38.9962	46.9271
		10.00	5.00	-8.38250*	1.96496	.000	-12.3480	-4.4170
			15.00	11.53250*	1.87352	.000	7.7516	15.3134

		20.00	34.57917*	1.87352	.000	30.7983	38.3601
	15.00	5.00	-19.91500*	1.96496	.000	-23.8805	-15.9495
		10.00	-11.53250*	1.87352	.000	-15.3134	-7.7516
		20.00	23.04667*	1.87352	.000	19.2658	26.8276
	20.00	5.00	-42.96167*	1.96496	.000	-46.9271	-38.9962
		10.00	-34.57917*	1.87352	.000	-38.3601	-30.7983
		15.00	-23.04667*	1.87352	.000	-26.8276	-19.2658

Annex K Task 11 Data

K.1 Physiology Raw Data

K.1.1 Electrolytes and Hematology

	Specimen	Baseline	Post-Exposure	1 hour	2 hour	3 hour	4 hour
Na	9013	140	144	134	140	133	133
	9010	136	136	135	133	134	140
	9009	140	147	140	139	139	140
	9012	140	144	138	138	138	138
	9011	141	140	145	139	138	138
	Average	**139.4**	**142.2**	**138.4**	**137.8**	**136.4**	**137.8**
	Stnd. Dev.	**1.9**	**4.3**	**4.4**	**2.8**	**2.7**	**2.9**
K	9013	4.2	4.7	4.7	4.7	4.5	4.3
	9010	4	4.1	4.2	4.3	4.4	4.5
	9009	4.1	5	4.4	4.6	4.7	4.9
	9012	4.3	4.3	4.7	4.6	4.7	4.7
	9011	4.3	5	4.8	4.6	4.5	4.5
	Average	**4.2**	**4.6**	**4.6**	**4.6**	**4.6**	**4.6**
	Stnd. Dev.	**0.1**	**0.4**	**0.3**	**0.2**	**0.1**	**0.2**
Hematocrit	9013	22	26	22	22	19	20
	9010	24	25	21	20	21	21
	9009	29	32	29	24	23	22
	9012	24	29	24	22	21	22
	9011	22	25	22	22	22	21
	Average	**24.2**	**27.4**	**23.6**	**22.0**	**21.2**	**21.2**
	Stnd. Dev.	**2.9**	**3.0**	**3.2**	**1.4**	**1.5**	**0.8**
Hemoglobin	9013	7.5	8.8	7.5	7.5	6.5	6.8
	9010	8.2	8.5	7.1	6.8	7.1	7.1
	9009	9.9	10.9	9.9	8.2	7.8	7.5
	9012	8.2	9.9	8.2	7.5	7.1	7.5
	9011	7.5	8.5	7.5	7.5	7.5	7.1
	Average	**8.3**	**9.3**	**8.0**	**7.5**	**7.2**	**7.2**
	Stnd. Dev.	**1.0**	**1.1**	**1.1**	**0.5**	**0.5**	**0.3**

K.1.2 Blood Gases and Alkaloids

	Specimen	Baseline	Post-Exposure	1 hour	2 hour	3 hour	4 hour
PCO_2	9013	42.0	88.9	53.8	50.2	51.2	50.1
	9010	47.2	57.4	47.8	42.1	43.3	43.2
	9009	43.4	85.0	43.5	40.4	38.9	38.5
	9012	52.5	83.1	48.2	51.2	47.7	51.1
	9011	49.3	83.6	47.6	44.8	39.6	38.5
	Average	**46.9**	**79.6**	**48.2**	**45.7**	**44.1**	**44.3**
	Stnd. Dev.	**4.3**	**12.6**	**3.7**	**4.8**	**5.3**	**6.1**
PO_2	9013	244	282	294	420	335	321
	9010	377	347	436	390	449	406
	9009	371	421	391	447	481	425
	9012	336	251	302	351	259	246
	9011	249	292	305	336	323	283
	Average	**315.4**	**318.6**	**345.6**	**388.8**	**369.4**	**336.2**
	Stnd. Dev.	**64.8**	**66.9**	**64.1**	**46.3**	**92.6**	**77.4**
HCO_3	9013	28.2	27.2	31.9	32.9	34.7	35.7
	9010	32.3	30.8	35.2	34.4	34.5	34.1
	9009	25.0	22.5	24.1	28.0	28.9	29.5
	9012	28.2	24.6	27.1	29.2	28.4	29.5
	9011	26.6	26.9	28.6	29.2	28.3	28.7
	Average	**28.1**	**26.4**	**29.4**	**30.7**	**31.0**	**31.5**
	Stnd. Dev.	**2.7**	**3.1**	**4.3**	**2.8**	**3.3**	**3.2**
Lactate	9013	0.85	8.75	1.3	0.45	0.5	0.52
	9010	0.59	3.71	0.79	0.71	0.71	0.66
	9009	0.57	12.12	1.91	0.53	0.39	0.35
	9012	<0.3	8.33	0.82	0.36	<0.3	<0.3
	9011	0.38	6.61	0.61	0.43	0.54	0.5
	Average	**0.60**	**7.90**	**1.09**	**0.50**	**0.54**	**0.51**
	Stnd. Dev.	**0.19**	**3.08**	**0.53**	**0.13**	**0.13**	**0.13**
pH	9013	7.435	7.094	7.381	7.424	7.439	7.461
	9010	7.444	7.338	7.475	7.520	7.509	7.506
	9009	7.370	7.031	7.352	7.449	7.478	7.492
	9012	7.338	7.080	7.358	7.364	7.382	7.370

	9011	7.340	7.115	7.387	7.422	7.462	7.481
	Average	**7.385**	**7.132**	**7.391**	**7.436**	**7.454**	**7.462**
	Stnd. Dev.	**0.051**	**0.119**	**0.049**	**0.056**	**0.048**	**0.054**

K.1.3 Vital sign data

	Specimen	Baseline	Post-Exposure	1 hour	2 hour	3 hour	4 hour
CO	9013	3.5	6.1	4.2	4.0	3.9	3.8
	9010	4.4	5.6	4.6	3.6	4.0	3.6
	9009	4.4	5.5	4.4	3.7	3.2	3.0
	9012	4.9	6.8	4.3	4.1	4.1	3.7
	9011	5.9	10.1	5.9	5.5	4.8	4.7
	Average	**4.6**	**6.8**	**4.7**	**4.2**	**4.0**	**3.8**
	Stnd. Dev.	**0.9**	**1.9**	**0.7**	**0.8**	**0.5**	**0.6**
HR	9013	55	114	62	57	56	54
	9010	77	70	73	62	64	63
	9009	85	95	78	66	58	59
	9012	74	84	60	60	62	59
	9011	119	121	109	91	78	67
	Average	**82.0**	**96.8**	**76.4**	**67.2**	**63.6**	**60.4**
	Stnd. Dev.	**23.4**	**21.0**	**19.7**	**13.7**	**8.6**	**4.9**
MAP	9013	74	74	80	76	79	81
	9010	90	89	78	85	77	77
	9009	72	71	85	76	74	74
	9012	76	72	87	79	72	72
	9011	96	88	71	70	63	67
	Average	**81.6**	**78.8**	**80.2**	**77.2**	**73.0**	**74.2**
	Stnd. Dev.	**10.7**	**8.9**	**6.3**	**5.4**	**6.2**	**5.3**
Temp	9013	38.00	38.31	38.31	38.28	38.30	37.99
	9010	38.64	38.52	38.07	37.74	37.81	37.97
	9009	38.28	38.29	37.59	37.40	37.20	37.75
	9012	38.18	38.12	37.69	37.60	37.47	37.45
	9011	38.11	38.29	38.05	37.72	37.44	37.62
	Average	**38.24**	**38.31**	**37.94**	**37.75**	**37.64**	**37.76**
	Stnd. Dev.	**0.24**	**0.14**	**0.30**	**0.33**	**0.43**	**0.23**

Annex L Final Report from Caleton University

REPORT FOR WAYNE STATE UNIVERSITY

ELECTRICAL CHARACTERIZATION

AND

EXAMINATION OF 20 XREP ROUNDS

prepared by Dave Dawson

Research Associate

approved by Dr. Andy Adler

Professor, Biomedical Engineering

Systems and Computer Engineering

Carleton University

September 30, 2011

REPORT FOR WAYNE STATE UNIVERSITY
ELECTRICAL CHARACTERIZATION
AND
EXAMINATION OF 20 XREP ROUNDS

Purpose:

The purpose of this report is to provide information on the electrical characteristics and performance of 20 rounds of the XREP shotgun shell electronics package. This work was funded, in part, by a contract to Carleton University (CU), Department of Systems and Computer Engineering, by Wayne State University, Department of Medicine.

Twenty rounds were provided to Carleton University by Wayne State University in early August 2011. These rounds contained only the electronics package since the propellant and firing mechanism had been removed prior to shipping to CU.

Method:

Our investigation followed 2 tracks:

1. Physical and mechanical. During the physical and mechanical examinations of two rounds we identified:
    a. conducting paths of the contact barbs,
    b. which components would produce electronic firing without destruction of the impact clips on the front-facing barb disk,
    c. which components were not necessary for electronic firing,
    d. optimum ways to obtain a signal from the electronics package. At the same time we looked for a way to re-fire the rounds since the first firing was designed to be the only firing due to an unknown consumable component in the electronics package. We isolated and removed batteries from one round and identified places where we could insert a replacement voltage.

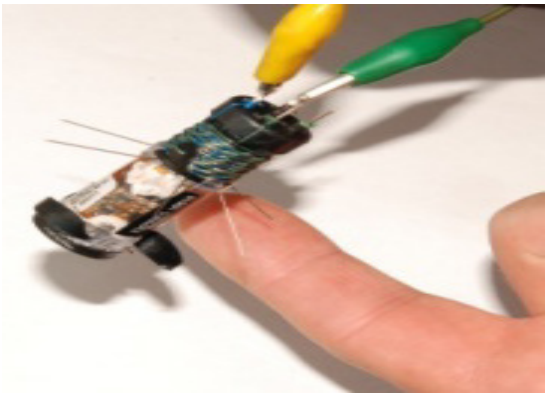

Figure 24: Principal conducting path

2. Electronic. We successfully captured signal from eleven rounds by pulling the trigger tab which was under compression but insulated from the electronics bed. When the trigger tab was pulled, the power supply was connected to the electronics package.

Figure 25: Trigger tab location

3. We were able to capture pulse trains and isolate individual waveshapes. The signal was sampled at various rates between 500 KS/s and 2 MS/s. For a small sample of waves we calculated total charge per pulse from 3 sample waveshapes in each pulsetrain (approximately pulses 10, 50, and 80 or later) to validate the integrity of the waveshape. We measured voltages and burst lengths and calculated pulse repetition frequencies.

Waveshapes were stored in .psdata format files and converted to .csv files for each buffer in the Pico Scope software acquisition train. A portion of one such file is included for illustration in this report at Appendix B.

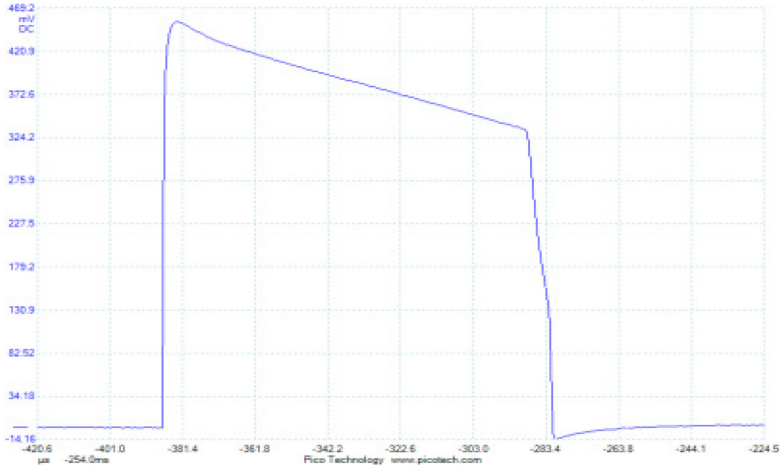

Figure 26:Single pulse waveshape geometry

Equipment:

All the equipment

we used for the physical and mechanical investigation was simple hand tools and low velocity / low impact power tools.

Our electronics test equipment consisted of a Pico Scope 4224 20 MHz dual channel oscilloscope, Dell Vostro laptop computer, Pico Scope 6.5.78.5 software, calibrated 600 ohm loads and Tektronix 6015A| high voltage probes. All connections were made in accordance with sound engineering practice and laboratory procedures. We also took some signals simultaneously with National Instruments pxi-5122 and Tektronix 3012 oscilloscopes but we found these instruments to yield less satisfactory results than the Pico Scope due to memory limitations and software malfunctions inherent in this equipment.

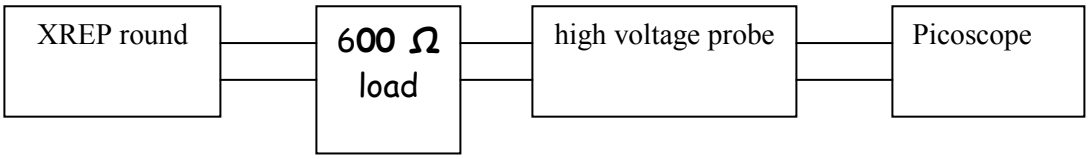

General Observations:

1. Pulse rates (pulses per second) were very stable in every round we examined.
2. Pulse trains demonstrated a brief interruption of 2-4 pulses twice in a pulse train of 100 pulses at approximately 1/3 and 2/3 of the way along the pulse train.

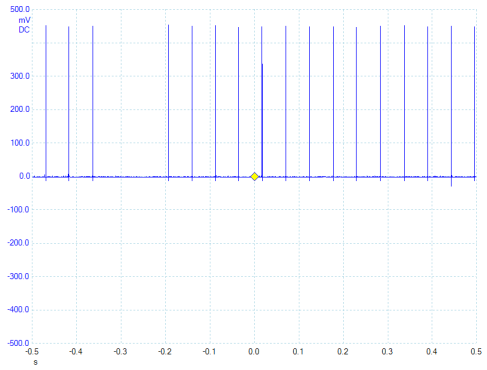

Figure 27: typical interruption in pulse train

3. The fidelity of waveshapes (geometry) was consistent over all the pulses we examined. We did not see any stray emissions, unwanted chatter or oscillations in the waveshapes.
4. Voltage amplitudes were within specifications published by the manufacturer. (450-550V). Specific values for each round are found in Appendix C.
5. Charge per pulse (50-90 µC) was within specifications published by the manufacturer. Specific values for each round are found in Appendix C.
6. Burst lengths of the pulses were the most variable characteristic of every pulse we examined but this characteristic was not specified by the manufacturer. We calculated an average burst length over the 11 rounds of 114µs although these lengths varied from 65µs to 161µs.

Table 1: Continuity Measurements to determine conductive paths

Continuity measurements (ohms)			
Front of barb disk		Blue wire (includes closest adjacent post)	To blue wire = 0 To black wire = ∞ To Rear-facing barbs = ∞ To Cholla barbs = ∞ To uninsulated tether = ∞
		Black wire (includes closest adjacent post)	To blue wire = ∞ To black wire = 0 To Rear-facing barbs = ∞ To Cholla barbs = ∞ To uninsulated tether = ∞
		Green Kevlar (1) Not a conductor	To blue wire = ∞ To black wire = ∞ To Rear-facing barbs = ∞ To Cholla barbs = ∞ To uninsulated tether= ∞
		Green Kevlar (2) Not a conductor	To blue wire = ∞ To black wire = ∞ To Rear-facing barbs = ∞ To Cholla barbs = ∞ To uninsulated tether= ∞

Back of barb disk		Rear-facing barbs (2) (common)	To blue wire = ∞ To black wire = ∞ To Rear-facing barbs = 0 To Cholla barbs = 0 To uninsulated tether = 0
		Uninsulated tether Is a conductor	To blue wire = ∞ To black wire = ∞ To Rear-facing barbs = 0 To Cholla barbs = 0 To uninsulated tether= 0
Top of electronics space		Cholla barbs (6) (common)	To blue wire = ∞ To black wire = ∞ To Rear-facing barbs = 0 To each other = 0 To uninsulated tether= 0

Results:

1. We were able to remove the hard plastic casing of the round to verify battery condition and fire the round without breaking the break-away pins on the barb disk at the head of the round or any destructive disassembly which would inhibit further mechanical investigation.
2. We successfully captured a large number of non-bipolar (ie dc) pulses from each round and verified the performance in accordance with the manufacturer's published performance specification found at appendix A. A tabulation of our results is found at Appendix C.
3. The single pulse waveshape from the original firing of each package was a simple descreasing triangular wave imposed on top of a square wave. Unlike the X-26 and M-26 emissions, this is not a complex waveshape.
4. We were able to re-fire the electronics manually on some of the rounds but the results were not significant. Although the re-fired waveshape was geometrically similar to the original, it was 0.01x the amplitude and roughly 50x the burst length.

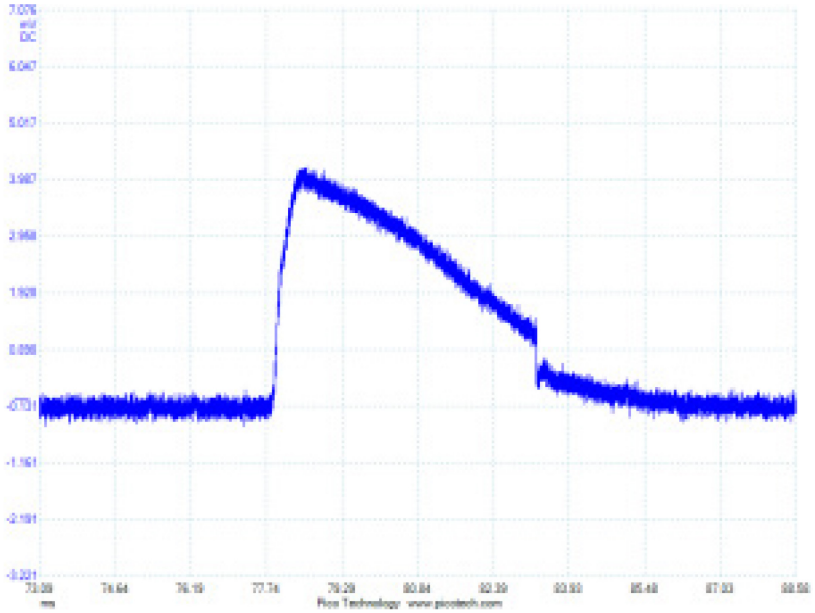

Figure 28: manually re-fired pulse

5. We did not successfully identify or isolate the consumable component which prevents re-firing the electronics so each pulse train that we captured was unique.

6. Nine rounds did not produce any usable results. We did not get a trace on either the first original firing or any indication of energy on re-firing. Measurement of the battery

voltage on 3 of the rounds indicated a short circuit between positive and negative terminals. A case-by-case analysis of why rounds did not fire is found in Appendix C.

7. Two of the nine rounds did not produce a usable trace because we were uncertain of the conductive paths between the black front-facing barbs and the rear-facing barbs.
8. Four of the nine rounds had been already fired. We presume that the trigger tab, which is quite fragile in its placement near the propellant assembly, had been pulled out during the removal of the propellant assembly.
9. Three of the nine rounds did not fire even though the trigger tab was intact before we pulled it.

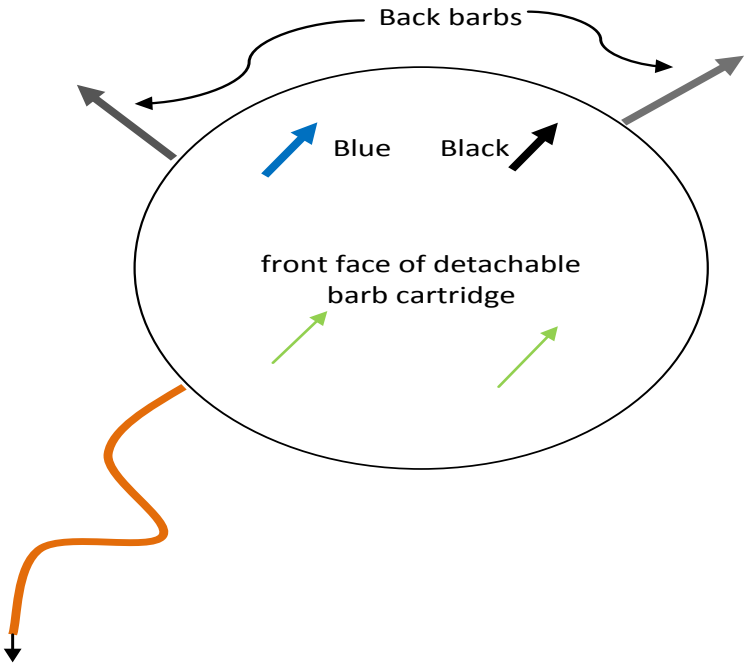

Figure 6: front barb disk

Appendix A: Manufacturer's XREP performance specification

Title: TASER® XREP™ Electronic Control Device (ECD) Specifications
Department: Research and Development
Version: 2.0
Release Date: 12/7/2009

Law Enforcement Models

Model	Model No.	Color	Range
XREP™ ECD	50002	Black	15' [4.57 m] minimum,[1,5] up to approximately 100' [30.48 m] max

Specifications

1. Output specifications[2,3,4]
   Waveform: DC Pulse
   Charge: 50–90 microcoulombs (µC)
   Pulse duration: 250–405 microseconds (µS)
   Pulse rate: 19 ± 1 pulses per second (pps)
   Peak loaded voltage: 450–550 volts (V)
   Cycle time: 20 ± 2 seconds
2. Operating temperature range: -4 °F [-20 °C] to 122 °F [50 °C]
3. Storage temperature range: -40 °F [-40 °C] to 167 °F [75 °C]
4. Relative humidity: Up to 85% (non-condensing)

Characteristics

1. Muzzle velocity[5]: Approximately 242 fps from TASER X12™ by Mossberg® 12-gauge shotgun. Approximately 266 fps from 18.5" Cylinder bore 12-gauge shotgun, any maker.
2. Blunt force impact energy[5] at 18": Approximately 44 foot pounds with 266 fps muzzle velocity. Approximately 36 foot pounds with 242 fps muzzle velocity.
3. Power source: Battery of two 3V DL1/3N Lithium cells connected in series.
4. Body design: Two-piece, main body and nose
5. Separation Method: Six pins shear upon impact separating the nose from the main body of the round.
6. Patent: U.S. 7042696, 7057872, 7218077, 7280340, 7327549, 7580237, and other patents pending.

Features

1. Propulsion: Custom high-low chamber design
2. Electrical connections
   Primary: Nose
   Secondary: Rear-facing barb, wire, six Cholla probes, two nose electrodes.
3. XREP ECD projectiles can be used with the TASER X12 and standard manufactured model single shot, double barrel, or pump action 12-gauge shotguns with a 2.75" to 3.5" chamber, designed to accept ammunition produced per SAAMI Standard Z.299.2-1992, sold to the market. XREP ECD projectiles will fire from a semi-automatic shotgun, but they will not cycle the action[6].
4. Warranty: 1-year failure to fire standard warranty[7].

Physical Characteristics[8]

	XREP ECD Projectile
Length of finished round inside shell (L)	2.62" [6.65 cm]
Length of projectile from bottom of wad to top of nose, minus probes	2.01" [5.1 cm]
Tether spread length	14" ± 1" [35.56 ± 2.5 cm]
Weight, projectile (approximate)	0.62 oz [18.3 g]
Weight, cartridge (approximate)	0.95 oz [27 g]
Stabilization method	Fins

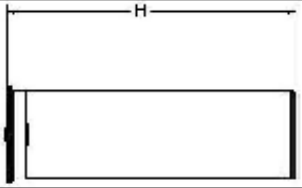

[1] The minimum safe distance for an XREP ECD projectile from the shotgun muzzle is 15 feet [4.57 meters].
[2] Product specifications may change without notice; actual product may vary from this picture.
[3] Pulse rate, charge, and peak voltage specifications at room temperature. Operating at temperatures below 32° F [0° C] can significantly reduce each output specification.
[4] Output specifications are derived from averaging 8 pulses while firing into a 2000 Ω (ohms) non-inductive resistive load at room temperature.
[5] Muzzle velocities and blunt force impact energies are approximate figures. These values may change due to environmental conditions.
[6] **XREP ECD projectiles will not fire through a choked shotgun barrel.**
[7] The warranty is for XREP ECDs fired from standard manufactured model single shot, double barrel, or pump action 12-gauge shotguns sold to the market. Additional terms and conditions may apply. Contact TASER International or visit www.TASER.com for additional warranty information.
[8] Dimensions and weights are for reference only.

TASER

Appendix B: extract from a CSV format of raw data file of a typical waveshape.

One sample every 0.0005 ms = 0.5 µs

$$fsample = \frac{1}{\frac{0.5(e-6)s}{Sample}} = \frac{2MSamples}{s}$$

Time,Channel A
(ms),(mV)

0.00000000,0.00000000
0.00050000,-0.61042600
0.00100000,-0.54938340
0.00150000,-0.61042600
0.00200000,-0.61042600
0.00250000,-0.61042600
0.00300000,0.00000000
...
...
...
524.28499868,-0.61042600
524.28549868,-0.61042600
524.28599868,-1.09876700
524.28649868,0.00000000
524.28699868,-0.61042600
524.28749868,-1.09876700

Appendix C: tabulation of results

		Action & Observations	Result
		Continuity tests, conducting paths identified, disassembly, polarity of batteries identified, signal taken from front (blue and black) barbs, original fire	V_{max} = 452V, V_{min} = 333V, Q = 66.3µC, prf = 20pps Burst length = 101.4µs
		Manual re-pulsing. Diminishing and distorting waveshape with successive manual re-pulses	V_{max} = 4.146V, V_{min} = 1.337V, Burst length = 5 ms
		Signal taken from front blue and 1 back-facing barb, original fire	V_{max} = 402V, V_{min} = 240V, Q = 80.25µC, prf = 20pps Burst length = 150µs
		Manual re-pulsing. Diminishing and distorting waveshape with successive manual re-pulses. No defined V_{min}, smooth decay	V_{max} = 4.548V, Burst length = 16 ms
		Further disassembly, remove batteries, manual repulsing, insert 4.98V dc in place of battery	Waveshape like X-26

		Original fire, black front barb > back barb. Not a conducting path.	No energy recorded
		Original fire, black front barb > back barb. Not a conducting path.	No energy recorded
		Exposed ± terminals without disrupting case Measure residual voltage on DLi cells. Don't need insertion of dc V.	$V_{residual}$ = 5.53V diminishing to 3.9V after 15 manual pulses
		Exposed ± terminals without disrupting case. Measure residual voltage on DLi cells	Batteries appear shorted. No re-pulsing possible
		Dual channel sensing	No energy recorded
		Blue to black front barbs.	V_{max} = 455V,

		Single channel sensing	V_{min} = 348V, Q = 67µC, prf = 20pps Burst length = 100µs

			Dual channel sensing. Blue to black Ch.A. Blue to back Ch.B. First 3 pulses showed evidence of processor decision-making on best path. First 3 pulses ChA < ChB and burst length was 230 µs, but the remainder of pulse train ChA > ChB. The amplitude was adjusted and then the burst length.	V_{maxA} = 410V, V_{maxB} = 332V V_{minA} = 242V, V_{minB} = 208V Q_A = 46.2 µC, Q_B = 37.4 µC Q_{total} = 83.6 µC prf = 20pps Burst $length_{stable}$ = 120µs
			did not fire. Unable to re-pulse	
			Dual channel sensing. Blue to black Ch.A. Blue to back Ch.B. Observed interruptions in pulse train in 6, 11 & 16. 3, 5, 2 pulses missing respectively. Total pulse train = 369 pulses in 20 buffers. Evaluation of pulse 10, pulse 50 and pulse 350 follows.	Coarse averages V_{maxA} =355V, V_{max} = 267V V_{minA} = 216V,V_{minB} = 185V, Q_A = 35.6 µC, Q_B = 24.1 µC, Q_{total} = 59.7 µC prf = 18.45 pps Burst $length_{stable}$ = 112µs
				V_{maxA} = 356 V,V_{maxB} = 268 V V_{minA} = 216 V, V_{minB} = 188 V Q_A = 34.9 µC, Q_B = 22.6 µC Q_{total} = 57.6 µC Burst $length_{stable}$ =

			112 µs
			V_{maxA} = 350 V, V_{maxB} = 267 V V_{minA} = 216 V, V_{minB} = 186 V Q_A = 34.6 µC, Q_B = 22.6 µC Q_{total} = 57.2 µC Burst $length_{stable}$ = 112 µs
			V_{maxA} = 355 V, V_{minA} = 213 V V_{maxB} = 265 V, V_{minB} = 183 V Q_A = 37.4 µC, Q_B = 27.3 µC Q_{total} = 64.8 µC Burst $length_{stable}$ = 112 µs

		Single channel sensing. blue to black. Observed interruptions in pulse train in buffers 7 & 12. 5 pulses missing in each case respectively. Total pulse train = 317 pulses in 17 buffers. f_s = 1MS/s	V_{max} = 477V, V_{min} = 347V, Q = 60.1µC, prf = 19pps Burst length = 87.5µs
		No data recorded.	

			Single channel sensing. blue to black. only 1 buffer saved = 14 pulses. single hand operation. f_s = 5 MS/s	V_{max} = 460V, V_{min} = 350V, Q = 71.3µC, prf = 19.2pps Burst length = 106µs
			Single channel sensing. blue to back. 7 buffers saved. Observed interruption in buffer 2, pulses 32-35 missing. Single hand operation. f_s = 1 MS/s	V_{max} = 422V, V_{min} = 227V, Q = 89.5µC, prf = 19.3pps Burst length = 161µs
			Single channel sensing. blue to back. Observed interruptions in pulse train in buffers 2, 7, 12 . 3/4/5 pulses missing respectively. Total pulse train = 178 pulses in 16 buffers. f_s = 1 MS/s	V_{max} = 422V, V_{min} = 242V, Q = 87.1µC, prf = 19.2pps Burst length = 157µs
			Single channel sensing. blue to black. f_s = 1 MS/s. Trigger tab not visible, nor present. Insulating strip still in place. Fired electronics with finger compression of tab after removing insulating strip. 32 pulses captured.	V_{max} = 465V, V_{min} = 354V, Q = 75.2µC, prf = 18.5pps Burst length = 110s
			Dud. trigger tab missing. Unable to fire.	
			Dual channel sensing. Ch.A blue to black. Ch.B blue to back. Observed	V_{maxA} = 369V, V_{minA} = 227V V_{maxB} = 269V,

			interruptions in pulse train in buffers 2 & 7. 3,5 pulses missing respectively. Total pulse train = 300 pulses in 16 buffers. f_s = 500 kS/s	V_{minB} = 194V Q_A = 32.1µC, Q_B = 24.9µC Q_{total} = 57µC Prf = 18.5pps Burst $length_{stable}$ = 65µs
			Dud. Trigger tab present but it had been pulled out. Unable to fire.	
			Dud. Trigger tab missing. Unable to fire.	
			Dud. Trigger tab missing. Unable to fire.	

Appendix C (cont'd): Analysis of rounds that did fire

SN	V_{max} (V)	Q (µC)	Burst length (µs)	prf (pps)
000163 Ch. A	355	66	101	20
000163 Ch. B	267			
000289	455	67	100	20
000313	452	66	101	20
000340	460	71	106	
000344 Ch. A	410	84	120	20
000344 Ch. B	332			
000358 Ch. A	369	57	65	18.5
000358 Ch. B	269			
000366	422	90	161	19.3
000403	477	60	88	19
000430	465	75	110	18.5
000457	422	87	157	19.2
000509	402	80	150	20

Average V_{max} of single channel captures = 388V
Average V_{max} of Ch. A in dual captures = 378V
Average V_{max} of Ch. B in dual captures = 289V

Average Q (total) = 73µC

Average burst length = 114µs

Appendix D: Analysis of rounds which did not fire or for which no data was recorded:

SN	Fault
000015	Trigger tab was missing. Tab appears to have been pulled out during removal of propellant chamber. Dead round.
000025	No data recorded. Dead round.
000049	Trigger tab was missing. Tab appears to have been pulled out during removal of propellant chamber. Dead round.
000078	No data recorded-our error. Black front barb to back barb is not a conducting path.
000113	No data recorded-our error. Black front barb to back barb is not a conducting path.
000316	No data recorded. Dead round.
000319	Trigger tab was missing. Tab appears to have been pulled out during removal of propellant chamber. Dead round.
000384	Trigger tab was missing. Tab appears to have been pulled out during removal of propellant chamber. Dead round.
000426	No data recorded. Dead round.

Summary: 4 rounds trigger tab missing, thus round was dead.
3 rounds all parts present but round was dead.
2 rounds wrong conductive path.

Appendix E: Titles of raw data files

	File ID	
1.	XREP firing manual re-fire 2807201111h30...psdata	
2.	20110815 SN 000313.psdata	
3.	20110816-001 SN 000313 re-fire w ext PS.psdata	
4.	20110816-0001 sn 000313 re-fire w external ps.psdata	
5.	20110815-001 SN 000509.psdata	
6.	20110815-001 SN 000509 re-fire.psdata	
7.	20110817-001 SN 000078 re-fire w on board battery.psdata	
8.	20110817-001 SN 000078 random re-fire w on board	

	battery.psdata	
9.	20110819-001 SN 000289.psdata	
10.	20110819-001 SN 000289 re-pulse.psdata	
11.	20110819-001 SN 000344 parallel capture.psdata	
12.	20110819-001 SN 000344 re-pulsed data.psdata	
13.	20110819-001 SN 000426 parallel capture.psdata	
14.	20110831-001 SN 000163.psdata	
15.	20110920-0001 SN 000316.psdata	
16.	20110920-001 SN 000340.psdata	
17.	20110920-001 SN 000358.psdata	
18.	20110920-001 SN 000403.psdata	
19.	20110920-001 SN 000430.psdata	

20.	20110920-001 SN 000457.psdata	
21.	20110920-001 SN 000366.psdata	
22.	Size of all data files	

List of symbols/abbreviations/acronyms/initialisms

°	Degree
%	Percent
μC	Microcoulomb
3-RBID	3-Rib Ballistic Impact Dummy
A	Amphere(s)
ABFO	American Board of Forensic Odontologists
AIS	Abbreviated Injury Scale
ANOVA	Analysis Of Variance
BioSID	Bio-Side Impact Dummy
BPM	Beats Per Minute
C	Celcius
cm	Centimeter
COP	Circle Of Precision
dL	Deciliter
DLAR	Division of Laboratory Animal Resources
DND	Department of National Defense
DRDC	Defense Research and Development Canada
DRDKIM	Director Research and Development Knowledge and Information Management
ECG	Electrocardiogram
FPS	Feet Per Second
FPS	Frames Per Second
g	Gram
HCO3	Bicarbonate
Hz	Hertz
IACUC	Institutional Animal Care and Use Committee
K	Potassium
Kg	Kilogram
L	Liter
LAL	Laceration Assessment Layer
LED	Light Emitting Diode
LSD	Lease Significant Difference
m	Meters(s)
mm	Millimeters
mmHg	Millimeters of Mercury (Hg)
mMol	Millimole
m/s	Meters Per Second
Na	Sodium
Na	Not Available
NIH	National Institutes of Health
N*m	Newton Meter
PAL	Penetration Assessment Layer
PCO2	Partial Pressure of Carbon Dioxide
PCV	Packed Cell Volume
PO2	Partial Pressure of Oxygen

PPS	Pulses Per Second
R & D	Research and Development
RPS	Rotations Per Second
s	Second(s)
SPSS	Statistical Package for the Social Sciences
SRS	Surgical Research Services
TI	TASER International
UK	United Kingdom
USA	United States of America
V	Volt(s)
VC	Viscous Criteria
VCmax	Maximum Viscous Criteria Value
WSU	Wayne State University
XREP	eXtended Range Electronic Projectile

Glossary

3-RBID - The 3-Rib Ballistic Impact Dummy is a biofidelic mechanical surrogate used for evaluating injury risk of blunt ballistic impacts [3].

Abbreviated Injury Scale (AIS) - The abbreviated injury scale is an ordinal scale used in triage to rank the severity of injuries. The scale is from 1-6 with increasing severity (1-Minor, 2-Moderate, 3-Serious, 4-Severe, 5-Critical and 6-Unsurvivable). [9]

Accuracy - A measurement of how closely a measured value agrees with the true value. For the current study, this represents how close the measured X and Y coordinates of the point of impact are to the X and Y coordinates of the point of aim (typically the center of the target).

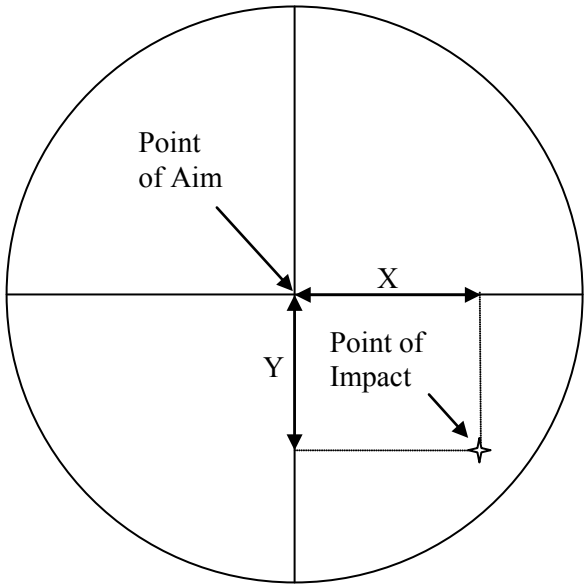

Figure 29 - Example of how accuracy is measured

Charge - A calculated value based on the value of voltage over time. The integral of the voltage over time shown below is used to calculate the amount of energy delivered by the XREP across a 600 ohm resistor.

Circle of Precision - The smallest circle in which all ten impacts for a given round fit. The center of the circle of precision is placed on the average X and Y coordinates.

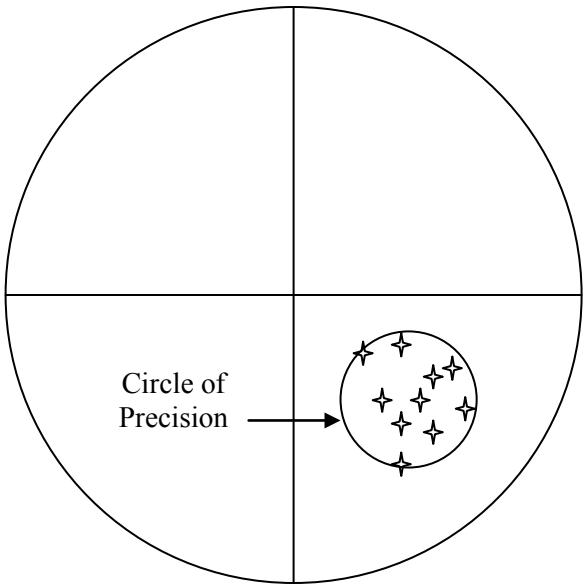

Figure 30 - Example of how circle of precision is measured

Fair Hit - A hit or impact is considered a fair hit if all required information is collected (velocity, video, etc) and the point of impact is no less than 1 inch from the edge of the surrogate, if a surrogate is being used.

Laceration Assessment Layer (LAL) - The external covering of the PAL used to assess the occurrence of laceration. The LAL is composed of an outer layer of natural (Sheep skin) chamois and an inner layer of 0.60 cm closed cell foam.

No Breakage - Classification for a round that, after being dropped, did not exhibit any flaws that would conceivably affect the round's performance. Abrasions and small deformities to the round's shotgun casing after being dropped were also classified as such.

Peak Current - The maximum current calculated for a single unique waveform using Ohm's Law

$$I = V / R$$

Equation 2 - Ohm's Law

Where I is the peak current, V is the peak voltage, R is the resistance. The manufacturer recommended load of 600 ohms was used.

Peak Voltage - The maximum voltage measured on a single unique waveform.

Penetration Assessment Layer (PAL) - The internal component of the penetration surrogate used to assess the occurrence of penetration. The PAL is composed of 20% ballistic gelatin.

Pitch - A measurement of the attitude of the projectile in-flight. Pitch is reported in degrees above (+) or below (-) horizontal. This variable describes the aerodynamic stability of the round. In the figure below, the pitch is the angle between the two lines (Figure 31)

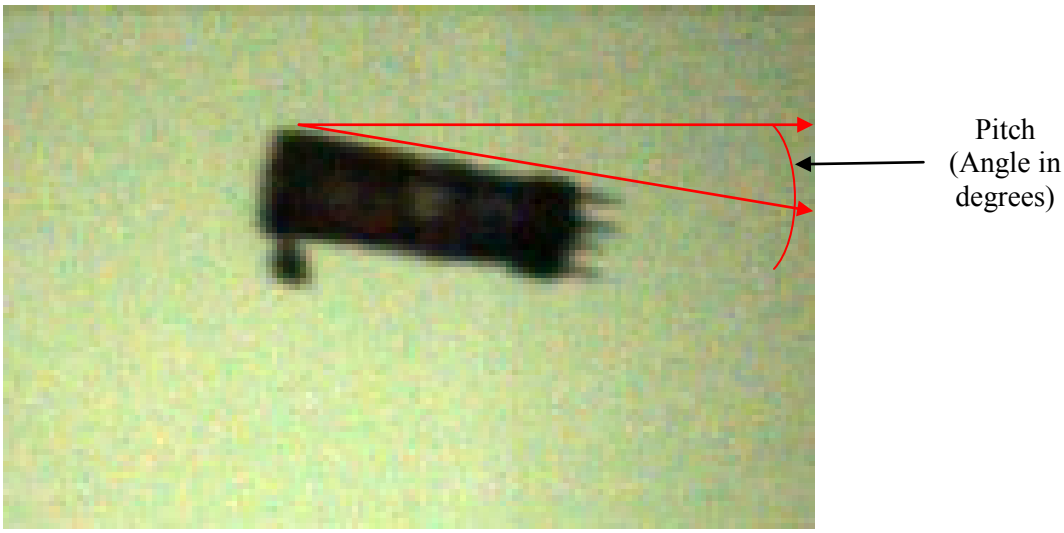

Figure 31 - Example of how pitch is measured

Precision - A measurement of how closely measured values agree with each other. For the current study, this represents how close the various impacts for a given test distance are to each other.

$$E = \int_{t=0}^{t=t\_end} V dt$$

Equation 3 - Equation for waveform charge

Where V is the voltage, t=0 is the start of the waveform and t_end is the end of the waveform

Primary Pulse Duration - A measurement of the time during which unique electrical waveforms are being generated.

Primary Pulse Frequency - A measurement of the quantity of unique electrical waveforms generated per second. The pulses per second (PPS) effect the quality of neuromuscular incapacitation (NMI) produced by the projectile.

Rotation - A measure of the number of rotations about the long axis of the projectile per second (RPS). The projectile is spin-stabilized and this variable also describes the aerodynamic stability of the round.

Slipped - The classification for a round that was displaced relative to the shotgun casing after being dropped. This displacement is positive for a displacement toward the muzzle end of the casing.

Viscous Criterion (VC) - An injury criterion empirically derived to correlate impact to severity of injury. The VC is calculated based on the amount of sternal deflection and the velocity at which the deflection occurs. VC has been validated as a useful tool in determining injury severity related to blunt ballistic impacts [16].

$$VC = \frac{Y_{CFC600}}{DefConst} * \frac{dY_{CFC600}}{dt}$$

Equation 4 - Equation for viscous criterion

Where Y is the thoracic deformation (m) filtered with a channel filter class 180, DefConst is the depth of half of the surrogate ribcage in (mm) and dY_{CFC600}/dt is the deformation velocity (m/s).

$$\frac{dY[t]_{CFC600}}{dt} = V[t] = \frac{8(Y[t+\Delta t] - Y[t-\Delta t]) - (Y[t+2\Delta t] - Y[t-2\Delta t])}{12\Delta t}$$

Equation 5 - Equation for chest deformation velocity

Where Δt is the time interval between measurements (s).

DOCUMENT CONTROL DATA

(Security classification of title, body of abstract and indexing annotation must be entered when the overall document is classified)

1. ORIGINATOR (The name and address of the organization preparing the document. Organizations for whom the document was prepared, e.g. Centre sponsoring a contractor's report, or tasking agency, are entered in section 8.)

Wayne State University
5057 Woodward Ave.
Detroit MI 48202
USA

2. SECURITY CLASSIFICATION (Overall security classification of the document including special warning terms if applicable.)

UNCLASSIFIED
(NON-CONTROLLED GOODS)
DMC A
Review: GCEC JUNE 2010

3. TITLE (The complete document title as indicated on the title page. Its classification should be indicated by the appropriate abbreviation (S, C or U) in parentheses after the title.)

Evaluation of the TASER eXtended Range Electronic Projectile (XREP)

4. AUTHORS (last name, followed by initials – ranks, titles, etc. not to be used)

Sherman, Donald; Bir, Cynthia

5. DATE OF PUBLICATION (Month and year of publication of document.)	6a. NO. OF PAGES (Total containing information, including Annexes, Appendices, etc.)	6b. NO. OF REFS (Total cited in document.)
March 2012	171	0

7. DESCRIPTIVE NOTES (The category of the document, e.g. technical report, technical note or memorandum. If appropriate, enter the type of report, e.g. interim, progress, summary, annual or final. Give the inclusive dates when a specific reporting period is covered.)

Contract Report

8. SPONSORING ACTIVITY (The name of the department project office or laboratory sponsoring the research and development – include address.)

Centre for Security Science
Defence R&D Canada
222 Nepean St. 11th Floor
Ottawa, ON Canada K1A 0K2

9a. PROJECT OR GRANT NO. (If appropriate, the applicable research and development project or grant number under which the document was written. Please specify whether project or grant.)	9b. CONTRACT NO. (If appropriate, the applicable number under which the document was written.)

10a. ORIGINATOR'S DOCUMENT NUMBER (The official document number by which the document is identified by the originating activity. This number must be unique to this document.)	10b. OTHER DOCUMENT NO(s). (Any other numbers which may be assigned this document either by the originator or by the sponsor.)
2012 XREP 04F	DRDC CSS CR 2012-003

11. DOCUMENT AVAILABILITY (Any limitations on further dissemination of the document, other than those imposed by security classification.)

12. DOCUMENT ANNOUNCEMENT (Any limitation to the bibliographic announcement of this document. This will normally correspond to the Document Availability (11). However, where further distribution (beyond the audience specified in (11) is possible, a wider announcement audience may be selected.))

13. ABSTRACT (A brief and factual summary of the document. It may also appear elsewhere in the body of the document itself. It is highly desirable that the abstract of classified documents be unclassified. Each paragraph of the abstract shall begin with an indication of the security classification of the information in the paragraph (unless the document itself is unclassified) represented as (S), (C), (R), or (U). It is not necessary to include here abstracts in both official languages unless the text is bilingual.)

The TASER XREP was assessed to provide a complete characterization as a less-lethal weapon. The characterization was undertaken to determine how the system performed under normal and special conditions. The characterization included an assessment of the physical/electrical design and durability of the system, in-flight aerodynamics and accuracy, risk of blunt and penetrating injuries as well as a physiological surrogate. Testing was performed in a laboratory setting to allow for control of environmental variables. All fired rounds were tested with a computer-controlled firing system. The overall accuracy of the projectile was found to decrease with distance. Vertical drop from the point of aim to the point of impact at a distance of 20 meters was -51.37 ± 4.79 cm when tested at 23°C. Testing at 50°C and -20°C showed significantly less vertical drop -31.90 ± 3.12 cm and -29.69 ± 10.23 cm respectively. The round was stable in flight and produced a very low risk of blunt trauma although penetration testing at 2 meters showed a high likelihood of penetration. The electrical output of the projectile was within the manufacturer's specification, continued to operate after impact and did not produce any persistent clinically significant effects in the swine model.

Le TASER XREP a été évalué pour fournir une caractérisation complète comme arme moins mortelle. La caractérisation a été entreprise pour déterminer comment le système se comporte dans des conditions normales et des conditions spéciales. La caractérisation comprenait une évaluation de la conception physique/électrique et de la durabilité du système, de la précision et de l'aérodynamique en vol, du risque de contusions et de blessures pénétrantes, ainsi qu'un substitut physiologique. Des essais ont été effectués dans un laboratoire pour permettre de contrôler l'environnement. Tous les projectiles lancés ont été testés à l'aide d'un système de tir commandé par ordinateur. On s'est aperçu que la précision globale du projectile diminue au fur et à mesure que la distance augmente. La chute verticale du point de visée au point d'impact à une distance de 20 mètres était de -51,37 ± 4,79 cm lorsque testée à 23 °C. Un essai à 50 °C et un à -20 °C ont démontré qu'il y avait une chute verticale beaucoup moins importante de -31,90 ± 3,12 cm et de -29,69 ± 10,23 cm respectivement. Le projectile était stable en vol et produisait un très faible risque de contusions bien que l'essai de pénétration à 2 mètres démontrait une probabilité élevée de pénétration. L'électricité produite par le projectile respectait la spécification du fabricant, ne cessait pas après l'impact et ne produisait pas d'effets persistants importants au niveau clinique chez le porc

14. KEYWORDS, DESCRIPTORS or IDENTIFIERS (Technically meaningful terms or short phrases that characterize a document and could be helpful in cataloguing the document. They should be selected so that no security classification is required. Identifiers, such as equipment model designation, trade name, military project code name, geographic location may also be included. If possible keywords should be selected from a published thesaurus, e.g. Thesaurus of Engineering and Scientific Terms (TEST) and that thesaurus identified. If it is not possible to select indexing terms which are Unclassified, the classification of each should be indicated as with the title.)

Taser; Less Lethal Weapons; Conducted Energy Devises